FOSSIL ENERGY

FE-15529-6

MHD ELECTRODE DEVELOPMENT

Quarterly Report for the Period January–March 31, 1980

By
John W. Sadler
Jeff Bein
Laurence H. Cadoff
Don L. Dietrick
James A. Dilmore
Edsel W. Frantti
Dave Jacobs
Edgar L. Kochka
Jack A. Kuszyk
S. K. Lau
Joseph Lempert
Jack C. Reck
Barry R. Rossing
James R. Schornhorst
Eugene E. Smeltzer

April 1980

Work Performed Under Contract No. AC01-79ET15529

Westinghouse Electric Corporation
Advanced Energy Systems Division
Pittsburgh, Pennsylvania

U. S. DEPARTMENT OF ENERGY

DISCLAIMER

Available from the National Technical Information Service, U. S. Department of Commerce, Springfield, Virginia 22161.

Price: Paper Copy $10.00
Microfiche $3.50

FE-15529-6
Distribution Categories UC-90g and UC-93

MHD ELECTRODE DEVELOPMENT

Quarterly Report for the Period
January-March 31, 1980

John W. Sadler
Jeff Bein
Laurence H. Cadoff*
Don L. Dietrick
James A. Dilmore*
Edsel W. Frantti
Dave Jacobs
Edgar L. Kochka
Jack A. Kuszyk
S. K. Lau*
Joseph Lempert**
Jack C. Reck
Barry R. Rossing*
James R. Schornhorst
Eugene E. Smeltzer*

*Westinghouse Research & Development Center
**Consultant

WESTINGHOUSE ELECTRIC CORPORATION
Advanced Energy Systems Division
P. O. Box 10864
Pittsburgh, Pa. 15236

APRIL 1980

PREPARED FOR THE
UNITED STATES DEPARTMENT OF ENERGY

Under Contract No. DE-AC-01-79-ET-15529

APPROVED:

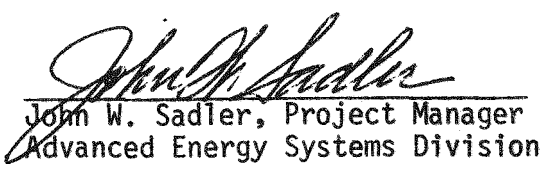

John W. Sadler, Project Manager
Advanced Energy Systems Division

TABLE OF CONTENTS

TABLE OF CONTENTS (Continued)

LIST OF TABLES

LIST OF FIGURES

LIST OF FIGURES (Continued)

I. ABSTRACT

Technical progress under DOE Contract DE-AC-01-79-ET-15529 during the January to March 1980 quarter is presented.

Platinum capped anodes and iron cathodes, operating in the slagging hot mode, have been included in WESTF Test 43. Further results of bonding studies in support of this test are presented. The results of thermal diffusivity measurements made by Battelle Pacific Northwest Laboratory (BPNL) of super-hot hafnia electrode and indium oxide current leadout materials are reported.

Laboratory electrochemical corrosion tests have been continued. Results reported herein indicate that Fe_3O_4 additions are effective in reducing polarization in Western slags. In comparison with cobalt oxide additions, the Fe_3O_4 addition provides significant cost advantages.

During this period, significant WESTF operations included WESTF Test 47, 42, 43 and 49. This test sequence included tests of: slagging cold metallics in the MTS II test section; hafnia and zirconia coupons in the WESTF test section (non-slagging super-hot conditions); platinum/iron run under slagging hot conditions in the WESTF test section, and, a test of the 0.5 $SrZrO_3 \cdot 0.5$ ($Sr_{.25}La_{.75}FeO_3$) material in the non-slagging super-hot mode in the MTS II test section.

Upon completion of WESTF Test 49, facility test operations were suspended and modifications of the facility, to support the addition of a 3 Tesla magnet, initiated. The status of design, procurement and modification activities is presented.

II. OBJECTIVE AND SCOPE OF WORK

In continuation of the program to develop MHD power generation to commercial feasibility, Westinghouse is conducting a program to develop improved electrode designs for open-cycle coal-fired MHD generator applications. The program includes the link between basic and supportive materials development and testing in an engineering test rig that offers an adverse MHD environment for extended periods of time.

Specific development activities of this program are as follows:

(a) Laboratory screening tests to provide preliminary electrochemical stability data on selected advanced or modified ceramic candidate electrode and insulation materials.

(b) Laboratory screening tests to evaluate the resistance of selected candidate anode materials to simulated arc impingements under a representative range of chemical and thermal conditions.

(c) Engineering rig tests of preferred electrode designs, selected on the basis of the screening test results and/or pertinent outside data, under simulated open-cycle coal-fired MHD operating conditions.

(d) Preparation and fabrication of experimental electrode materials, as warranted by favorable laboratory screening test results, to provide samples for engineering rig tests.

In addition to these four main development activities, this project includes providing such laboratory, design, test and analytical support as necessary to characterize test materials, and to determine such essential physical and chemical properties as are required to properly design the test specimens and to interpret and analyze test data. Dependent on development results, preferred electrode materials will be prepared for advanced testing in other DOE contractor facilities.

These objectives are being pursued in accordance with a statement of work which is consistent with the National Plan for MHD development formulated by DOE.

The major elements of the program are presented in a Work Breakdown Structure which is presented in Table 1. The Level I effort is the MHD Electrode Development Contract, and Level II consists of the following four tasks.

WBS 1.1 ELECTRODE AND INSULATOR MATERIALS
WBS 1.2 ENGINEERING TESTS
WBS 1.3 WESTF MODIFICATION
WBS 1.4 PROJECT MANAGEMENT AND DOCUMENTATION

WBS 1.1 - ELECTRODE AND INSULATOR MATERIALS

The objective of this task is to provide for the development, laboratory evaluation and fabrication of electrode and insulator materials. All necessary experimental material preparation, as well as fabrication of test samples for laboratory screening tests, engineering rig tests in the Westinghouse Electrode System Test Facility, WESTF (WBS 1.2), or other tests will be completed under this task. This task also includes supporting pre-test material characterization and laboratory screening tests used to evaluate the relative performance of candidate materials. These screening tests include electrochemical and anode arc impingement tests.

WBS 1.2 - ENGINEERING TESTS

The objective of this task is to provide for the engineering tests of promising electrode/insulator materials resulting from the WBS 1.1 activity. In particular, this task provides for the supporting design, test and post-test analysis effort as well as maintenance and operation of the engineering test rig, WESTF. Table 2 summarizes WESTF test capabilities.

This task incorporates the elements of planning, experiment design, test operations and post-test analysis and provides the close engineering design and test discipline necessary to effect successful electrode/insulating wall system development. In addition, final fabrication and assembly operations necessary to incorporate electrode and interelectrode insulating elements fabricated under WBS 1.1 into a complete assembly ready for testing in WESTF

TABLE 1

WORK BREAKDOWN STRUCTURE

(SUBELEMENTS TO DOE WBS 2.2.2)

- WBS 1.0 MHD ELECTRODE DEVELOPMENT
  - WBS 1.1 ELECTRODE AND INSULATOR MATERIALS
    - WBS 1.1.1 EXPERIMENTAL MATERIALS FABRICATION
      - MATERIAL DEVELOPMENT
      - MATERIAL CHARACTERIZATION
      - MATERIAL FABRICATION
    - WBS 1.1.2 LABORATORY SCREENING TESTS
      - ELECTROCHEMICAL TESTS
      - ANODE ARC TESTS
  - WBS 1.2 ENGINEERING TESTS
    - WBS 1.2.1 TEST ENGINEERING
      - DEVELOPMENT REQUIREMENTS
      - EXPERIMENT DESIGN
      - POST-TEST ANALYSIS
    - WBS 1.2.2 TEST ASSEMBLY FABRICATION
    - WBS 1.2.3 WESTF OPERATIONS
      - PRE-TEST ACTIVITY
      - TEST OPERATIONS
  - WBS 1.3 WESTF MODIFICATION
  - WBS 1.4 PROJECT MANAGEMENT AND DOCUMENTATION

I II III - SYSTEMS LEVEL

TABLE 2

WESTF TEST CAPABILITIES

Mass Flow	To 0.5 lb/sec
Combustion Temperature	To 2850^{o}K
Combustor Pressure	1 to 5 atm
Channel Velocity	Subsonic, 500 to 800 m/sec
Seeding	K_2CO_3 or K_2SO_4 wet with ash or char additions (Rosebud)
B Field	3 tesla, nominal - 3.3 tesla, objective
Fuel	Toluene/#2 Fuel Oil
Oxidant	Preheated air with oxygen enrichment
Data Collection	240 channels coupled with minicomputer
Test Duration	Up to 100 hours
Test Frequency	Up to 2 per month
Channel Configuration	12.5 cm^2 flow cross section
Startup Ramp, Minimum	$\approx$25^{o}K/min

will be provided under this task. Required test documentation and facility operating procedures will also be prepared.

WBS 1.3 - WESTF MODIFICATION

This task has been established to provide for the planned modification of WESTF. The primary element of this task is the addition of a conventional 3.0 tesla magnet.

WBS 1.4 - PROJECT MANAGEMENT AND DOCUMENTATION

This centralized management task provides the focal point for directing the activities which comprise the full project effort. The Project Manager is responsible for the proper definition, integration and implementation of the technical, schedule, contractual, and financial aspects of the program. Coordination of the preparation of required documentation will also be completed under this task.

III. SUMMARY OF PROGRESS TO DATE

During the January to March 1980 quarter, the principal areas of activity were as follows:

- Continuation of electrode and insulator material development activities with emphasis on investigating electrode attachment techniques.
- Continuation of anode/slag interface polarization electrochemical corrosion tests.
- Completion of WESTF Tests 42, 43, 47 and 49.
- Completion of design for WESTF Test 49 and completion of test section fabrication for WESTF Tests 43 and 49.
- Continuation of the design of the modified WESTF Test Section for use with the magnet (WESTF II).
- Continuation of magnet modification activities.
- Initiation of WESTF modifications as required for magnet installation.

Figure 1 summarizes the overall program schedule, based on the approved Project Management Summary Baseline Report, FY 80 Revision dated October 1979, and shows schedular status. As of the end of this quarter WESTF was shut down and modifications associated with magnet installation have been initiated.

Program activities are being redirected to provide emphasis in the engineering development and evaluation of slagging cold metallic electrodes. As a result a number of activities are now in a period of transition. Testing of slagging hot and non-slagging super-hot electrode systems will continue, but at a reduced level.

U.S. DEPARTMENT OF ENERGY

DOE Form CR-535 (1-78)

MILESTONE SCHEDULE AND STATUS REPORT

PAGE 1 OF 1

FORM APPROVED OMB NO. 38 R 0180

1. Contract Identification	2. Reporting Period	3. Contract Number
MHD ELECTRODE DEVELOPMENT PROGRAM	through 3/80	DE-AC-01-79-ET-15529

4. Contractor (name, address)
WESTINGHOUSE ELECTRIC CORPORATION
ADVANCED ENERGY SYSTEMS DIVISION
P. O. Box 10864 Pittsburgh, Pa. 15236

5. Contract Start Date: April 23, 1979

6. Contract Completion Date: September 30, 1980

7. Identification Number	8. Reporting Category (e.g., contract line item or work breakdown structure element)	9. Fiscal Years and Months																						10. Percent Complete	
		79				80																			
WBS		1Q	2Q	3Q	4Q	O	N	D	J	F	M	A	M	J	J	A	S							a) Planned	b) Actual
1.1	ELECTRODE AND INSULATOR MATERIALS																								
1.1.1	EXPERIMENTAL MATERIALS FABRICATION																								
1.1.2	LABORATORY SCREENING TESTS																								
1.2	ENGINEERING TESTS																								
1.2.1	TEST ENGINEERING																								
1.2.2	TEST ASSEMBLY FABRICATION																								
1.2.3	WESTF OPERATIONS																								
1.3	WESTF MODIFICATION																								
1.4	PROJECT MANAGEMENT AND DOCUMENTATION																								

11. Remarks

12. Signature of Contractor's Project Manager and Date	13. Signature of Government Technical Representative and Date
John W. Sadler	

Figure 1. Program Schedule and Status

1.0 WBS 1.1 - ELECTRODE AND INSULATOR MATERIALS

In addition to providing necessary test materials, for the laboratory screening tests and WESTF tests, and material characterization data required for the detail design activity, this task includes a number of electrode and insulator materials development and evaluation activities.

A number of candidate insulator materials have been evaluated on the basis of corrosion resistance in Western coal slag. On the basis of this immersion test (Reference 1), the following materials have been ranked as excellent:

Al_2O_3	Fused Cast	Carborundum
Al_2O_3-Cr_2O_3	Fused Cast	Carborundum
$MgAl_2O_4$-Cr_2O_3	Fused Cast	Carborundum
$MgAl_2O_4$	Fused Cast	Carborundum
$MgAl_2O_4$	Fused Cast	Trans-Tech
MgO	Fused Cast	Norton

Laboratory electrochemical corrosion tests and anode arc erosion tests have been conducted to evaluate the relative performance of candidate electrode materials. The following summarizes significant findings in these areas:

- A comprehensive model for understanding electrochemical reactions in slagging MHD channels has been developed (Reference 1).
- Zirconia based materials appear to be extremely promising candidate materials for use as anodes with Western slags under slagging hot and perhaps non-slagging super-hot conditions (Reference 2).
- Electrochemical corrosion is extremely sensitive to density and purity of electrode materials (Reference 2).
- Iron cathodes and platinum anodes form the most promising metal electrode combination identified to date for use under slagging hot conditions.

- Slag chemistry modification, through additions of transition metal ions, is effective in minimizing electrochemical corrosion and polarization (Reference 3).
- Laboratory scale anode arc tests indicate that TiB_2 coated copper may be comparable to platinum clad copper in the slagging cold operating mode (Reference 4).

As reported in Section IV-1.1.1, a satisfactory attachment technique was defined for the MIT material, 0.5 $(SrZrO_3)$·0.5 $(Sr_{0.25}La_{0.75}FeO_3)$, to be tested in WESTF Test 49. Results of BPNL thermal diffusivity measurements on a number of hafnia electrode and indium oxide current leadout materials are presented in Section IV-1.1.2. Continuing electrochemical corrosion test results are reported in Section IV-1.2.1. These results indicate that Fe_2O_3 additions are effective in reducing electrochemical stress in Rosebud slag.

2.0 WBS 1.2 - ENGINEERING TESTS

This task is directed towards the design, fabrication, test and post-test analysis of those electrode/insulator materials which undergo testing in the Westinghouse Electrode System Test Facility (WESTF). In comparison with laboratory screening tests, which generally couple only one or two aspects of the MHD channel environment, WESTF provides a realistic simulation of the MHD channel environment. Inclusion of magnetic field effects is planned, see WBS 1.3 below.

Table 3 provides a summary of WESTF tests completed to date. Implicit in this test summary are the following accomplishments:

- Satisfactory operation of WESTF: in the clean firing super-hot mode; in the slagging cold mode with Eastern and Western slags; in the slagging hot mode with Western slag.
- WESTF Tests 40 and 41, slagging cold electrodes, have established a correlation with laboratory and generator tests.
- Testing of electrodes and electrode materials supplied by others, including: AVCO, BPNL, and MIT.

During this quarter, as presented in Section IV-2.1.2, test section detail design activities have been redirected to reflect the emphasis to be given to slagging cold metallic systems. Results of these design activities are presented. Section IV-2.1.3 presents the results of the post-test analysis efforts completed this quarter. Fabrication activities are discussed in Section IV-2.2.

WESTF operating time during this quarter was 50 hours which included WESTF Tests 42, 43, 47 and 49. As of the end of this quarter the total WESTF operating time, defined as the cumulative time interval from combustor on to combustor off is 438 hours. Of this total time, 198 hours were accumulated under clean firing conditions and 240 hours were accumulated under slagging conditions.

3.0 WBS 1.3 - WESTF MODIFICATION

Activity within this task is directed towards extending the capabilities of WESTF and incorporating facility and operational improvements. The major activity is that associated with the addition of a conventional 3 Tesla magnet.

At the completion of WESTF Test 49 in mid-March, the facility was shut down for those modifications required by the magnet addition. Extensive rework of the facility is in progress.

In this regard, the design of the magnet modification has been completed and fabrication activities are in progress. The coil final assembly fixture has been received and essentially all fabrication activities have been completed. The outstanding magnet modification activity is the hydraulic and electrical checkout of the modified magnet.

Details of the design of the load bank, air preheater line isolation section, and other facility modification activities are presented in Section IV-3.0. As also reported in this section, upgrading of the mini-computer/DAS has been completed.

TABLE 3

WESTF TEST HISTORY

OPERATING MODE	CLEAN	CLEAN COLD	CLEAN SH	CLEAN SH	CLEAN SH	CLEAN SH	SLAG COLD
Test ID	D-7	W-35	W-36	W-37(2)	W-38(2)	W-39(2)	D-8
Test Section	Dummy	WESTF	WESTF	WESTF	WESTF	WESTF	Dummy
Approx. Date	5/77-6/77	7/77-9/77	9/77	10/77	11/77	1/78	6/78-9/78
Electrode Material(1)	NA	Cu	$LaCrO_3$	MAFF 31 MAFF 41 HfO_2 Comp.	$LaCrO_3$(3) $LaCrO_3ZrO_2$ $LaCrO_3$	$LaCrO_3$-$LaAlO_3$ $LaCrO_3$-$SrZrO_3$ $LaCrO_3$ MAFF 31	NA
Insulator Material	NA	$MgAl_2O_4$	$MgAl_2O_4$ MgO	$MgAl_2O_4$	$MgAl_2O_4$ MgO	$MgAl_2O_4$ MgO	NA
T_E, °C	NA	400-100	1700	1700+	1700+	1700+	NA
J, amp/cm^2	NA	To 1.0	1.0	1.0	1.0	1.0	NA
Q, w/cm^2	NA	~90	~30	~30	~30	~30	NA
B, Tesla	NA	NA	NA	NA	NA	NA	NA
Axial Field, Kv/m	NA	No	No	No	No	No	NA
Ash Type	NA	NA	NA	NA	NA	NA	Rosebud
Seed	K_2CO_3	K_2CO_3	K_2CO_3	K_2CO_3	K_2CO_3	K_2CO_3	K_2CO_3
SO_2 Level, m/o	--	--	--	--	--	--	--
Duration-Hrs.	NA	22	20	20	20	20	NA

OPERATING MODE	SLAG COLD	SLAG COLD	NON-SLAG SH	NON-SLAG SH	CLEAN SH	NON-SLAG SH	SLAG COLD
Test ID	W-40	W-41	D-9	D-10	D-11	45	47
Test Section	WESTF	WESTF	MTS(6)	Transition	Transition	MTS	MTS II
Approx. Date	10/78-1/79	1/79-8/79	9/79	10/79	11/79	12/79	1/80
Electrode Material(1)	Cu	Cu-Pt (+) Cu-W/Cu (-)	$LaCrO_3$	NA	NA	Zirconia	Cu-Pt (+) Cu (-)
Insulator Material	$MgAl_2O_4$	BN	MgO	MgO	MgO	NA	MgO
T_E, °C	150/275	150	To 1900	NA	NA	1800	150
J, amp/cm^2	To 1.25	0.9	NA	NA	NA	0.9	1.0
Q, w/cm^2	~125	~125	--	NA	NA	30	~125
B, Tesla	NA	NA	NA	NA	NA	NA	NA
Axial Field, Kv/m	Yes	Yes	No	No	No	No	No
Ash Type	Eastern	Eastern	Rosebud	Rosebud	--	Rosebud	Rosebud
Seed	K_2CO_3	K_2CO_3	K_2CO_3	K_2CO_3	K_2CO_3	K_2CO_3	K_2CO_3
SO_2 Level, m/o	0.01	0.01	0.01	0.01	0.01	0.06	0.3
Duration-Hrs.	14(4)	63(5)	5(7)	13(5)	11	9	7

(1) Anode and Cathode Unless Otherwise noted
(2) U-02 Phase III Proof Test
(3) With ZrO_2
(4) Four Runs
(5) Two Runs
(6) Materials Test section
(8) BPNL Material
(9) MIT Material

TABLE 3

WESTF TEST HISTORY (Continued)

OPERATING MODE	NON-SLAG SH	SLAG HOT	NON-SLAG SH				
Test ID	42	43	49				
Test Section	WESTF	WESTF	WESTF				
Approx. Date	1/80	3/80	3/80				
Electrode Material[1]	Hafnia Based[8] Zirconia Based	Pt (+) Fe (-)	$LaFeO_3$, $SrZrO_3$, $SrFeO_3$[9]				
Insulator Material	NA	$MgAl_2O_4$ Al_2O_3	MgO				
T_E, °C	1250 to 1750	1050-1400	1700				
J, amp/cm^2	0	1.0	1.0				
Q, w/cm^2	15 to 30	60-115	40				
B, Tesla	NA	NA	NA				
Axial Field, Kv/m	No	No	No				
Ash Type	Rosebud	Rosebud	Rosebud				
Seed	K_2CO_3	K_2CO_3	K_2CO_3				
SO_2 Level, m/o	0.06	0.06	0.06				
Duration-Hrs.	22	13	8				

4.0 WBS 1.4 - PROJECT MANAGEMENT AND DOCUMENTATION

Significant project documentation issued during this quarter included the following:

- Quarterly Report, October-December 1979.
- Monthly Project Management Reports

A project review meeting was held with DOE personnel in January 1980 to review technical areas of emphasis within the contract Scope of Work. As a result of this meeting and subsequent discussions steps have been initiated to emphasize the engineering development and evaluation of slagging cold electrodes, including alternatives to the use of platinum as the reference anode material. Activities associated with hot wall materials will be continued, however, at a reduced level.

IV. DETAILED DESCRIPTION OF TECHNICAL PROGRESS

A work plan is being formulated to reflect the emphasis to be directed to the engineering development and evaluation of cold metallic electrodes in support of CDIF/ETF. The basic methodology of this work is: to systemmatically investigate the effect of the MHD environment on channel materials and designs; to clearly identify the material corrosion mechanisms which are operative; to assess the effect of test variables on corrosion/erosion rates; to select and evaluate materials which are resistant to these conditions, and, to establish correlations between laboratory screening, engineering test rig and generator tests. This approach will establish a sound data base and will accelerate the development of slagging cold electrodes in a very cost-effective manner.

The work program is intended to address a number of technical issues applicable to slagging cold metallic electrodes, including interelectrode insulators and channel sidewall elements. These issues include:

- Plasma sulfur content
- Electrode/slag interface temperature
- Magnetic field strength
- Current density
- Combustor stoichiometry (O_2)
- Ash injection versus coal combustion
- Eastern versus western coal (ash)
- Axial field
- Heat flux
- Slag modification
- Slag carryover percentage

With regard to the slagging hot and non-slagging super-hot operating modes, appropriate systems will be investigated, however, at a reduced level.

As a result of the emphasis to be given to slagging cold metallic electrode systems, a number of changes are being effected in the detail effort under this contract. In particular a number of on-going design activities have been re-directed towards supporting WESTF operations in the slagging cold operating mode (see Section IV - 2.1.2). In addition, a number of laboratory activities, directed towards slagging cold metallic electrodes have been initiated (see Section IV - 1.1). In view of the emphasis now being directed towards the slagging cold electrodes, a number of previously defined WESTF tests have been deferred, see Section IV - 2.1.1.

1.0 WBS 1.1 - ELECTRODE AND INSULATOR MATERIALS

1.1 WBS 1.1.1 - Experimental Materials Fabrication

1.1.1 Material Development

Electrode Materials

WESTF Test 43

The platinum caps for WESTF Test 43 (10 mil thick foil) were attached to high density alumina by a diffusion bonding technique which was summarized in Reference 3. During this quarter, further evaluations of typical joints were completed. Micro-optical inspection of the ceramic-metal interface revealed an exceptionally tight seal with no visible micropores. However, a 'reaction' zone, as shown in Figure 2, was detected. This zone was analyzed using the SEM/EDAX to resolve its identity. A line profile across the interface showed a sharp transition from Pt to Al_2O_3 and no apparent diffusion zone. A spot analysis near the bond region also revealed only single elemental areas and no detectable impurities. A possible explanation for the 'zone' is that it is just the etched area of the alumina caused by the cleaning treatment prior to the bonding operation. The 40% nitric acid solution could have enough of an effect to change the microstructure of the alumina near its surface.

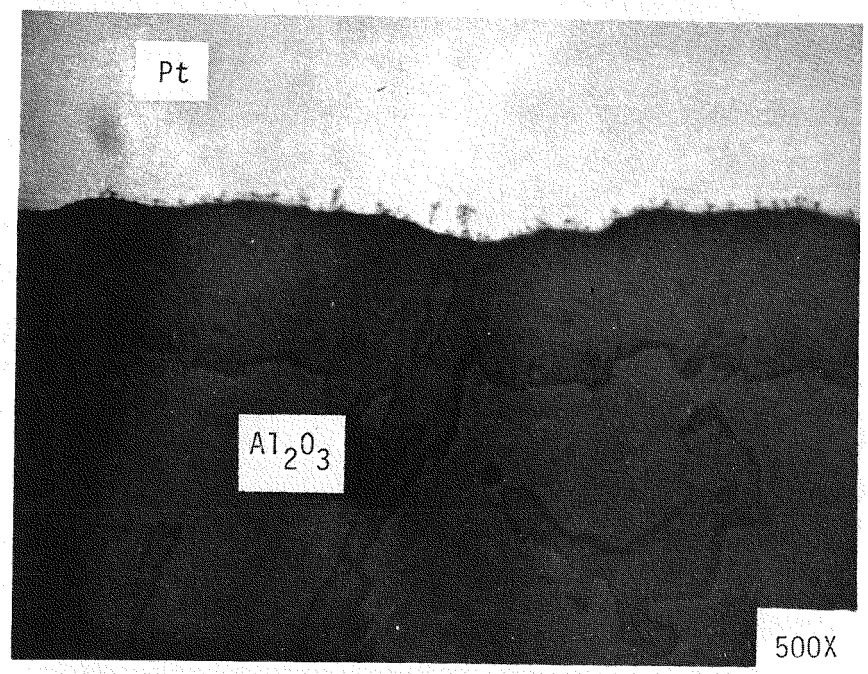

(A) Pt/Al_2O_3 Bond

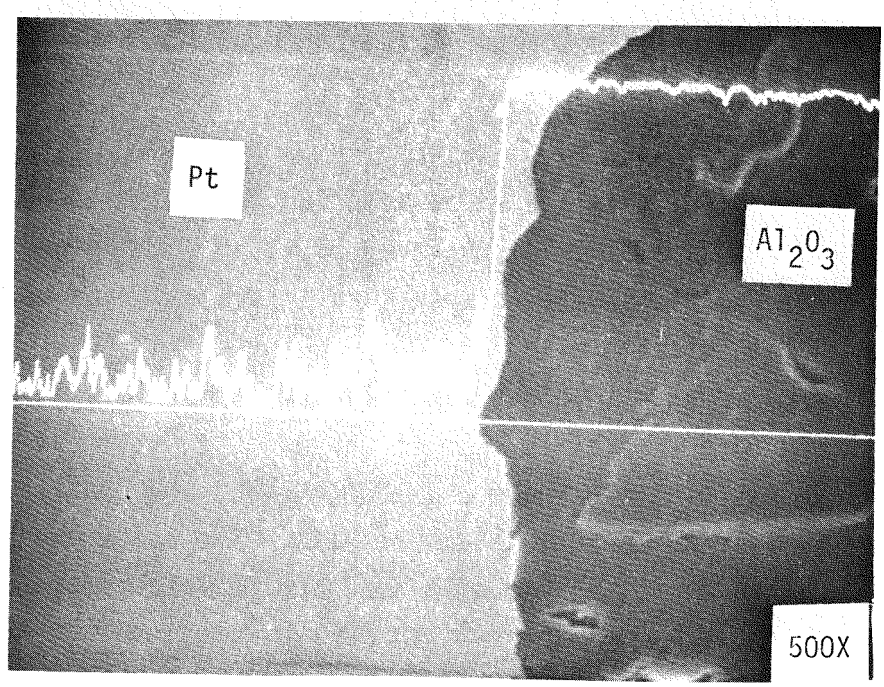

(B) Line Profile of Pt/Al_2O_3

Figure 2. Diffusion Bonding of Platinum to Al_2O_3

TiB_2 Clad Copper

TiB_2 clad copper specimens showed, in earlier and very limited arc erosion tests, an arc erosion rate that was comparable to platinum clad copper (References 1 and 3). Based on these results, it was concluded that the system merits further investigation as a cold wall electrode.

With the program changing to emphasize cold wall alternatives to platinum, further development work on TiB_2 has been initiated to provide improved samples for evaluation. For the earlier arc erosion tests, the TiB_2 coatings were applied by Chemical Vapor Deposition (CVD) from a chloride system. Due to the high deposition temperature required and the large differences in the thermal expansion coefficients of copper and TiB_2, these coatings exhibited many surface cracks. In order to minimize the coating thermal stresses and maximize adhesion, coating deposition by sputtering is being investigated. Sputtering offers the potential of producing a copper-TiB_2 graded interface that should improve the thermal shock resistance of this system. These samples will be evaluated in laboratory screening tests prior to inclusion in WESTF tests.

Platinum Clad Copper

Platinum is the current baseline anode material for slagging cold wall electrodes. An in-house evaluation of a thin sputtered platinum coating on copper showed that short exposures to elevated temperatures, such as those used in brazing with silver-copper eutectic alloy, results in the formation of brittle, ordered alloy phases and Kirkendall voids. Thus, a further evaluation of a platinum clad copper MHD anode from WESTF Test 41 was made to determine if comparable effects were observed. This anode was made by AVCO and consisted of a 20 mil platinum foil silver soldered to a copper base. The anode was run in WESTF Test 41 for a total of 49.6 hours with seed and 62.7 hours at temperature (Reference 5).

Anode No. 18 from WESTF 41 was selected for evaluation, as-tested and with further heat treatments in a vacuum furnace for one minute at 600°C and 20 hours at 250°C. A cross-section of the as-tested anode and of the braze interface (Easy Flow 45) is shown in Figure 3. The platinum thickness is nominally 20

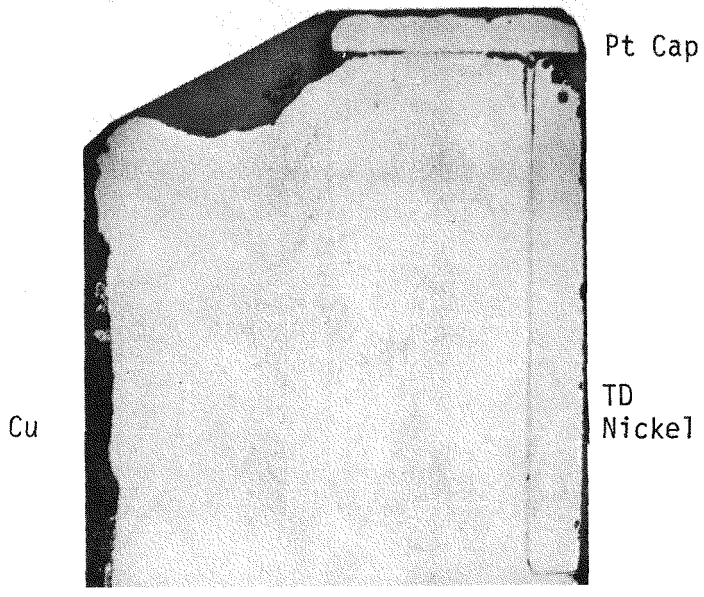

(A) Cross-Section (10X)

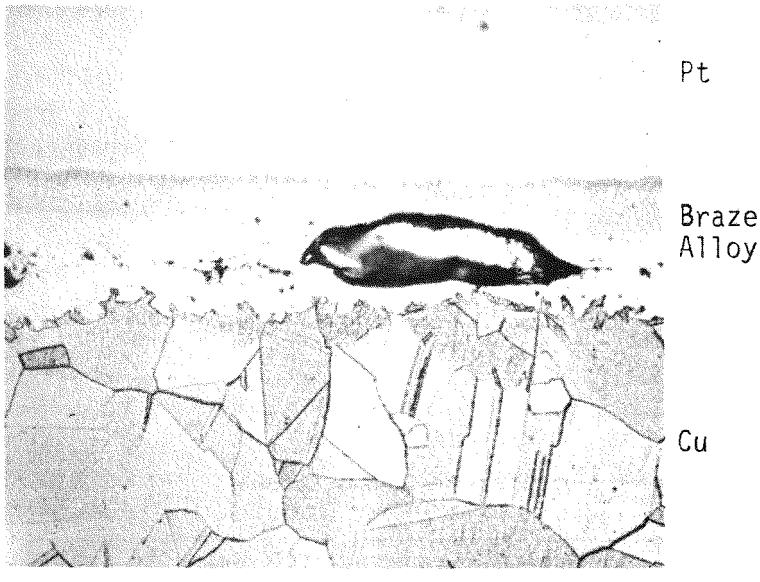

(B) Braze Interface (500X)

Figure 3. Cross-Section of Anode No. 18 from WESTF Test 41

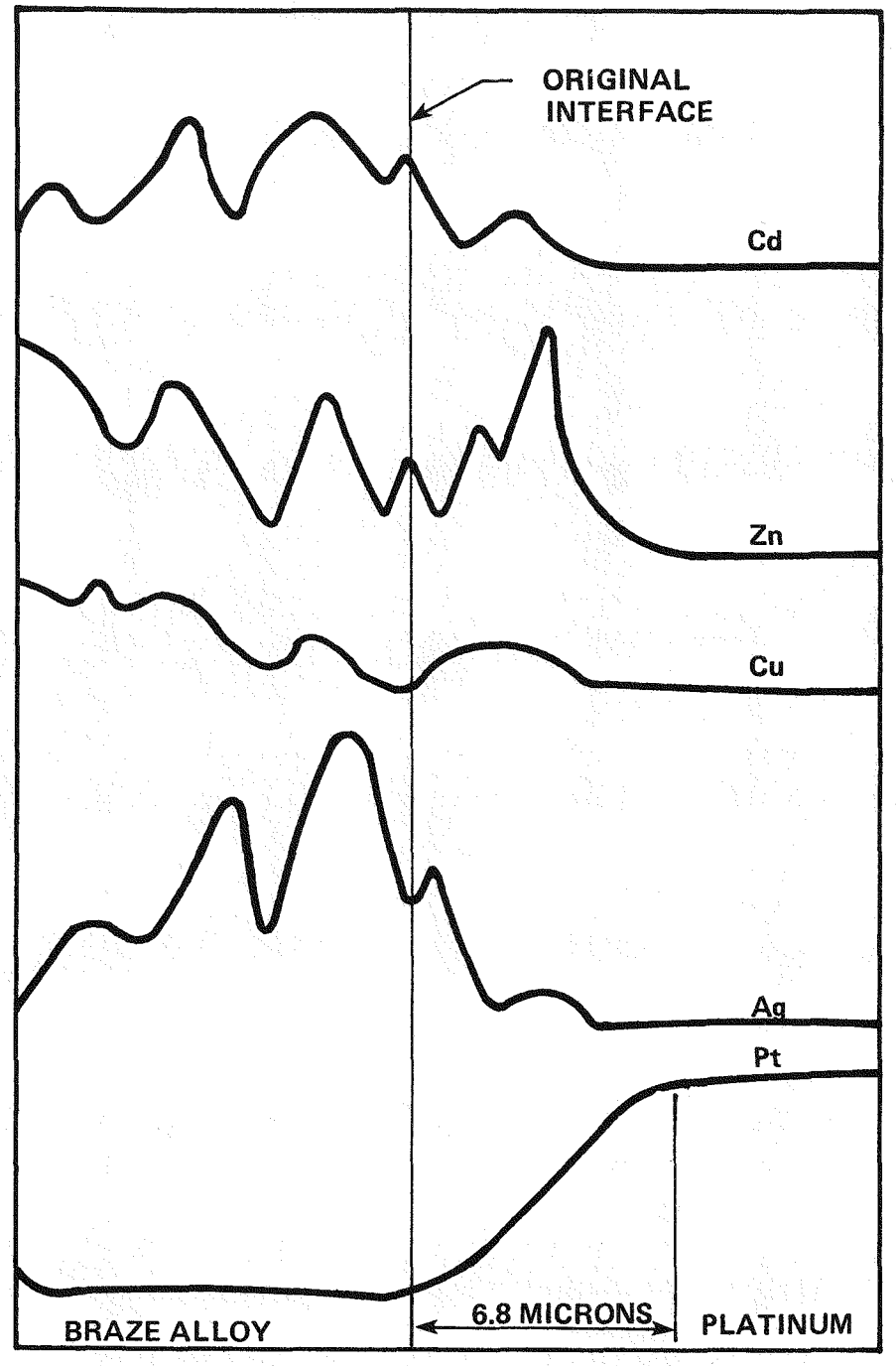

Figure 4. Relative Concentration Profiles Across a Silver Braze Alloy/Platinum Interface

mils; the major arc created surface depression seen in Figure 3a is 3 mils deep. The braze interface shown in Figure 3b contains both large and small voids. An x-ray trace across the braze/Pt interface shows diffusion of the brazing alloy constituents into the platinum, but not at a rate high enough to create Kirkendall voids. All of the braze alloy constituents have diffused into the platinum. The silver concentration drops off quickly at the platinum interface. Segregation of constituents within the braze alloy is also evidenced by the contour of the concentration lines. These traces are shown in Figure 4. SEM photographs of the platinum and copper surfaces are shown in Figure 5. The platinum surface shows very discrete arc craters whereas the copper surface is generally eroded away.

Photomicrographs of the braze area of samples that were heat treated as described above are shown in Figure 6. The maximum heat treatment temperature was limited to 600°C because the silver solder used has a melting temperature of 607°C. Areas of major voids apparently increased, and, as shown by a subsequent x-ray analysis, the increase was apparently due to the loss of silver, cadimum, and zinc during the vacuum heat treatment. Although it is not known to what extent these elements would thermally volatilize in the MHD environment, it is possible that selective volatilization and oxidation will degrade the interface over a period of time and result in the loss of the platinum cap. Further work is needed on the resistance of brazing materials and attachments for long term performance in MHD environments.

Insulator Materials

Laboratory scale slag compatibility testing of candidate insulator materials was deferred due to the number of WESTF tests run during the quarter.

Insulators which had shown good slag corrosion resistance in the previous laboratory scale experiments were incorporated in several WESTF tests. A spinel ($MgAl_2O_4$) obtained from Norton Company, has shown promise in MHD air preheater applications (Reference 6). To evaluate its performance under MHD channel conditions, the downstream transition section of WESTF Test 45 was lined with

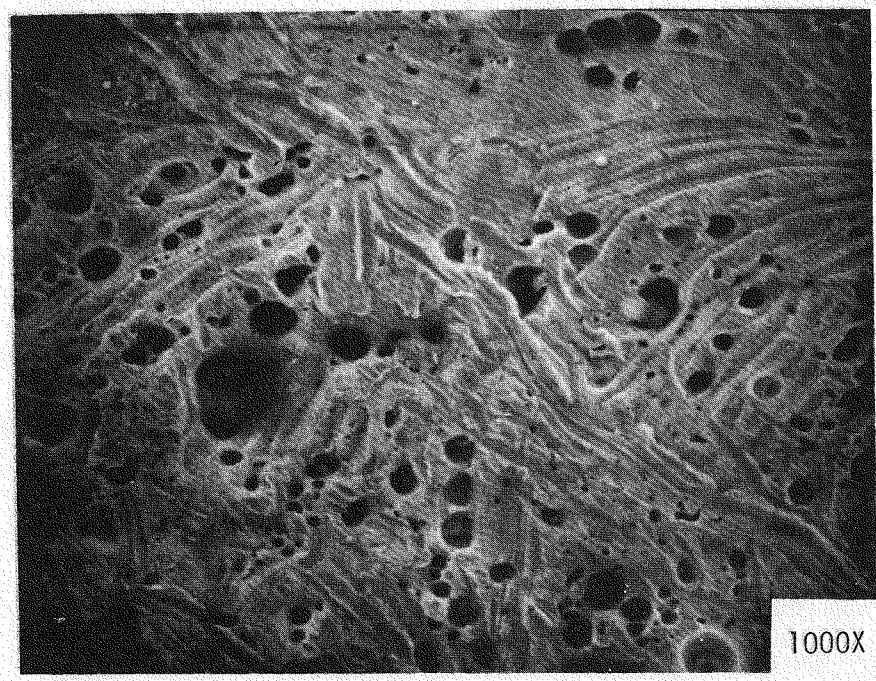

(A) Platinum Surface

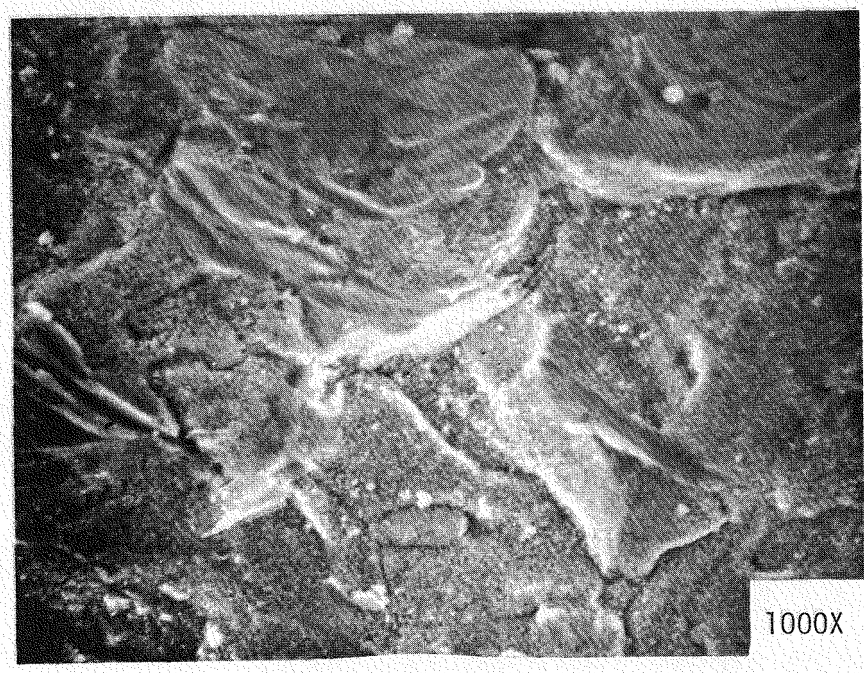

(B) Copper Surface

Figure 5. SEM Photographs of Exposed Platinum and Copper Anode 18 from WESTF Test 41

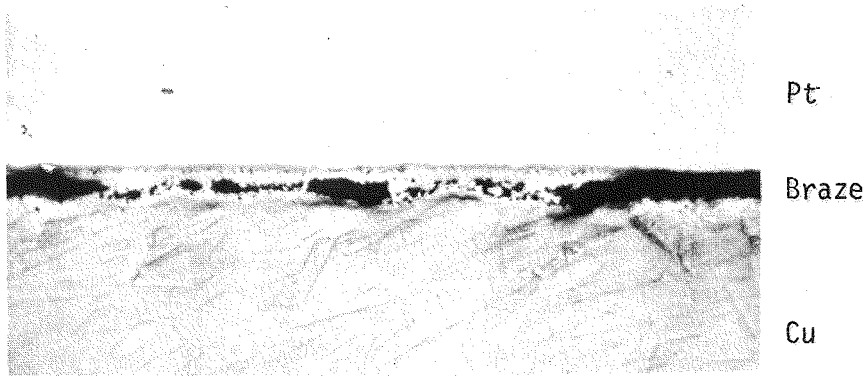

(A) 1 Min., 600° C, 10^{-4} torr

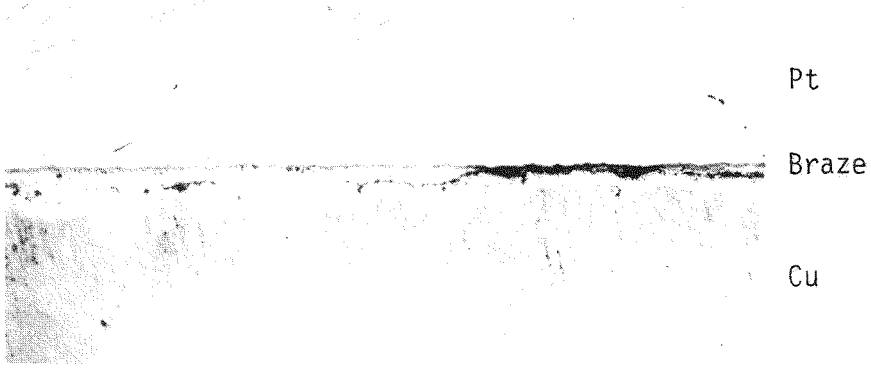

(B) 20 Hrs., 250° C, 10^{-4} torr

Figure 6. Braze Areas of Anode 18 From WESTF Test 41 after Additional Vacuum Heat Treatments

the spinel. A portion of the downstream piping was also lined with a magnesia castable for a comparison of their erosion/corrosion rates. The test was run for a total of six hours and the surface temperature of the castables was estimated at 1700°C. Figure 7 displays a cross-section of the slag/castable interfaces for both MgO and $MgAl_2O_4$. In both materials the slag has penetrated into the surface and a definite reaction zone is visible. A region 0.060-0.070" thick in both castables has been pervaded. The mechanism of attack is quite similar in both cases. The slag penetrates the surface pores and dissolves the matrix phase which surrounds the $MgAl_2O_4$ or MgO grog grains. This in turn allows the erosive action of the plasma to sweep away the now loosened grains. The matrix (bonding phase) is definitely the weak constituent of both castables even though the magnesia relies on a chromate bonding system and the spinel a calcium aluminate bond. Impurities (Si, Ca, Al, S) which would tend to react with the liquid slag are also detected in the matrix of both materials. With these results, one is unable to show a superiority of one castable over the other. Slag compatibility tests of longer duration are needed to fully evaluate their performance.

Two commercial fused cast refractories which have shown excellent slag corrosion resistance in small scale laboratory tests were incorporated in the exit transition section of WESTF Test 42. The materials, Al_2O_3-Cr_2O_3 and $MgAl_2O_4$-Cr_2O_3, were designed to run at a surface temperature of 1625°C for an eight hour duration. They were attached to water-cooled copper using a silicon silastic. The refractories were pried off at the completion of the test and mounted for optical examination. Both materials revealed a very thin layer of slag deposited on its surface but there was no penetration through the surface. No slag interaction with either insulator could be detected. The only deleterious signs were the fractures running perpendicular to the surface in $MgAl_2O_4$-Cr_2O_3 and the slight crazing appearance of the microstructure in Al_2O_3-Cr_2O_3. These fracture pheonomena are probably the result of the fairly rapid cooldown utilized to preserve "at temperature effects" in the test channel and prevent condensation of seed and slag.

Attachment Techniques

A successful attachment technique was developed for bonding indium oxide doped hafnia current leadout material to nickel mesh, which is proposed for use in the

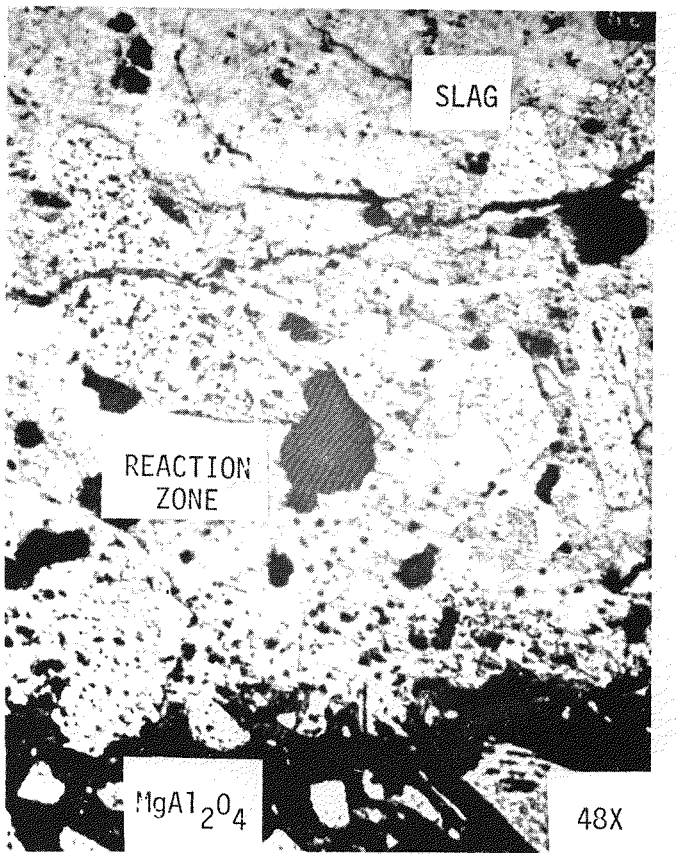

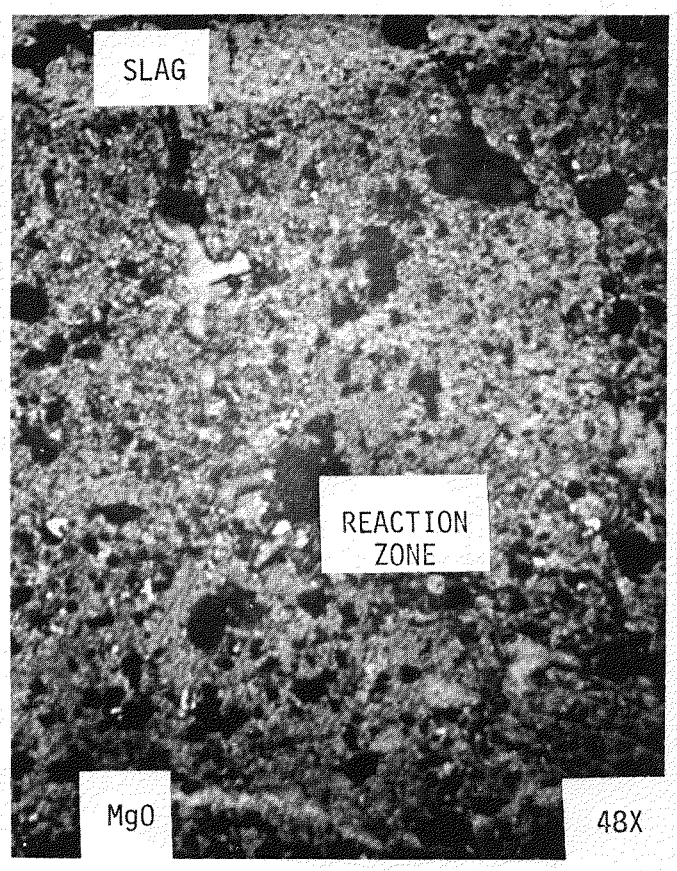

Figure 7. Slag Corrosion of $MgAl_2O_4$ and MgO Castables after 6 Hours at~1700° C

electrode structure for subsequent WESTF tests. A plasma sprayed layer of nickel, 2-3 mils thick, was first applied to the surface of the ceramic. The material was then brazed to the nickel mesh with a high temperature Cu-Ag braze for 1.5 minutes at 10^{-5} atm. A strong bond was achieved and there appeared to be total adhesion between the ceramic and mesh, as evidenced by the photomicrograph of the interface in Figure 8a. Several sample attachments were subsequently heated at 500°C (the proposed attachment design temperature) for 100 hours to observe any deterioration of the bond. No loss of bond strength was detected. A DC current ($1A/cm^2$) was finally induced through the attachment to simulate electrical power generation. A constant current was applied for 48 hours with no apparent detrimental effect on the bond.

An attachment method was also developed for the electrodes in WESTF Test 49, 0.5 $SrZrO_3$ - 0.5 ($Sr_{.25}La_{.75}FeO_3$) bonded to copper mesh. The initial bonding trials focused on trying to achieve a direct seal between the ceramic and metal mesh without the necessity of metallizing the ceramic surface. This met with little or no success. A plasma sprayed layer of copper was then applied to the ceramic prior to brazing. Very weak bonds were attained, principally due to the peeling away of the metallized layer. Subsequently, attempts were made to obtain a satisfactory attachment by sputtering a thin layer ($\sim$7 microns) of copper onto the ceramic and bonding with a high temperature copper-silver braze. The resultant bond, as shown in Figure 8b, was very strong and had good adherence throughout. The three electrode pairs to be tested in WESTF Test 49 will be attached in the manner just described. The list of brazing trials run on .5 $SrZrO_3$ · .5 ($Sr_{.25}La_{.75}FeO_3$) is tabulated in Table 4.

The attachment techniques developed for electrode system have not always resulted in an optimum bond being used. As a result, there has been speculation that attachment failures, rather than material failures, could have been a cause of unsuccessful electrode material testing in the past. To eliminate some of the concern, a more systemmatic study of bonding techniques, especially where ceramic to metal joints are involved, will be initiated. The investigation will include the development of a secure bonding technique for each individual ceramic/metal

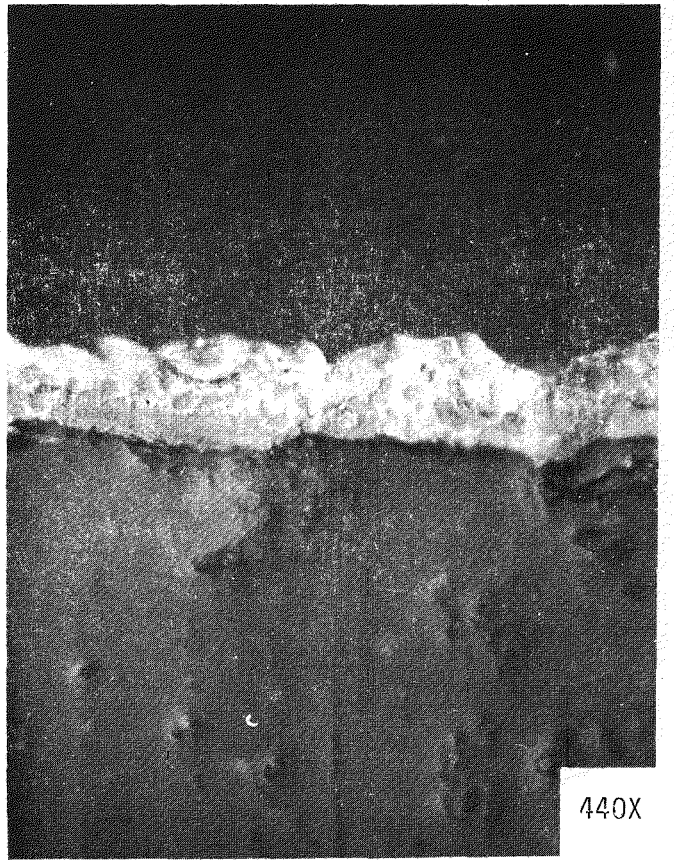

(A) 30 m/o In_2O_3 · 20 m/o $PrO_{1.8}$
3.0 m/o Yb_2O_3 · 47 m/o HfO_2
Bonded to Nickel Mesh

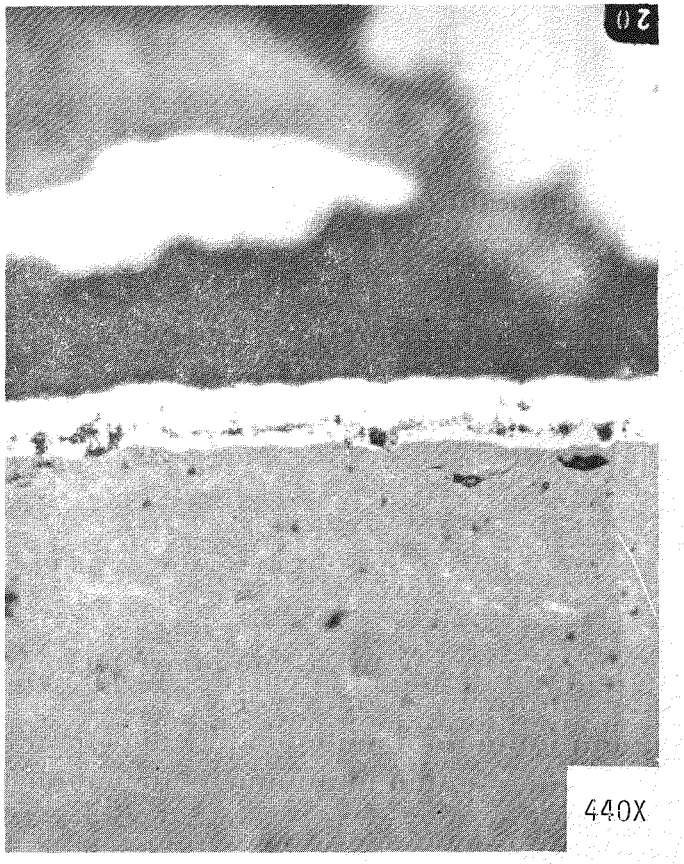

(B) 0.5 $SrZrO_3$ · 0.5 $(Sr_{.25}\ La_{.75}\ FeO_3)$
Bonded to Copper Mesh

Figure 8. Ceramic to Metal Mesh Attachment

TABLE 4

ATTACHMENT CONDITIONS AND RESULTS FOR BONDING

0.5 $SrZrO_3$ - 0.5 $(Sr_{0.25}La_{0.75}FeO_3)$* to Copper Mesh

TRIAL	CERAMIC PREPARATION	BRAZE	BONDING PARAMETERS TEMP. (°C)	TIME(Min.)	Atm.	REMARKS
1	None	TICUSIL	850	3.5	10^{-5}	Very weak bond, slight pull caused attachment failure.
2	None	Cu-Ag	779	3.5	10^{-5}	Weak bond, not good wetting of ceramic.
3	2 mil thick plasma sprayed Cu applied to surface	Cu-Ag	779	3.5	10^{-5}	Weak bond, sprayed layer doesn't appear to adhere well.
4	2 mil thick plasma sprayed Cu applied to surface	Cu-Ag	779	2.0	10^{-5}	Shorter brazing time doesn't seem to remedy peeling of plasma sprayed copper.
5	2 mil thick plasma sprayed Cu applied to surface	Cu-Ag	779	30 sec.	10^{-5}	Still very weak bond, plasma sprayed copper won't adhere to ceramic with any regularity.
6	7 micron thick sputtered Cu applied to surface	Cu-Ag	779	2.5	10^{-5}	Very good bond achieved, manual pulling does not effect attachment.
7	7 micron thick sputtered Cu applied to surface	Cu-Ag	779	2.5	10^{-5}	Very good bond achieved, manual pulling doesn't disrupt bond.

*Material processed and supplied by Massachusetts Institute of Technology, Dr. R. Cannon.

system. The reliability of a particular bonding method will be evaluated from micro-optical examination, along with tensile testing of the joint.

1.1.2 Material Characterization

Thermal Conductivity

The thermal conductivity of four ceramic electrode materials to be run in future WESTF tests were redetermined by BPNL. These materials included 0.5 $SrZrO_3$ · 0.5 ($Sr_{.25}La_{.75}FeO_3$), to be run in WESTF Test 49, and .28 $PrO_{1.83}$ - 0.5 Yb_2O_3 · .67 HfO_2, .06 $Tb_4O_7Y_2O_3$·.07Y_2O_3·.87 HfO_2, and .30 In_2O_3·.20 $PrO_{1.83}$·.03 Yb_2O_3· .47 HfO_2, compositions to be run in a subsequent WESTF test. The thermal diffusivities were measured by BPNL using a laser pulse technique from near room temperature to temperatures up to 1600°C. The thermal conductivity, given in Figures 9 through 12, was calculated from the thermal diffusivity, room temperature density, thermal expansion and the specific heat.

The data taken on cooling was used to draw the curves. This data will be used in sizing the electrodes to satisfy their appropriate test conditions. The thermal conductivity of a fourth electrode composition, .43 In_2O_3 · .03 Tb_4O_7 · .04 Y_2O_3 · .50 HfO_2 (MMM), is presently being measured at BPNL.

Electrode Materials

Subsequent WESTF tests using the MTS II test section will incorporate hafnia based compositions which will be graded to different oxide current leadouts. Specifically, the compositions are:

Composition	BPNL Identity	Sintered Density (g/cc)
$.28PrO_{1.83}·0.5Yb_2O_3·.67HfO_2$	A	8.10
$.06Tb_4O_7·.07Y_2O_3·.87HfO_2$	B	8.26
$.30In_2O_3·.20PrO_{1.83}·.03Yb_2O_3·.47HfO_2$	LLL	8.15
$.43In_2O_3·.03Tb_4O_7·.04Y_2O_3·.50HfO_2$	MMM	---

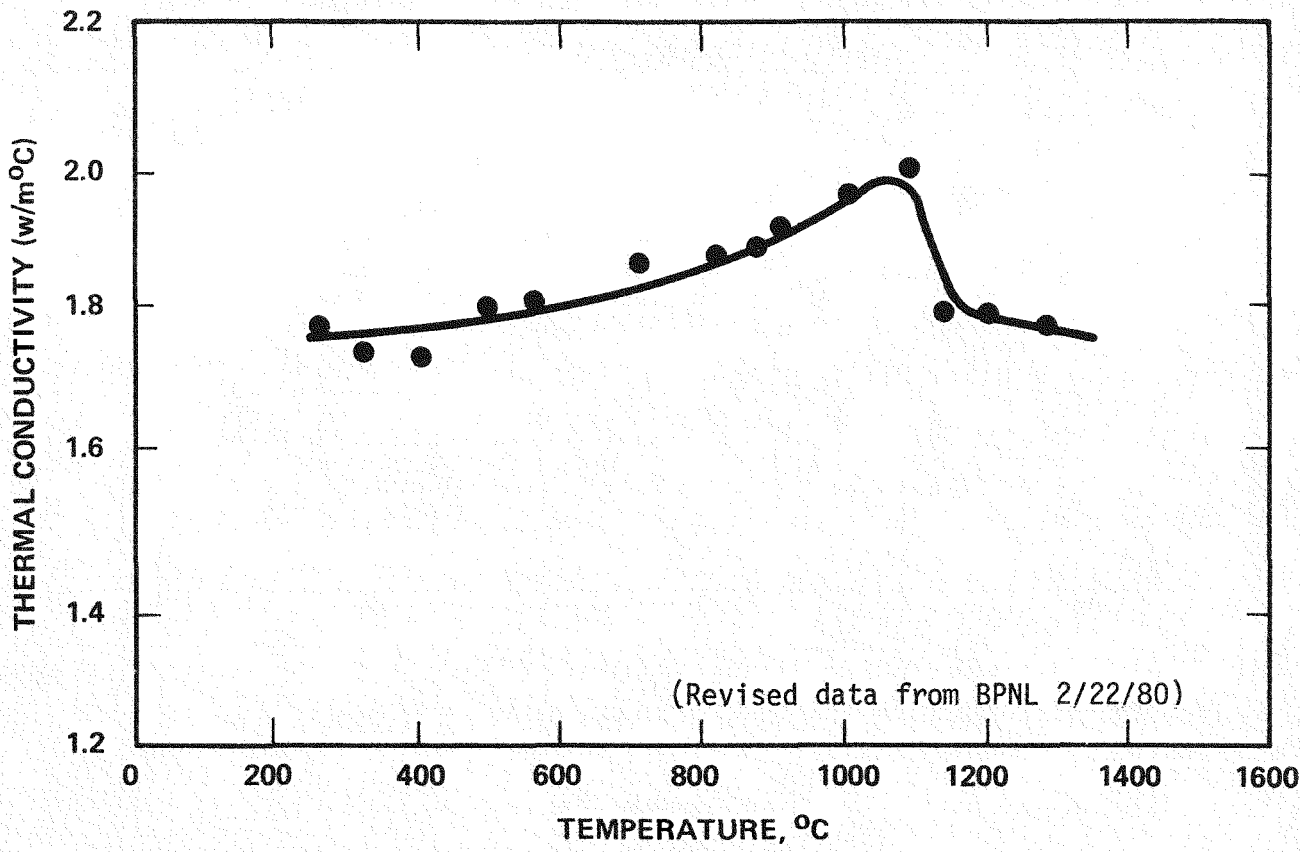

Figure 9. Thermal Conductivity of 0.5 $SrZrO_3$·0.5 ($Sr_{.25}$ $La_{.75}$ FeO_3)

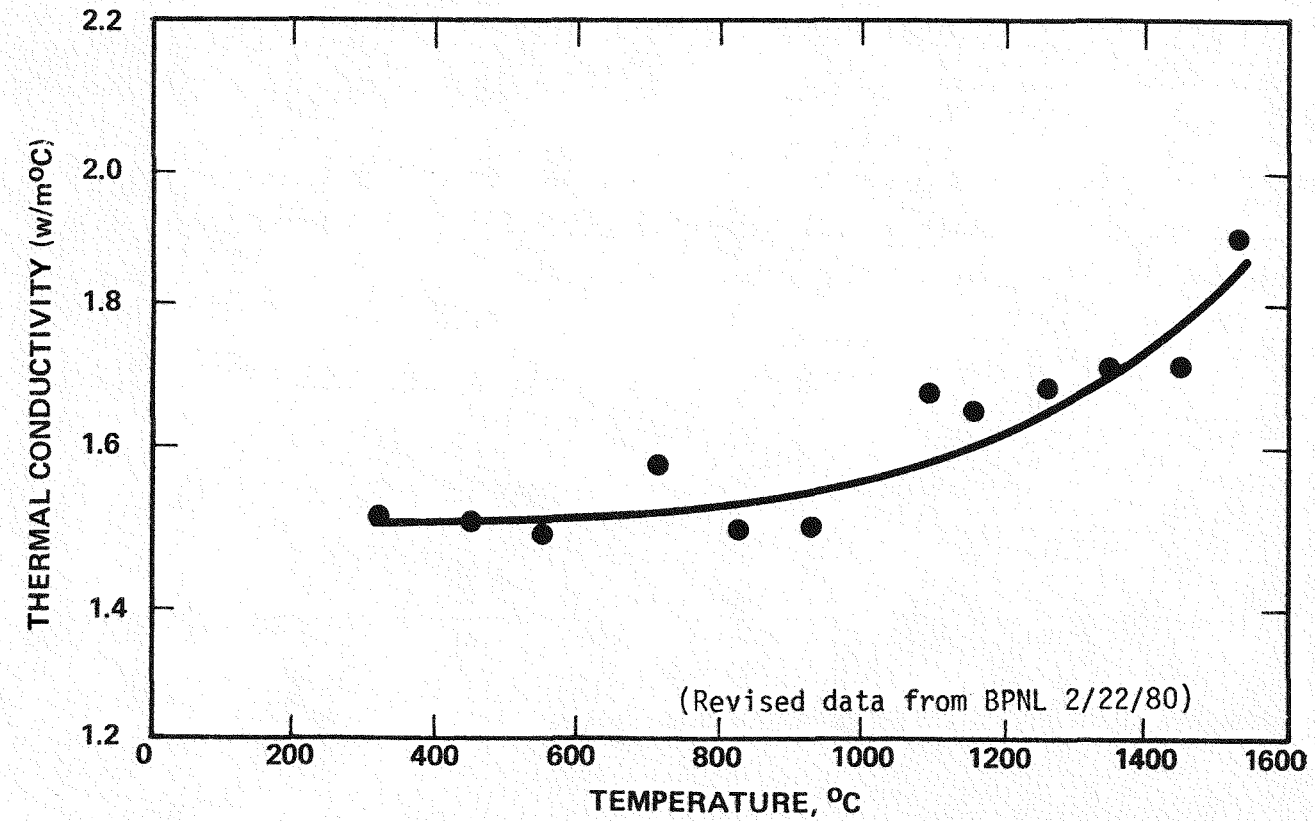

Figure 10. Thermal Conductivity of .28 $PrO_{1.83}$·.05 Yb_2O_3·.67HfO_2 (Hafnia 'A')

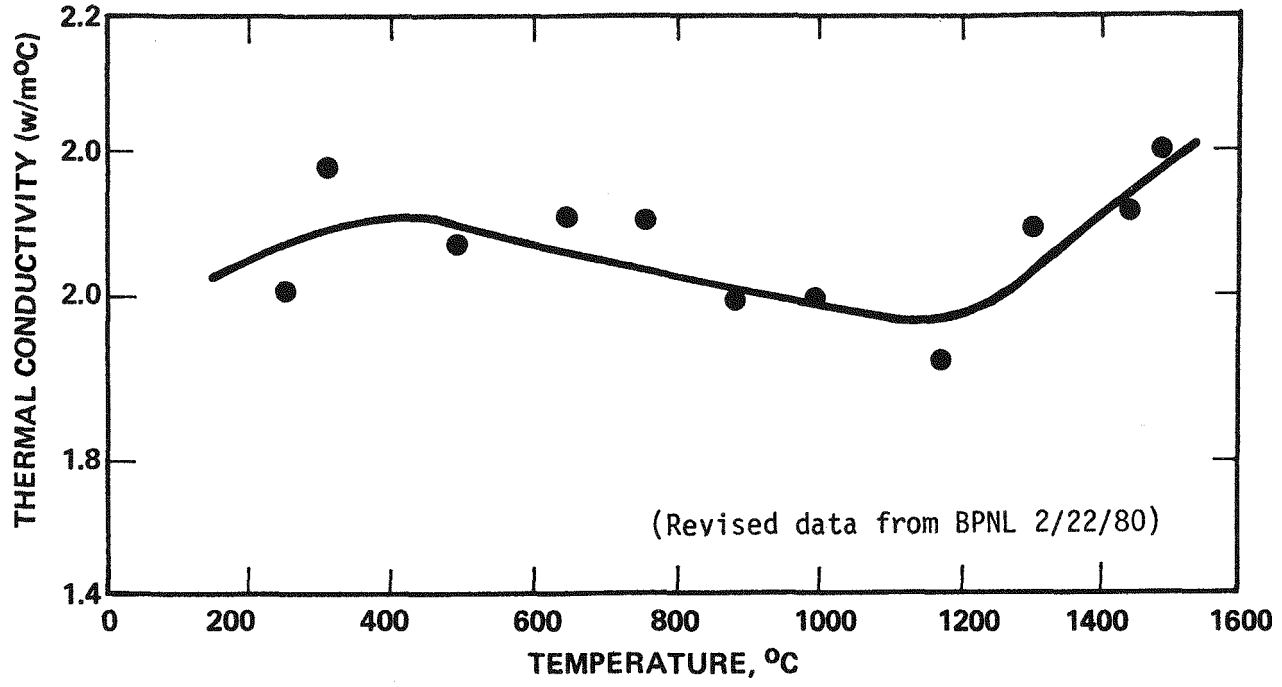

Figure 11. Thermal Conductivity of .06$Tb_4O_7$$Y_2O_3$·.87 HfO_2 (Hafina 'B')

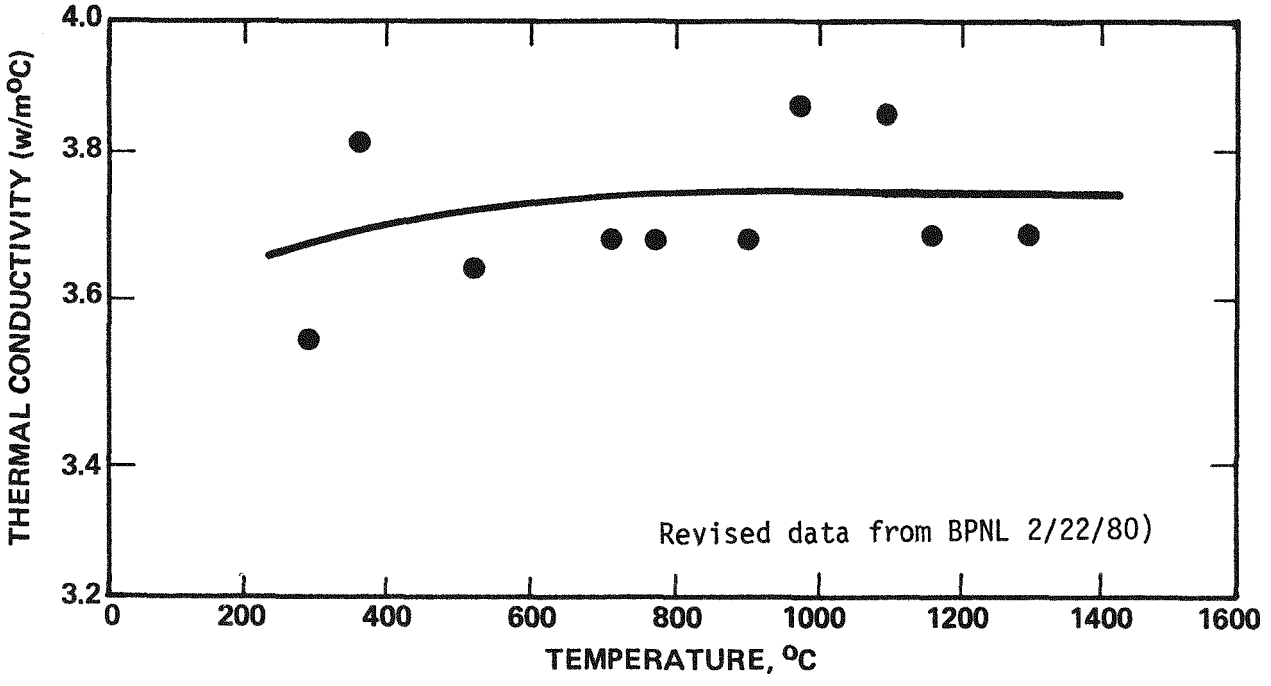

Figure 12. Thermal Conductivity of .30 In_2O_3·.20 $PrO_{1.83}$·.03Yb_2O_3·.47HfO_2 (LLL)

The two leadout materials, LLL and MMM, contain a large percentage of In_2O_3 to increase the low temperature electrical conductivity. All four compositions were fabricated from powders which were processed by a coprecipitation technique. The powders were then cold pressed and sintered at ~1600°C for up to 20 hours to obtain densities up to 98% of theoretical. Because of the thermal expansion coefficient difference between the leadout materials and the base compositions it was necessary to press and sinter 'sandwich' discs as shown in Figure 13. The base material, A or B, was pressed between a leadout layer of either LLL or MMM. This sandwich effect eliminates bowing and cracking at the interface caused by stress build-up from shrinkage differences. After determining the right electrode thicknesses for the design conditions, the discs can then be ground to eliminate one of the leadout layers.

1.2 WBS 1.1.2 - Laboratory Screening Tests

1.2.1 Electrochemical Corrosion Tests

Polarization Measurements

Polarization measurements of Western coal slags modified with Fe_2O_3 additions with 304 stainless steel electrodes were made using a technique similar to that described earlier (Reference 3). The major difference between these most recent tests and the earlier tests were that the electrodes were immersed only about 1/2" into the molten slag bath compared to the 1" depth previously used.

Tests were run at about 1350°C, in W-50 Rosebud slag (Reference 7) containing 10 w/o K_2O to which various amounts of Fe_2O_3 were added. The concentration of iron oxide given in terms of Fe_3O_4 content in the slag is presented in Table 5. The results of these tests are given in Figures 14 and 15 and Table 5.

The overall shape of the polarization curves in Figures 14 and 15 are similar to those obtained earlier when the role of Co_3O_4 additives in slag was investigated. In all cases, there is a tendency for ohmic (linear current - voltage behavior) or electronic conductivity at the cathode at low current density and non-ohmic or ionic conductivity at high current density. The opposite relationships occur at the anode. The effect of iron on slag polarization at the cathode is manifested in two ways. With increasing Fe content, there is a marked decrease in "mean

Figure 13. Hafnia Based Electrodes with Oxide Current Leadouts

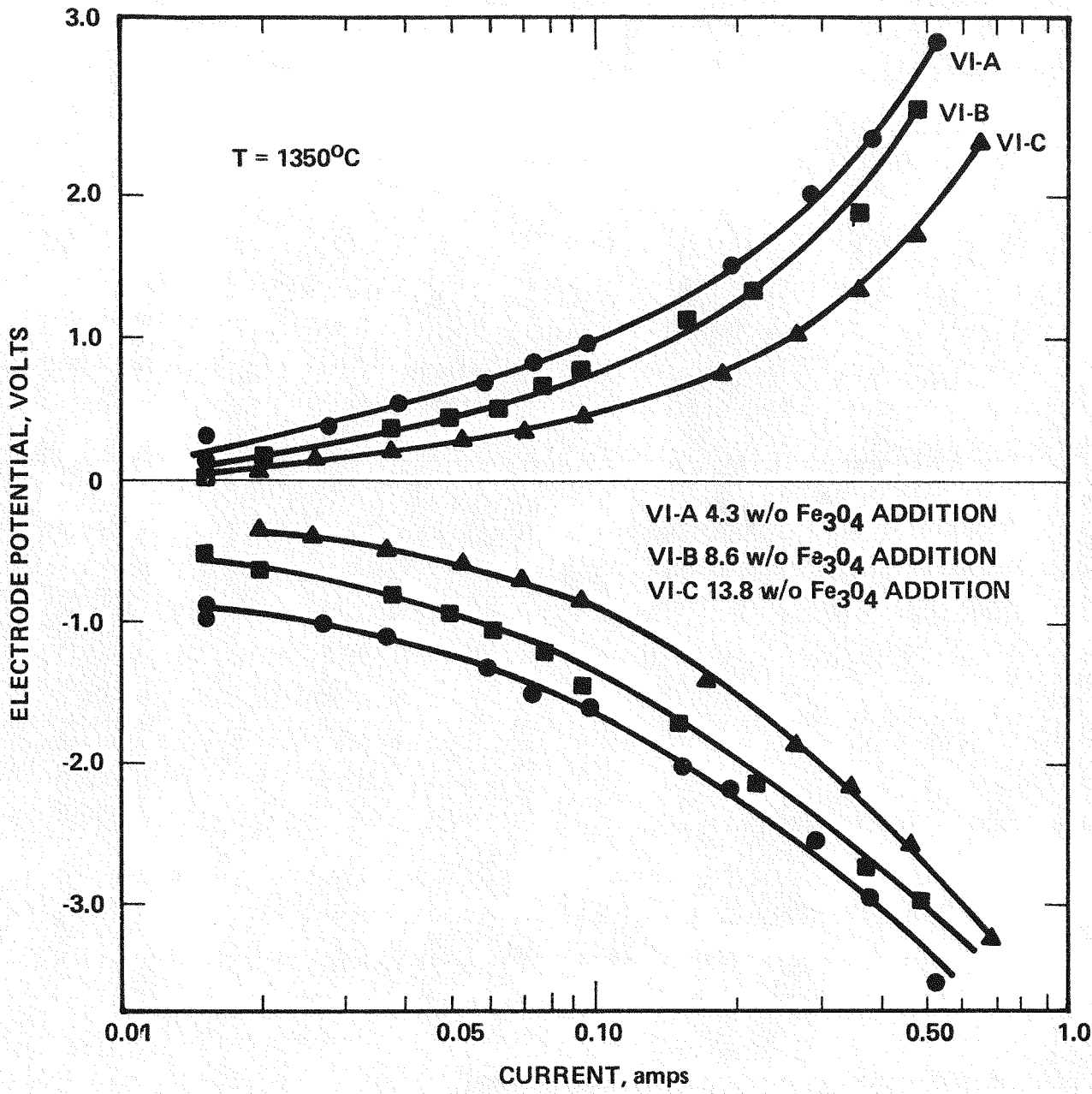

Figure 14. Electrode Polarization of 304 Stainless Steel in Fe_3O_4 Modified Rosebud Slag

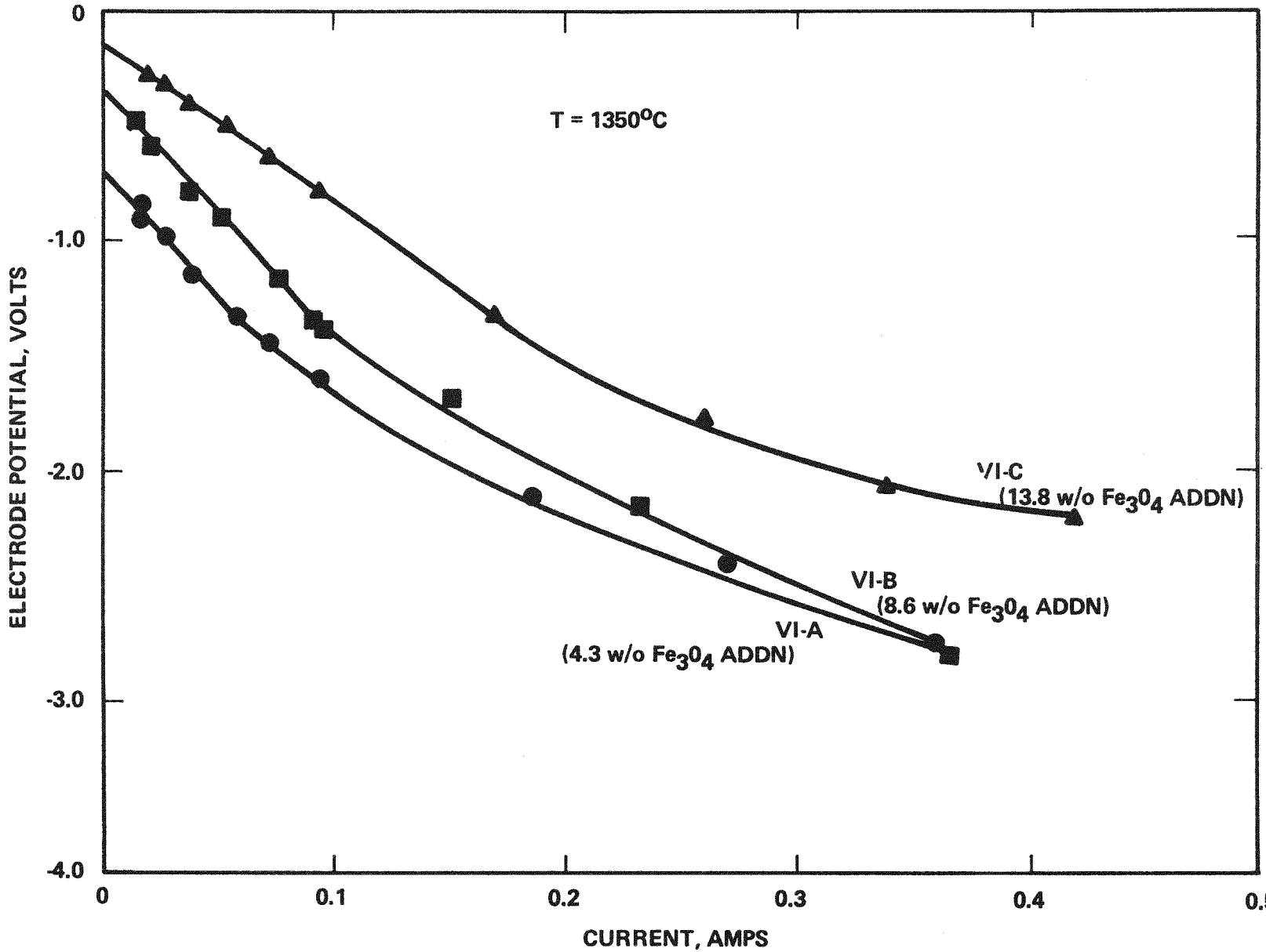

Figure 15. Cathode Polarization Curves for Rosebud Slag with Fe_3O_4 Additions. 304 SS Electrodes

TABLE 5

POLARIZATION OF STAINLESS STEEL 304 CATHODE IN W-50 ROSEBUD SLAG* WITH Fe_3O_4 ADDITIONS

RUN ID	Fe_3O_4 ADDITIONS w/o	m/o	MEAN RESISTANCE CATHODE, Ω	CRITICAL RESISTANCE CATHODE, Ω
V1-A	4.3	1.2	21.1	29
V1-B	8.6	2.6	15.4	14.6
V1-C	13.8	4.4	7.9	7.8

*10 w/o K_2O

resistance", $\bar{R}$ ($\Delta E/\Delta I$) in the ohmic or electronically conducting portion of the polarization curve (Figure 15) and there is a decrease in R_c (E/I), the "critical resistance" at which the conduction mechanism changes from electronic (linear) to ionic (semilogarithmic). This data is summarized for the cathode in Table 5. $\bar{R}$ is a measure of the change in total electrical resistivity of the slag while R_c reflects changes in both the total resistance as well as the electronic contribution to the resistivity of the slag. Therefore, these results conservatively imply that the total conductivity and perhaps as well the electronic transference number of the slag, increase about 2.5 fold when 4.3 m/o Fe_3O_4 is added to a Western Rosebud slag.

Figure 16 is a plot of normalized mean conductance ($1/\bar{R}$) versus mole percent Fe_3O_4 and mole percent Co_3O_4 (Reference 3) in W-50 Rosebud slag. These results indicate that iron oxide additions are equally as effective as Co_3O_4 (at least at low concentrations) in minimizing polarization and electrical resistance of molten slags. Since iron oxides are at least 20 times less expensive than cobalt oxides, great economies can be obtained if Fe_3O_4 is used as an additive to minimize the electrochemical stresses (ECS) in coal slags.

1.2.2 Anode Arc Erosion Studies

In preparation for further use of the anode arc test rig in the screening of slagging cold electrode materials, the general test methodology is being reviewed to improve the effectiveness of this laboratory screening test.

A major problem has been in developing suitable methods of applying the corrodent (slag and/or seed) to the surface of the test samples such that it would not be blown away by the action of the arc. Earlier studies have used water based slurries of slag/seed which were painted on the sample surface. However, it was clear that large portions of the energy of the arc were dissipated in evaporating the water vehicle. Furthermore, water is a polar fluid and hence its presence could artifically accelerate electrochemical type reactions.

New studies have linked at using non-polar glycerin and glycols as the slurry vehicle, but these fluids also tend to dissipate the energy of the arc. Recently,

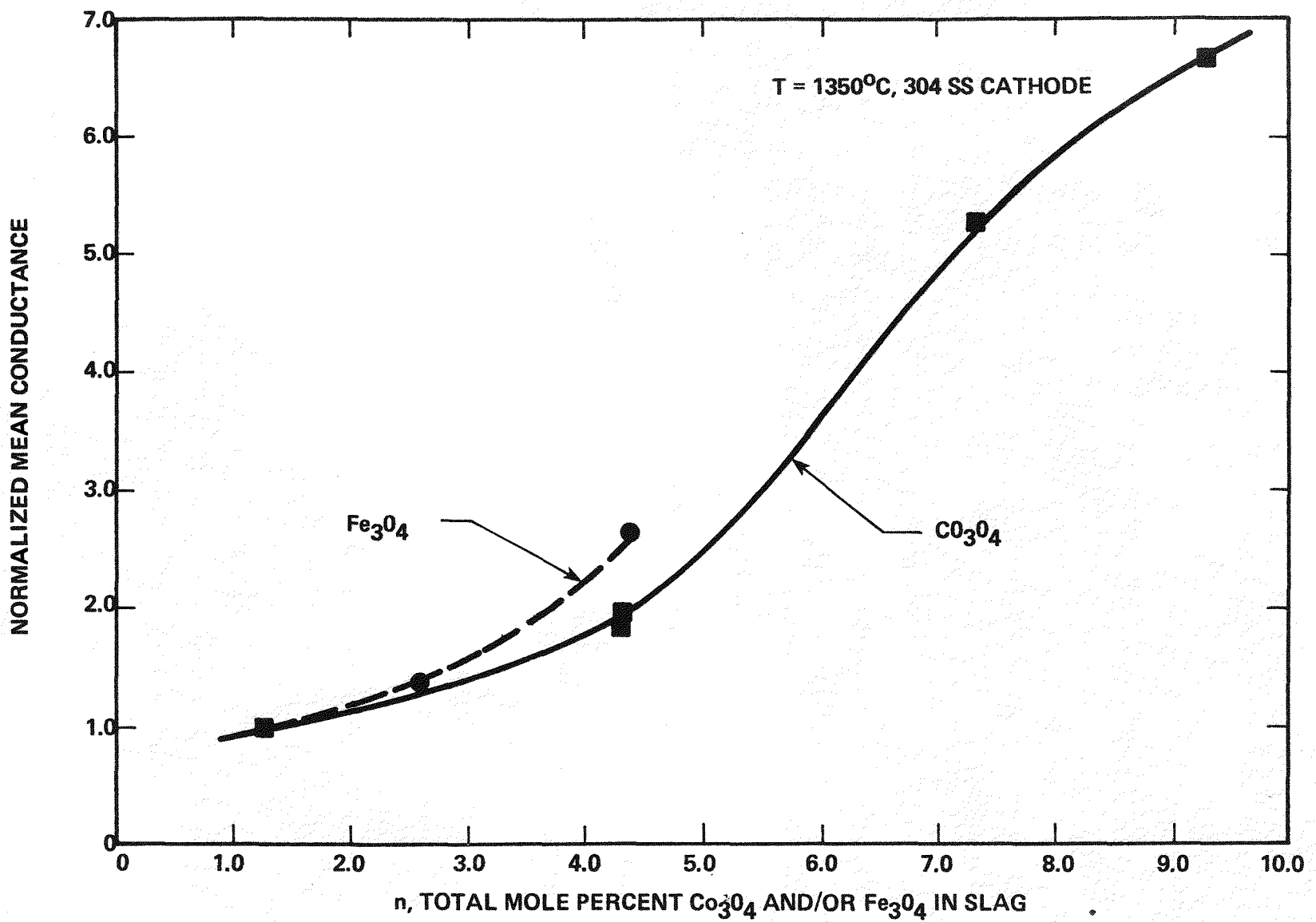

Figure 16. Effect of Transition Metal Oxides or Normalized Mean Conductance ($1/\bar{R}$) of Rosebud Slag at Cathode

a new technique has been developed which may haye considerable promise. It has been found that when the flame of an oxy-acetylene torch is used to heat the sample, dry powder corrodents which are dusted on the sample surface become "sticky" enough to adhere. Then when the arc impinges on the sample, the corrodent remains in place and a reasonably good facsimile of arc accelerated corrodent attack seems to be attained. Investigations are continuing as to whether this new torch-arc impingement test can simulate the arc corrosion morphology obtained under actual channel conditions.

2.0 WBS 1.2 - ENGINEERING TESTS

2.1 WBS 1.2.1 - Test Engineering

2.1.1 Development Requirements

During this quarter, Test Specifications were issued for WESTF Test 47 (Final) and WESTF Test 49 (Preliminary and Final). During the prior quarter, Preliminary Test Specifications had been issued for the following WESTF Tests:

- WESTF Test 44 - Hafnia electrodes (WESTF II)
- WESTF Test 46 - Insulating materials (Non-slagging super-hot)
- WESTF Test 48 - Insulating materials (Non-slagging super-hot)
- WESTF Test 50 - Hafnia electrode materials (MTS II).

These tests will be redefined and redesignated in view of the basic change in emphasis in WESTF testing.

WESTF Test 47

The Final Test Specification for WESTF Test 47 was issued. This test provided for the evaluation of the performance of platinum clad copper in a slagging cold, western slag, environment. An important objective of this test was to provide for the initial operation and checkout of the Type II Materials Test Section (MTS II).

The Type II Materials Test Section consists of a water cooled stainless steel casing lined with a refractory castable insulation and fitted with three removable water cooled electrode/insulator assemblies on both the anode and cathode walls.

The electrode surface exposed to the slag/plasma is 0.75 in. diameter (0.442 in^2) and is contained within a cylindrical boron nitride (lava on the cathode side) insulator with a 0.25 in. wall thickness. The anode wall will consist of 0.010 in. platinum clad copper electrodes. The cathode electrodes will be run without any cladding or coating.

The test section instrumentation includes two Ir/Rh thermocouples, one positioned in the gas stream that can be retracted and one imbedded in the 0.3 in. thick castable insulation. These are both located in the top insulating wall in relation to the channel. In addition, the center cathode electrode was designed with a sight port for viewing the surface of the Pt clad anode electrode.

WESTF Test 49

The objective of WESTF Test 49 was to evaluate the performance of 0.5 $SrZrO_3 \cdot 0.5$ ($Sr_{.25}La_{.75}FeO_3$) processed and supplied by MIT in a non-slagging super-hot MHD environment.

The testing will use the Type II Materials Test Section (MTS II). The electrode surface exposed to the slag/plasma is 0.75 in. diameter (0.442 in^2) and is contained within a cylindrical MgO insulator with a 0.25 in. wall thickness. The cylindrical insulator extends 0.407 inches from the electrode surface and then is replaced by boron nitride insulation underneath. Both the anode and cathode walls will consist of discs of 0.5 $SrZrO_3 \cdot 0.5$ ($Sr_{.25}La_{.75}FeO_3$) (0.257 inches thick) brazed to copper mesh (0.062 inches thick, 40% dense) which, in turn, is brazed to water-cooled copper. The ceramics have been sized to achieve the average design surface temperatures in mid-position of 1700°C for the electrode and 1550°C for the insulator.

The test section instrumentation includes two Ir/Rh thermocouples, one positioned in the gas stream that can be retracted and one imbedded in the MgO insulation. Both are located in the top insulating wall in relation to the channel. In addition, a Type S thermocouple, sheathed in Inconel 600, was positioned in each ceramic electrode 0.157" from the plasma surface.

2.1.2 Experiment Design

The design of the WESTF II test section is being revised in accordance with the emphasis to be given to the development and evaluation of slagging cold metallic electrodes. The primary constraint on the design of the test section has been the available space within the magnet bore. The flow passage dimensions have been established at 1.25 x 1.80 in., which includes an assumed slag layer thickness of approximately 2 mm (0.080 in.).

In order to improve the electrical performance of the insulating walls (sidewalls) and to provide better access for the viewport, which will be used to observe slag formation and movement, as well as arcing phenomena, the 1.80 inch dimension was selected as that which characterizes the electrode separation. This will provide improved electrical performance of the sidewall and will maximize the viewing depth into the test section.

The following sections discuss the design of the view-port, and the redesign of the MTS II and WESTF II test sections.

MTS II Viewport

A viewport has been designed to fit directly downstream of the Materials Test Section (MTS II). This sightport allows one to view the entire surface of one of the downstream electrodes in the MTS. Such phenomena as slag flow across the electrode face and non-uniform current transfer (arcing) can then be observed during the course of a test run.

The viewport, as shown in Figure 17, consists of a 19 inch long stainless steel pipe with a 5.5 inch inside diameter. Extending from this pipe at a 20° angle is a lateral sighting arm with a 2.5 inch inside diameter. The angle and position

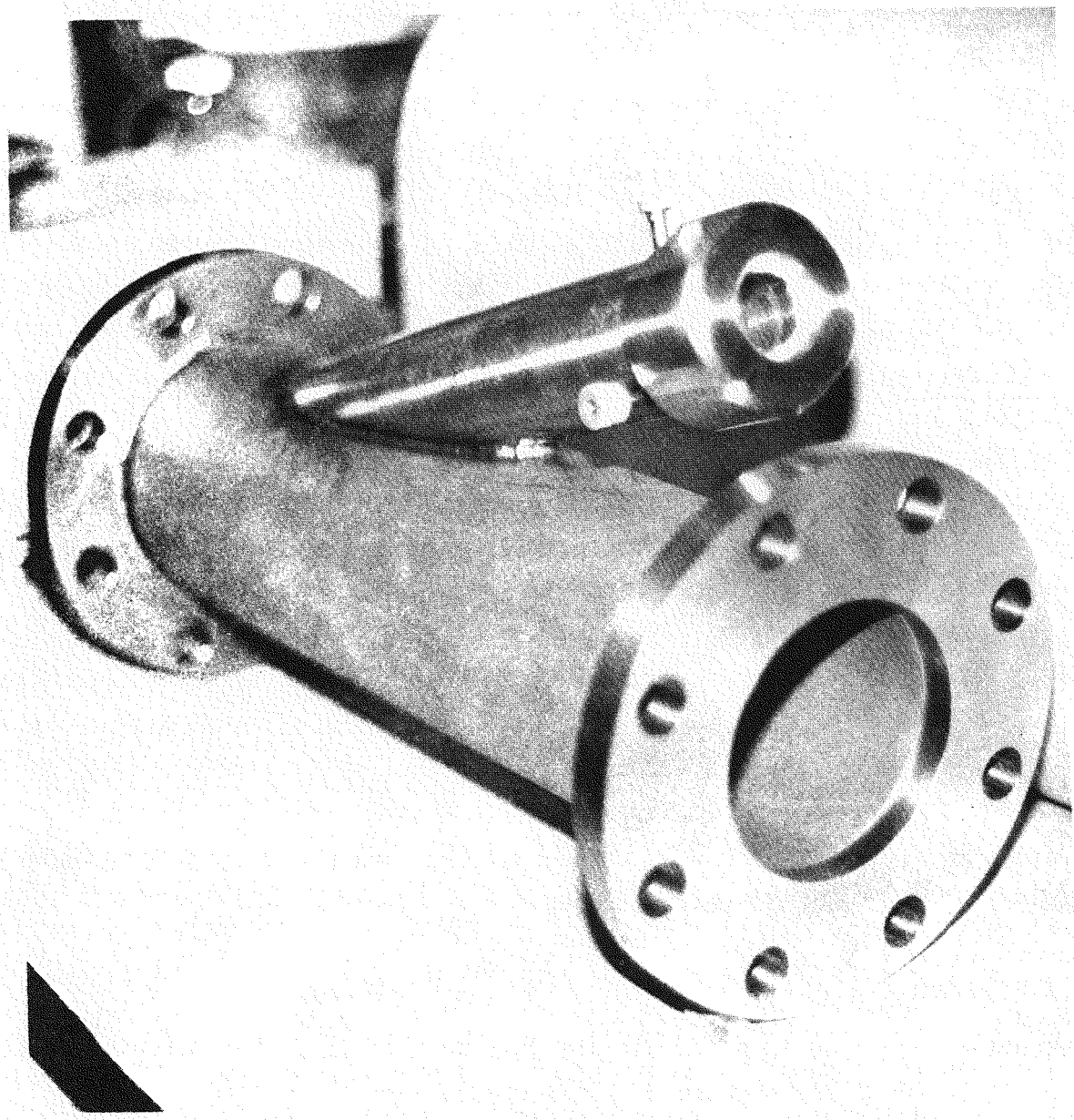

Figure 17. MTS II Viewport

of the sight tube is such that a limited amount of plasma and/or slag/seed will travel up the arm. The end of the viewport has a threaded stainless steel cap which supports a 3/8 inch thick quartz window. A fitting was provided for introducing an inert gas into the viewing arm to eliminate any film buildup on the window. In addition, a manually operated metal shutter, as shown in Figure 18, was installed to insure against any large slag particles from hitting the quartz when the viewing port is not in use. The vessel was designed so that magnesia castable could be applied to the inside of both pipes for insulation. In addition, a water jacket surrounding the vessel is needed to transfer the heat.

MTS II Test Sections

Due to the selection of new channel dimensions, as discussed above, two new materials test sections are being designed to replace the Type II Materials Test Section previously defined (Reference 3). The decision was made to design separate cold wall and hot wall test sections due to the realization that a single test section could not adequately satisfy all test conditions. Because refabrication was necessary it was also deemed desirable to reorient the electrodes to facilitate the use of the viewport discussed above. The reorientation consisted of placing the electrodes in the narrow walls to maximize the channel dimension controlling the viewing depth.

The slagging cold wall Material Test Section (MTS Cold), shown schematically in Figure 19, consists of a stainless steel shell which is internally water cooled. The channel walls contain 0.125 inch by 0.125 inch transverse grooves with a 0.375 inch pitch. These grooves are filled with a castable ceramic to assist in the formation of a slag coating.

The hot wall Material Test Section (MTS Hot), shown schematically in Figure 20, also consists of stainless steel and is internally water cooled. Its channel walls are lined with Norton MgO and castable ceramic in the configuration shown. The Norton MgO, with its high purity, is used to reduce the effects of contaminants that would be carried on to the electrodes if the upstream walls were composed of castable ceramic.

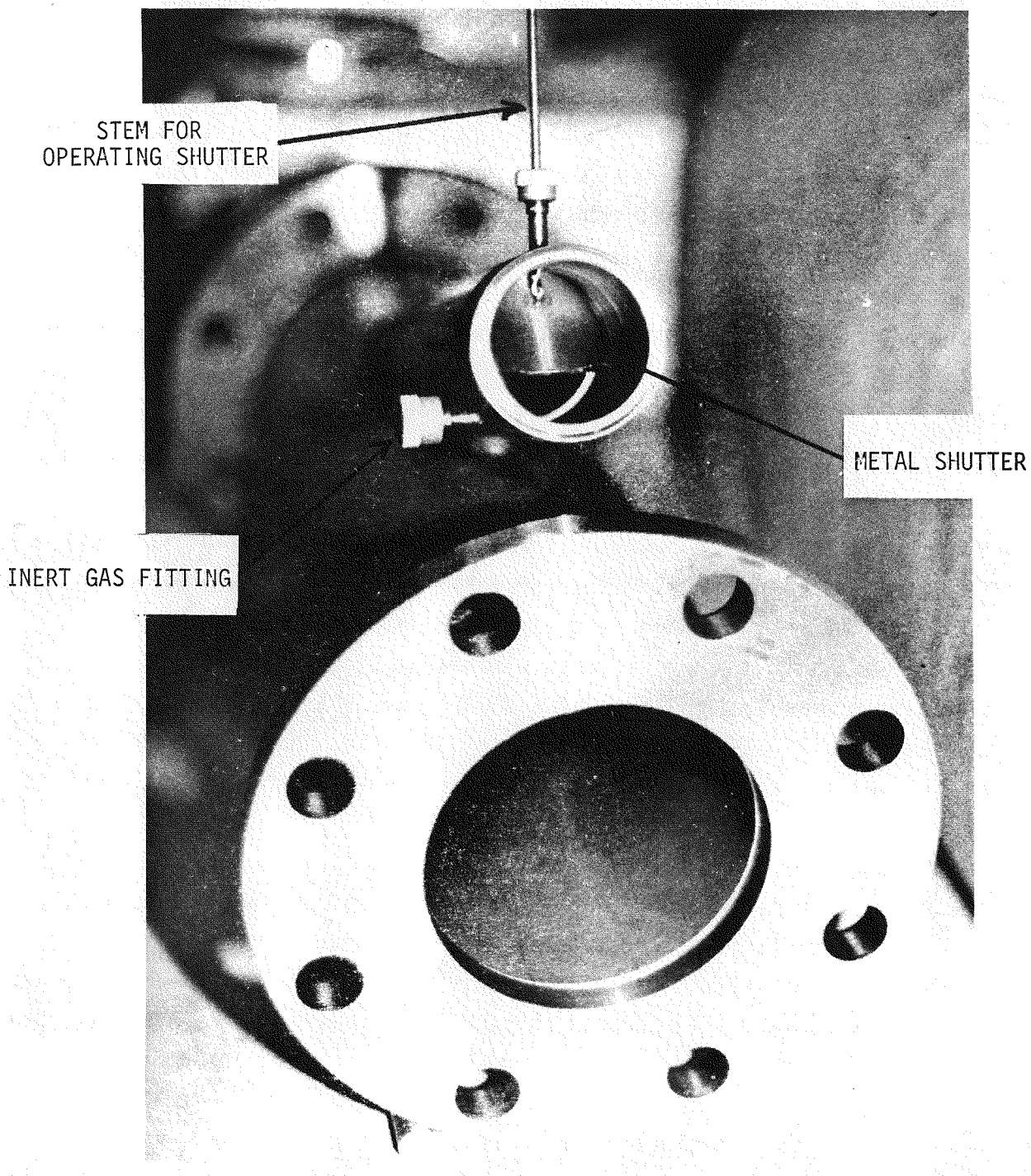

Figure 18. View of Manual Shutter in The MTS II Viewport

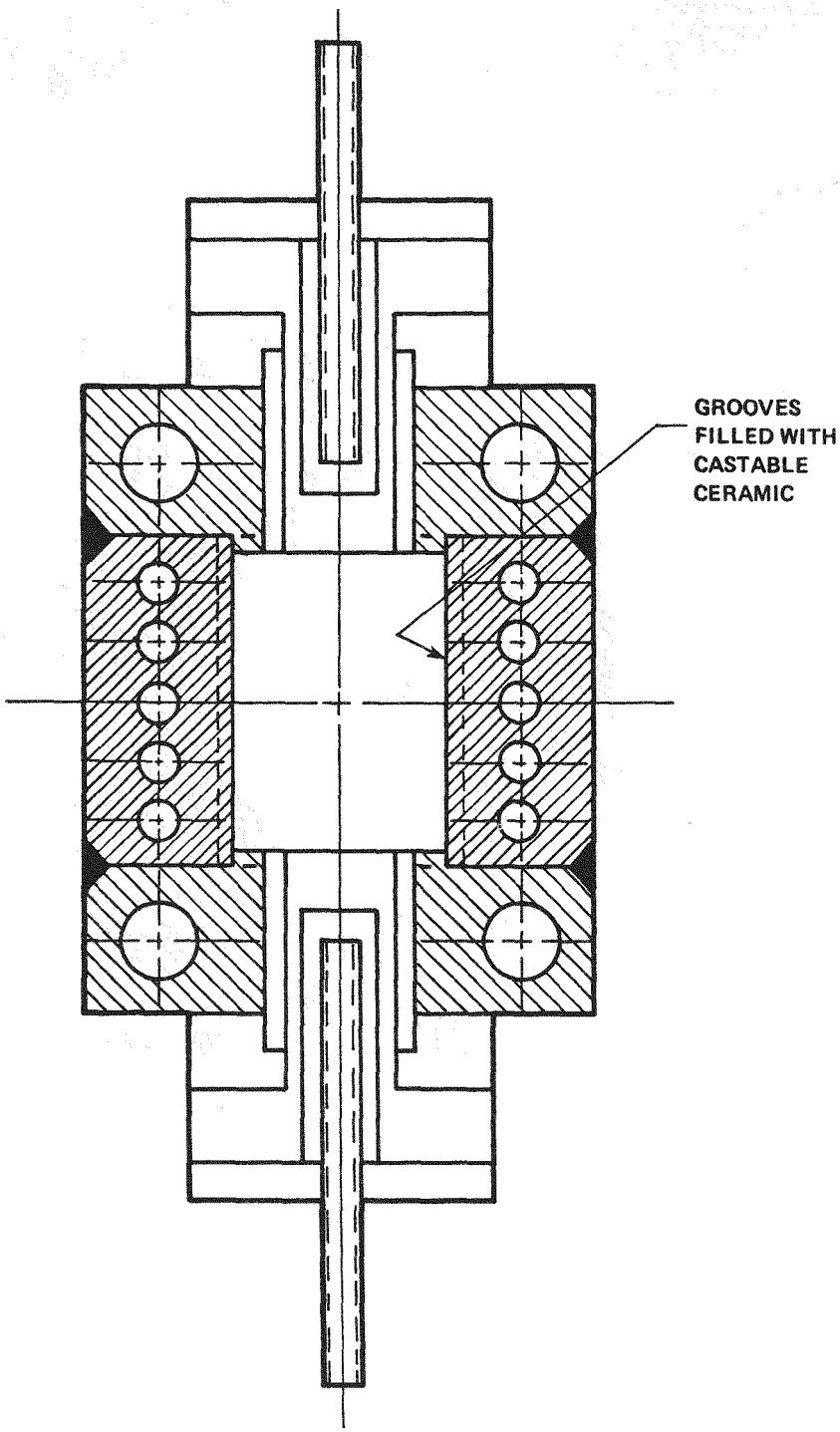

Figure 19. Cold Wall MTS II

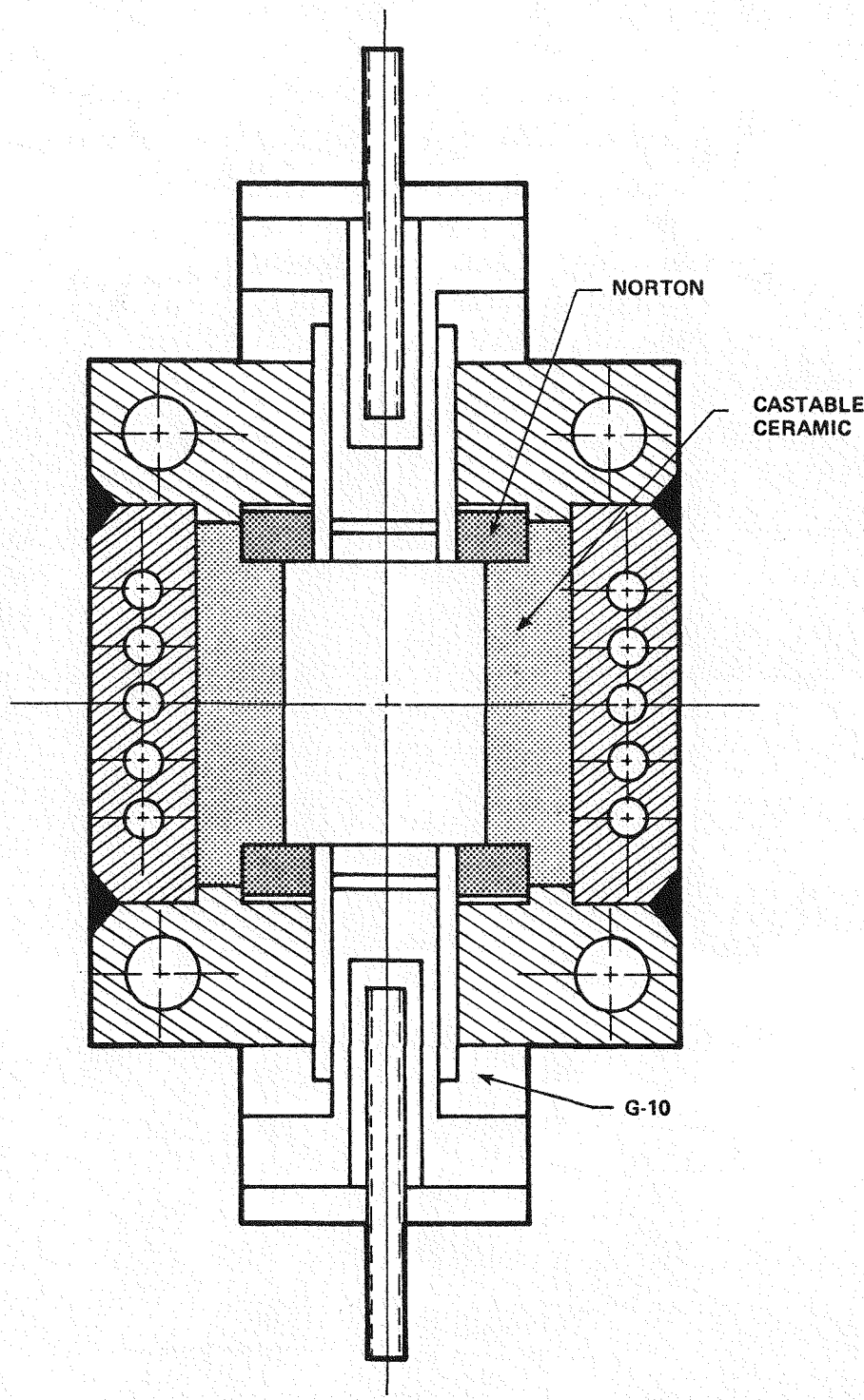

Figure 20. Hot Wall MTS II

The electrodes (four pair maximum) are similar to those previously used. The electrodes are surrounded by 0.125 inch thick insulators to aid in removal and electrically isolate the samples. The thickness of the insulators was reduced to accommodate the changes in channel dimensions and orientation of the electrodes.

MTS II Thermal Model

The type II Materials Test Section (MTS II) is intended for use as a general purpose test bed for screening tests of electrode materials in WESTF in the absence of magnetic field effects. Figure 21 is a schematic representation of MTS II which will be used to test materials in the slagging hot and non-slagging super-hot operating modes. The test section consists of a refractory lined water-cooled casing which contains three removable water-cooled electrode/insulator sample assemblies on both the anode and cathode walls. The MTS II configuration to be used for the screening of slagging cold electrodes is essentially the same as the above. The primary difference is that a continuous refractory lining is not used, but rather the metal liner contains shallow grooves which are oriented transverse to the direction of plasma flow. These grooves are filled with a castable refractory which functions to promote slag adherence.

General equations have been developed for the thermal analysis and sizing of the sample disk, primary insulator and the channel liner. These equations reflect the use of one-dimensional analyses and are based on the general MTS II configuration shown in Figure 22. The sample is a cylindrical disk which is attached via a suitable attachment technique to a copper water jacket; frequently, this attachment is achieved using an intermediate metallic mesh. The sample disc and copper base is surrounded along its height by a cylindrical insulator. In order to achieve the desired insulator plasma side surface temperature, and at the same time thermally protect the epoxy spacer, the space behind the primary insulator is filled by a secondary insulator. Both the sample disc and the insulator(s) are cooled by water flowing into the copper jacket via the water delivery tube.

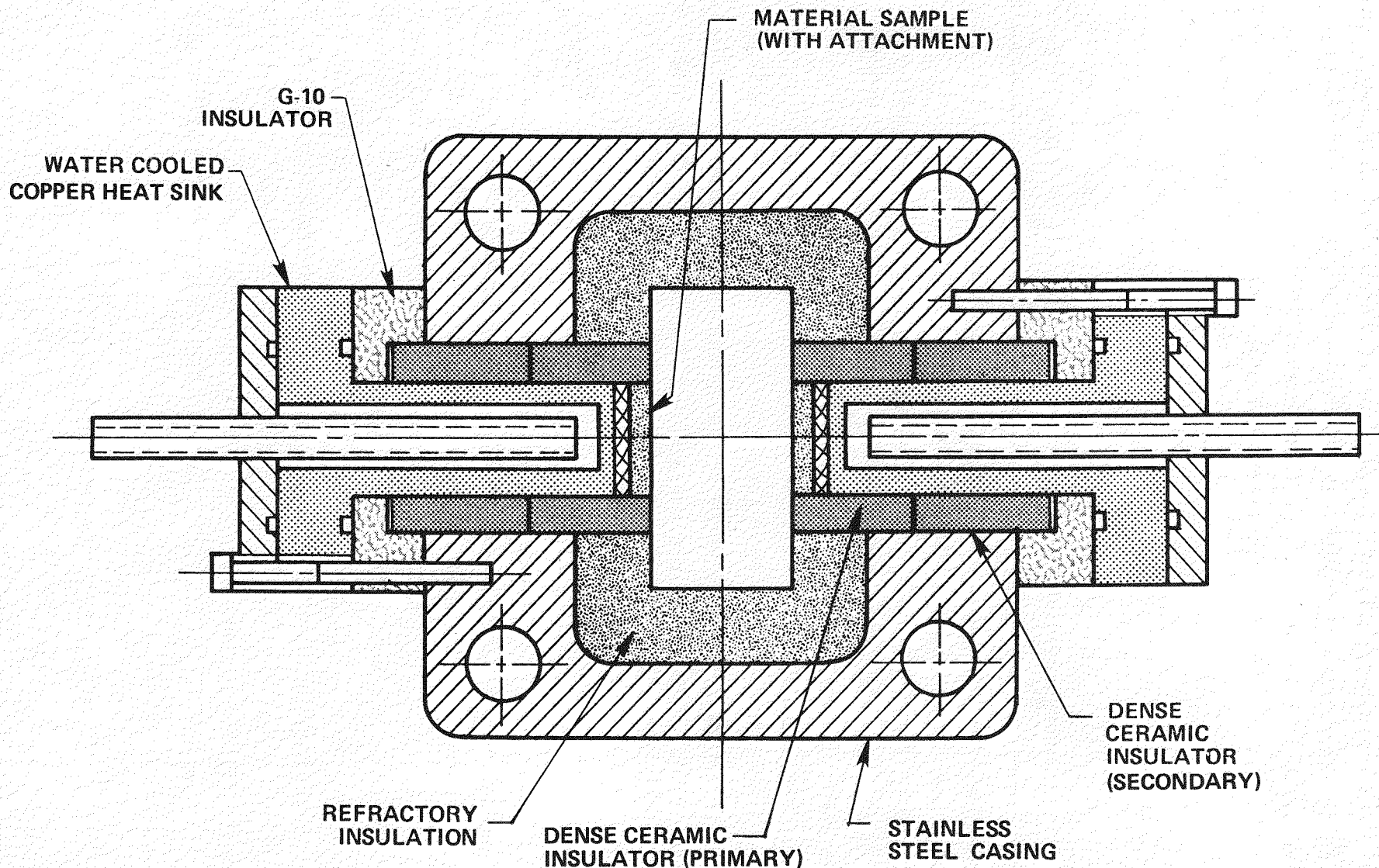

Figure 21. Type II Materials Test Section Schematic

1. Sample Disk
2. Mesh
3. Copper Water Jacket
4. Primary Insulator
5. Secondary Insulator
6. Channel Liner
7. Shim
8. Wall of Test Shell
9. Spacer
10. Water Delivery Tube
11. Coolant (water) Channel

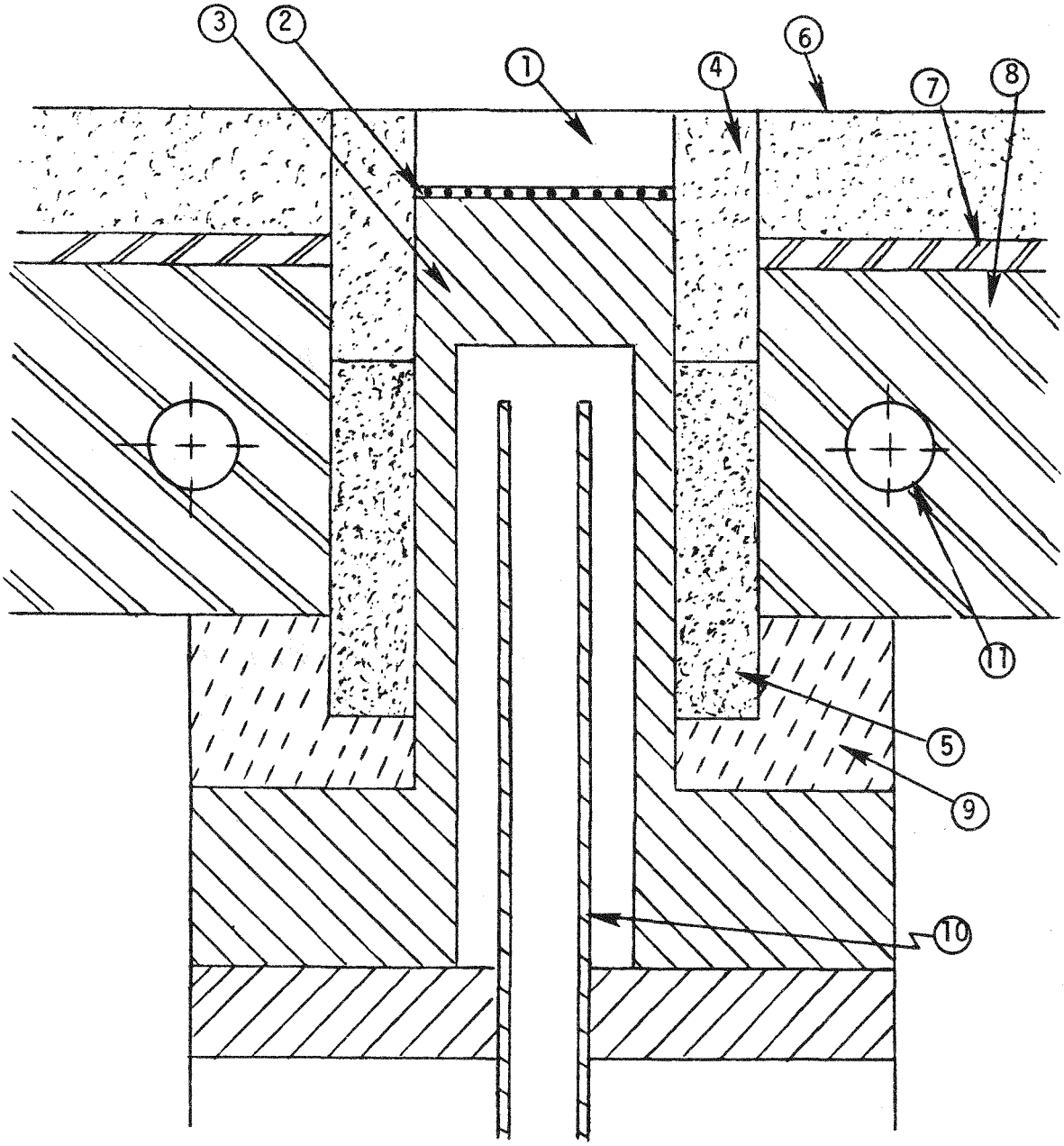

Figure 22. The MTS Configuration

The diameters of the sample disk and insulator are fixed, however, the heights are defined on a test-by-test basis so as to yield the electrode and insulator surface temperatures required by the particular experiment.

The reuseable portion of the test section consists of a metallic shell which is cooled by internal water flow and by surface heat transfer to ambience. The thickness of the shell's wall is fixed by design as is the internal flow cross section. However, the channel liner's thickness is somewhat adjustable by the use of a metallic shim placed between the liner and the shell. If a specific liner surface temperature is required, then the relative thicknesses of the shim and liner may be computed to yield the required condition.

The general equations developed for the thermal analysis and sizing of the sample disk, the primary insulator and the channel liner were used for WESTF Test 49 as reported below.

WESTF II Test Section

During this quarter, revisions were made in the basic design of WESTF to reflect the increased emphasis on testing slagging cold wall electrode and insulator systems and include the following:

- Change in electrode pitch to permit direct correlation with test results from the AVCO generator program (Mark VII).
- Change in cross-channel electrode separation to permit the viewing of a maximum number of electrodes through a viewport incorporates in the test passage.

The pitch most commonly used in the AVCO generator program is 0.70 in. (Reference 8).

The reference design for this pitch will consist of a 0.625 inch electrode and a 0.075 inch interelectrode insulator. The individual frames will contain two electrodes and two peg type insulating wall elements per frame. The peg type insulating wall elements were redesigned to give the maximum segmentation possible in the small duct and to reflect operation in the slagging cold mode.

The metal insulating wall elements will be grooved and the groove filled with a castable ceramic for slag retention and protection of the metal surface. Electrode designs for the initial runs will be selected to correlate with AVCO's studies.

The initial WESTF II design had an anode to cathode separation of 1.25 inch and an insulating sidewall separation of 1.8 inch. In designing for a cold wall channel, an allowance was made for an .080 inch thick slag layer. Therefore, a channel cross-section of 1.41 x 1.96 inch prior to slag coating was established. In order to maximize the number of electrodes that can be seen through a viewport installed at the left end of the channel, the 1.96 inch dimension was selected for the anode to cathode separation, and the 1.41 inch dimension then became the distance between insulating sidewalls. The viewport will be designed to be interchangeable with both WESTF II and MTS II test sections.

WESTF Test 49

The objective of WESTF Test 49 was to screen and evaluate the performance of 0.5 $SrZrO_3 \cdot 0.5$ ($Sr_{.25}La_{.75}FeO_3$) processed and supplied by MIT in a non-slagging super-hot MHD environment.

The test requirements were:

Test Section	MTS II (1 x 2)
Plasma Temperature, K	2600
Pressure, atm	1.1 atm
Mass Flow, kg/s	0.14 kg/s
Operating Mode	Non-slagging super-hot
Surface Temp., Te, $°C_2$	1700 avg., midposition
Current Density, A/cm^2	1.0
Axial Field, kV/m	0
Magnetic Field, tesla	0
Surface Temp., T_{ins}, °C	1550-avg., midposition
Ash	Rosebud
Seed	K_2CO_3
SO_2 Level, m/o	0.1
Time at Conditions, hrs	~8
Electrode Water Flow, gph	24/sample
Channel Wall Water Flow, gph	300

The test article was the Type II Materials Test Section (see Figure 21) with a 1 x 2 inch flow cross-section, a water-cooled stainless steel casing lined with magnesia castable insulation (Permanente 165), and with three removable water-cooled electrode/insulator assemblies on both the anode and cathode walls.

The electrode surface exposed to the slag/plasma was 0.75 inch diameter (0.442 in^2) and was contained within a cylindrical MgO insulator with a 0.25 inch wall thickness. The cylindrical insulator extended 0.407 inch from the electrode surface and then was replaced by boron nitride insulation underneath. Both the anode and cathode walls consisted of discs of 0.5 $SrZrO_3 \cdot 0.5$ ($Sr_{.25}La_{.75}FeO_3$) (0.257 inch thick) brazed to copper mesh (0.062 inch thick, 40% dense) which, in turn, was brazed to water-cooled copper.

The test section instrumentation included two Ir/Rh thermocouples, one positioned in the gas stream that can be retracted and one imbedded in the MgO insulation. These are both located in the top insulating wall in relation to the channel. In addition, a Type S thermocouple sheathed in Inconel 600 was positioned in each ceramic electrode 0.157" from the plasma surface.

The thermal design and pretest analyses of WESTF Test 49 were completed. The design analysis was directed toward specifying the nominal test conditions and the sizes of the test components which will yield the required surface temperatures. The pretest thermal analysis was intended to verify the design calculations and to provide an overview of the anticipated temperatures and heat flows during nominal operating conditions.

The thermal conductivity data for the sample material was measured by BPNL and is shown in Figure 23. Over the range of measurement, i.e., $200 < T < 1400°C$, the data are independent of temperature with a mean value of 0.01844 W/cm-C° and a standard deviation of 8.44×10^{-4}. Furthermore, the electrical resistivity of the sample material is also independent of temperature with a nominal value of 1.0 ohm cm (Reference 9).

The salient results of the analyses are summarized in Table 6. The required heights of the sample disk and primary insulator were 0.654 and 1.033 cm,

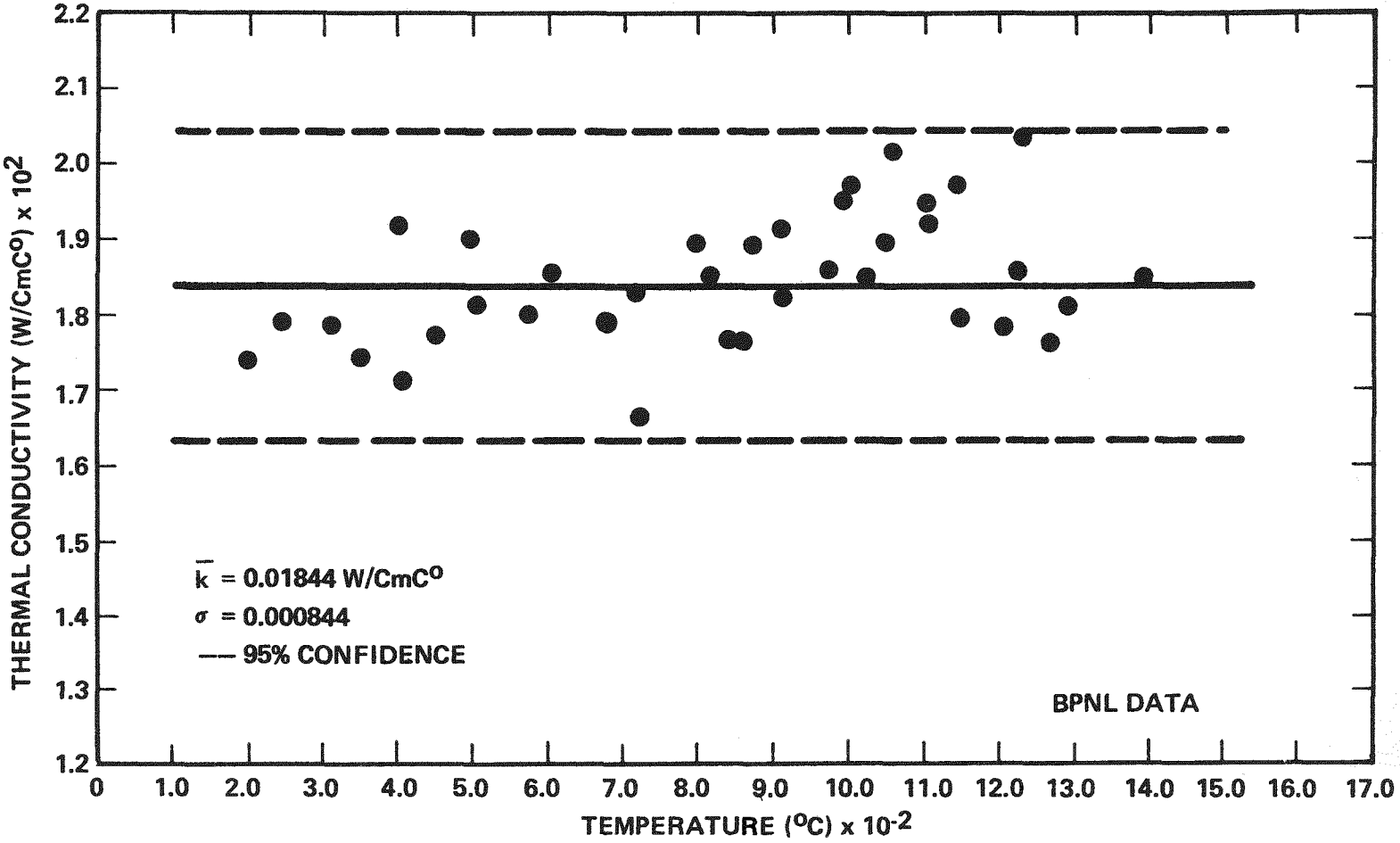

Figure 23. Thermal Conductivity of 0.5 $SrZrO_3 \cdot 0.5(La_{0.75}Sr_{0.25}FeO_3)$ (M-162)

TABLE 6

SUMMARY OF THE DESIGN AND THERMAL ANALYSES FOR WESTF TEST 49

Materials

Sample: $0.5SrZrO_3 \cdot 0.5Sr_{0.25}La_{0.75}FeO_3$ (M-162)

Mesh: Copper (0.062 in thick, 40% T.D.)

Primary Insulator: MgO (Norton, 85% T.D.)

Secondary Insulator: BN (hot pressing direction:axial)

Channel liner: Permanente 165

Dimensions (nominal)

Height of sample disk: 0.654 cm (0.257 in)
Height of primary insulator: 1.033 cm (0.407 in)
Thickness of channel liner: 0.762 cm (0.300 in)

Test Conditions (nominal)

Plasma temperature: 2327°C (2600°K)
Plasma mass flow rate: 140 gm/sec

Thermal Conditions (nominal)

Item	Heat Flow		Temperature (°C)	
	Total (W)	Per Area (W/cm^2)	Surf. Toward Plasma	Surf. Away from Plasma
Sample disk	126	44.4	1690	102
Copper Mesh	128	45.0	102	33
Copper Water Jacket	128	45.0	33	21
Primary Insulator	368	72.9	1568	82
Electrode Wall: Channel Liner	3150	44.2	1694	717
Test Shell	3150	44.2	717	330
Horizontal Wall: Chan. Liner	2391	50.2	1608	371
Test Shell	2391	50.2	371	120

respectively. These heights were determined on the basis of a nominal plasma temperature of 2600 K and a nominal mass flow rate of 140 gm/sec. These plasma conditions are midrange values; thus, the potential for in-test control and adjustment is maximal.

The thermal analysis summarized in Table 6 verified that, within acceptable limits, the required test conditions are achieved by the nominal dimensions and flow conditions. Specifically, the sample disk is shown to operate with a surface temperature of 1690°C while that of the insulator is 1568°C.

2.1.3 Post-Test Analysis

WESTF Test 42

WESTF Test 42 was a screening test of hafnia and zirconia electrode material coupons and insulating wall materials under non-slagging super-hot conditions. The primary objective of the test was to provide relative performance data for these materials over a range of temperatures and in the absence of electrical or magnetic fields.

The test was conducted on January 22-23, 1980 and the operating time, combustor on to combustor off, was 22.2 hours. A buildup of slag at the exit of the test channel was encountered which necessitated shutoff of the slag/seed injection system prior to completion of the test. As a result, only 8.7 hours of operation were with slag/seed flow. The hafnia materials were supplied by BPNL and BPNL participated in the conduct of the test.

Following test section disassembly the coupon/coupon holders from both walls were impregnated in mounting material, cut off from the copper bases and given to BPNL for detailed post-test characterization.

Since the post-test material characterization activity is in process at BPNL, the following sections are limited to post-test visual observations and results of the thermal data analysis.

Visual Observations

The "electrode" and "insulating" walls were brownish in color indicating that slag constituents had penetrated, at least to some extent, into all the channel materials. In general, the MgO coupon holders on both the A and C walls appeared to be somewhat more resistant to corrosion attack than the electrodes (See Figures 24 and 25). They are however highly cracked. The slag buildup on the A wall MgO is somewhat thicker than on the C wall. This suggests, that the A wall was cooler than the C wall and that liquid slag did flow over the A wall during some part of the test. On the upstream sections of the A and C walls, (area closest to transition section), there is a thick 3-5 mm buildup of solidified slag on the MgO which has partially spilled over onto electrodes A1 and C1.

"A" Wall Electrodes - The top segment of A-2, all of the A-3 and to a lesser extent both segments of A-5 exhibit moderate corrosion and these reacted surfaces have plastically sheared in the direction of plasma flow. The adjacent MgO insulators are relatively unaffected. Electrodes A1, A4 and A6 exhibit the least amount of attack.

"C" Wall Electrodes - The "C" wall materials were generally less corroded although somewhat more highly cracked than the "A" wall electrodes. Little surface attack was observed except for the central segments of C1 and C2.

Top and Bottom "Insulating Walls" - The insulating walls were generally covered with thin ($\sim$1-2 mm) slag layers. Slag thickness was greater at the bottom than at the top wall. Most of the heavy slag accumulation is at the upstream locations, indicative of lower temperatures in these regions.

Thermal Analysis

A preliminary thermal analysis of the test data has been completed and is summarized in Table 7. The heat fluxes and surface temperatures were computed from the time averaged readings of the thermocouples in the samples and in the water.

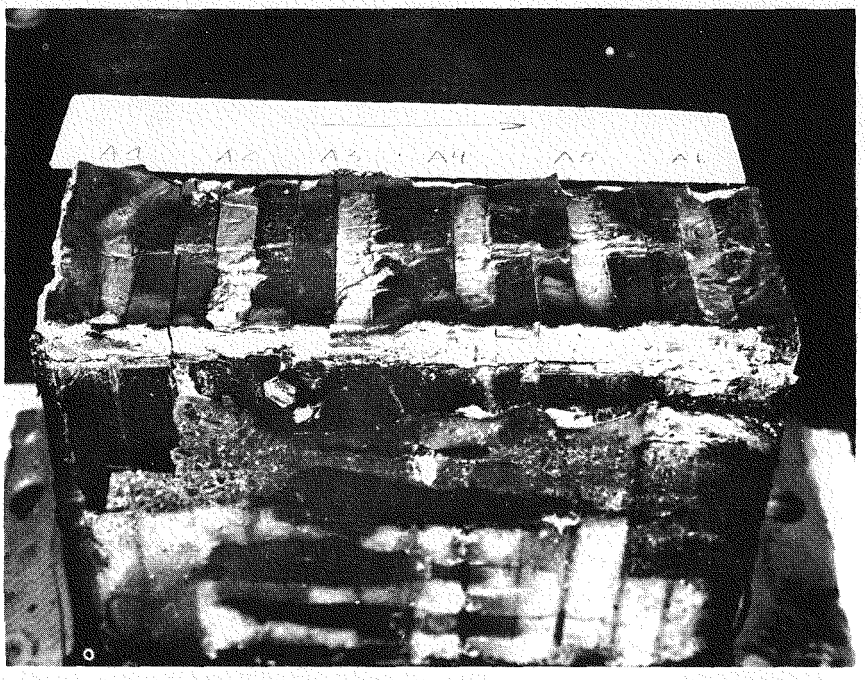

Figure 24. Appearance of Cathode Wall after WESTF Test 42

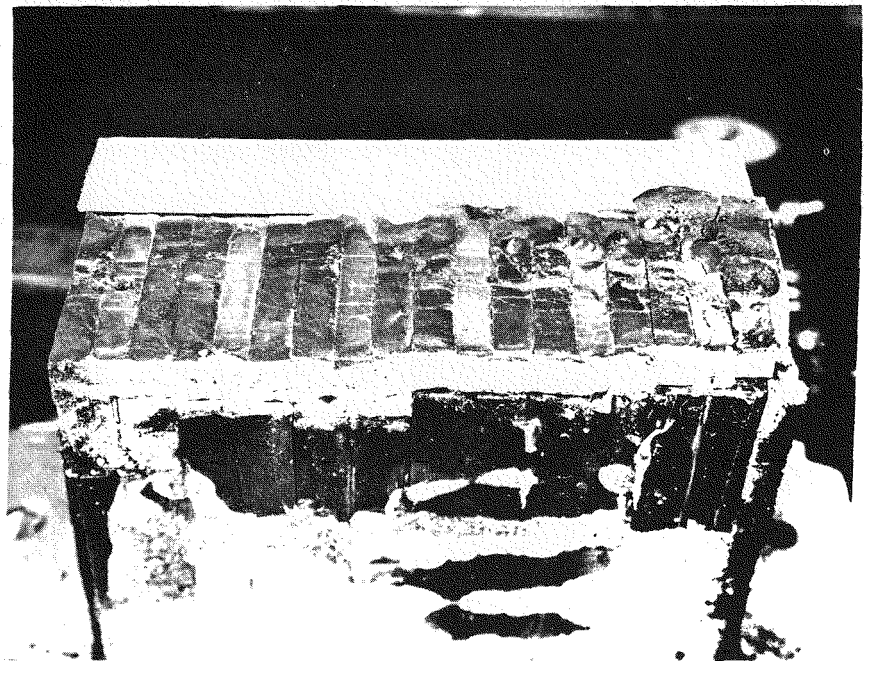

Figure 25. Appearance of Anode Wall after WESTF Test 42

TABLE 7

SUMMARY OF POST-TEST THERMAL ANALYSIS - WESTF TEST 42[a]

Pos.	Material	Thickness (cm) MgO	Thickness (cm) Sample	T/C Depth (cm)	T/C Temp. (°C)	Heat Flux (W/cm²)	Surface Temp. (°C)
A1	$12Y_2O_3 \cdot 88ZrO_2$ (M-155)	0.127	0.584	0.457	830	23.5	1740
A2	$15\ MgO_{.625}Ca_{0.375} \cdot 85\%ZrO_2$ (M-156)	0	0.508	0.406	840	28.5	1540
A3	$12Y_2O_3 \cdot 88ZrO_2$ (M-155)	0.254	0.673	0.457	1080	11.4[b]	1520[b]
A4	$15MgO_{.625}Ca_{0.375} \cdot 85ZrO_2$ (M-156)	0.254	0.762	0.457	920	20.8	1495
A5	$12Y_2O_3 \cdot 88ZrO_2$ (M-155)	0.127	0.686	0.457	500	11.3	940
A6	Hafnia D	2.413	0.762	0.457	925	15.6	1240[c]
C1	$Pr_{0.27}Yb_{0.09}Hf_{0.64}O_2$ (Hafnia A)	0.254	0.508	0.381	1020	32.5	1670
C2	$Tb_{0.20}Y_{0.10}Hf_{0.70}O_2$ (Hafnia B)	0.381	0.762	0.381	1100	26.0	1500
C3	$Pr_{0.27}Yb_{0.09}Hf_{0.64}$ (Hafnia A)	0.254	0.762	0.381	1075	24.2	1560
C4	$Tb_{0.20}Y_{0.10}Hf_{0.70}O_2$ (Hafnia B)	1.143	0.762	0.381	1035	20.9	1360
C5	$Pr_{0.27}Yb_{0.09}Hf_{0.64}O_2$ (Hafnia A)	0.508	0.762	0.381	995	21.3	1420
C6	$Tb_{0.20}Y_{0.10}Hf_{0.70}O_2$ (Hafnia B)	2.667	0.762	0.381	980	15.4	1270

NOTES: (a) The analyses are based on estimates of the time averaged conditions.
(b) Anode 3 is believed to have experienced a separation of bond; the computed values shown incorporate the effects of the separation.
(c) Anode 6 was viewed by the optical pyrometer; readings varied between 1370 and 1420°C throughout the test's duration.

The heat flux, Q, was computed according to

$$Q = \frac{(T_w - T_x)}{\frac{(S_s - X)}{\bar{k}_s} + \frac{S_m}{\bar{k}_m} + \Phi},$$

and the surface temperature, T_s, according to

$$T_s = T_x + XQ/\bar{k}_s,$$

where T_w = water temperature (= 6°C)

T_x = temperature indicated by the in-sample thermocouple

S_s = thickness of sample

S_m = thickness of MgO between sample and metal mesh

X = depth of thermocouple from plasma-surface

$\bar{k}_s$ = mean (temperature averaged) thermal conductivity of the sample

$\bar{k}_m$ = mean thermal conductivity of MgO (= 0.107 W/cm-°C)

Φ = combined (in-series) thermal resistances of the bonding materials, mesh and copper (= 23.11 °C/W, except for Anode 3 which was 73.11 °C/W).

The mean (temperature averaged) thermal conductivity of the WESTF Test 42 materials are as follows:

- 12 $Y_2O_3 \cdot 88ZrO_2$ - 0.0118 w/cm °C
- 15 $(Mg_{.625}Ca_{.375}) \cdot 85ZrO_2$ - 0.0166 w/cm °C
- $Er_{.82}Hf_{.18}O_2$ - 0.0227 w/cm °C
- $Pr_{.27}Yb_{.09}Hf_{.64}O_2$ - 0.0197 w/cm °C
- $Tb_{.2}Y_{.1}Hf_{.7}O_2$ - 0.0247 w/cm °C

In all cases, the in-sample thermocouple readings continually oscillated about their time averaged means with amplitudes of ~11%. Thus, corresponding oscillations are expected about the time averaged surface temperatures and heat fluxes given in Table 7. In the case of Anode 3, which is believed to have experienced a bond separation, Φ was taken to be 73.11 °C/W. This value includes the effect of an assumed 0.5 mm gap filled with plasma gas.

WESTF Test 43

Post-test visual examination of the iron cathode wall and Pt coated Al_2O_3 anode wall indicated that very extensive damage had occurred (See Figures 26 and 27). Except possibly for small areas of anodes 1, and 9-12, it appears that all the Pt coated Al_2O_3 segments popped off the mesh substrate. This occurred during the course of the test since the mesh was completely covered by a 1.5-2 mm thick brownish colored slag layer. A few large holes (~3 mm diameter) were observed in the interelectrode gap between anodes 2-3, 8-9, 11-12 possibley a result of intense arc damage.

Corrosion of the iron cathodes varied between moderate and very extensive. The slag covering was blacker than at the anode suggesting that it has a higher iron content. Insulators between cathodes 3-8 are all deeply undercut and are missing to a depth of at least 5 mm. The central section of electrodes 1-8 were moderately corroded while the top and bottom edges were somewhat more extensively attacked. The bottom two-thirds of cathodes 9-12 were highly corroded while the top third were moderately attacked. It is possible that cathode melting occurred at the cathode wall/bottom insulating wall interface for electrodes 9-12 suggesting that arcing was intense at that location. It is not clear at this time why the corrosion pattern differs significantly between upstream and downstream cathodes or as to why the downstream electrodes exhibited more material loss.

Thermal Analysis

A preliminary post-test thermal analysis of the WESTF 43 test data has been completed and is summarized in Table 8. Figures 28 and 29 illustrate the cathode and anode, respectively, that was tested in WESTF 43. The only

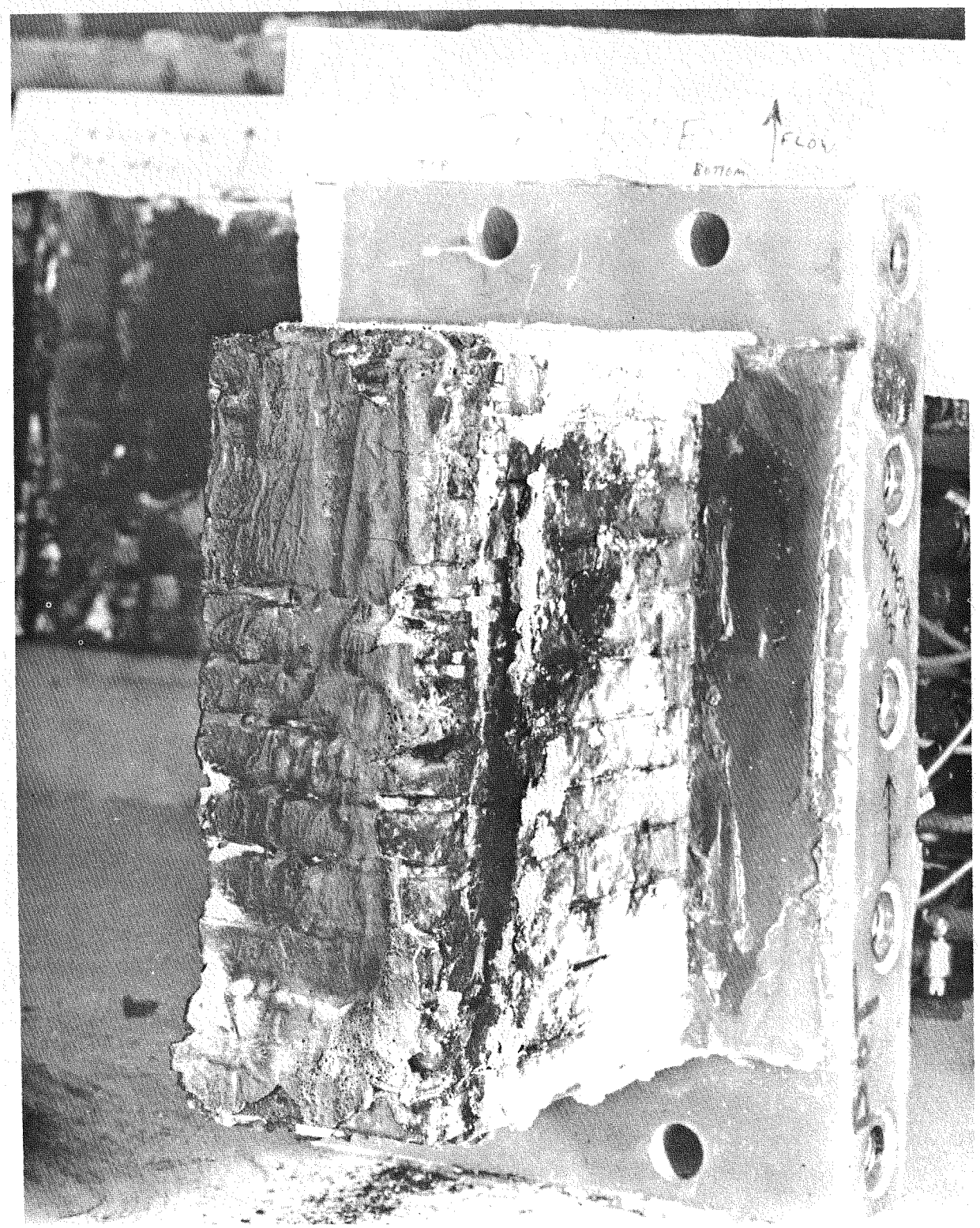

Figure 26. Appearance of Cathode Wall after WESTF Test 43

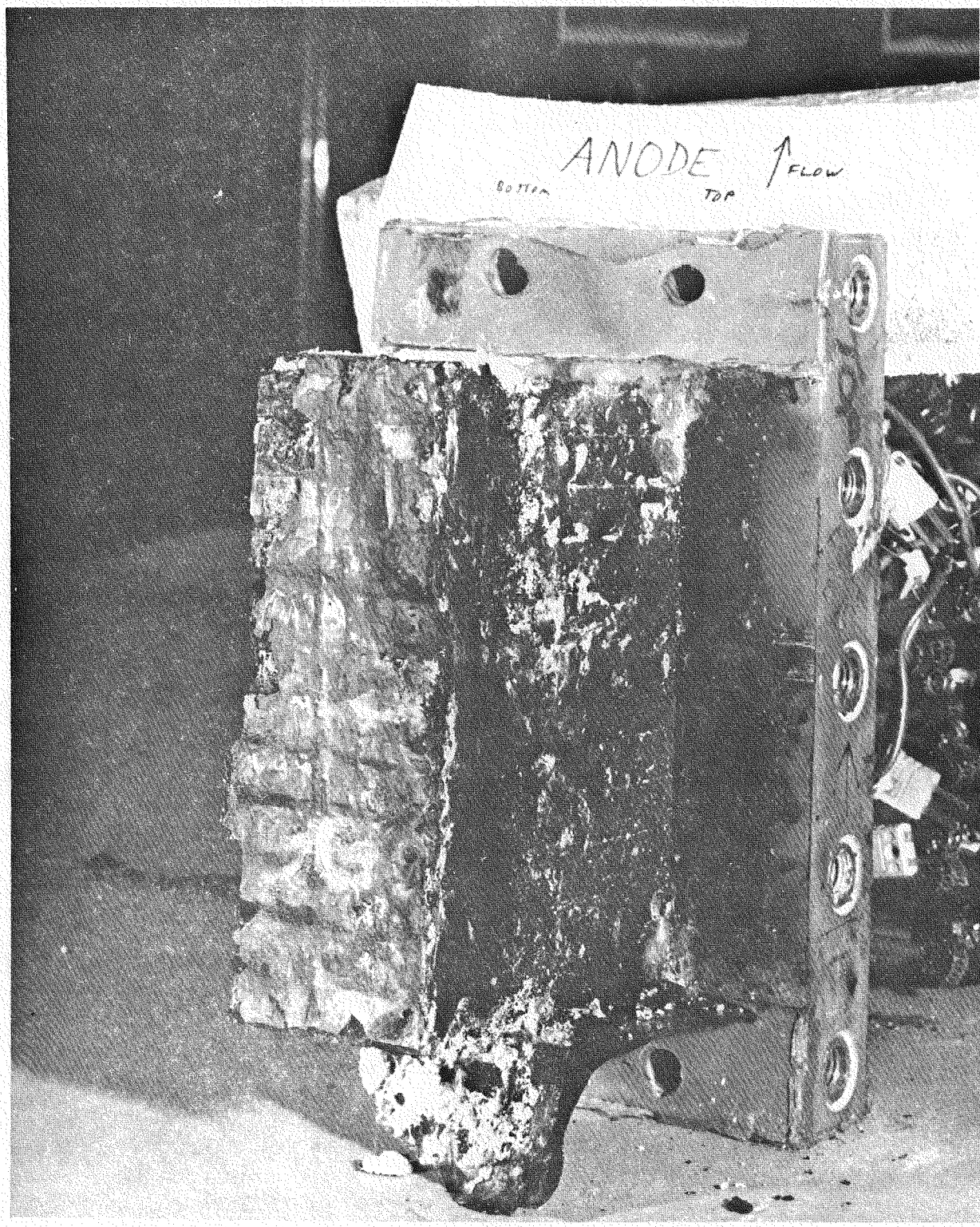

Figure 27. Appearance of Anode Wall after WESTF Test 43

TABLE 8

SUMMARY OF WESTF TEST 43 POST TEST THERMAL ANALYSIS*

ELECTRODE	THICKNESSES (cm)		THERMOCOUPLE DEPTH (cm)		HEAT FLUX (W/cm^2)	ELECTRODE SURFACE TEMPERATURE (K)	INSULATOR SURFACE TEMPERATURE (K)
	INSULATOR	CERAMIC	TC_1	TC_2			
Cathode 2 (C02)	1.118	1.016	0.203	2.266	80.6	1271	1489
Cathode 5 (C05)	1.326	1.224	0.203	2.474	91.5	1329	1596
Cathode 8 (C08)	1.910	1.808	0.203	3.058	62.9	1392	1577
Cathode 11 (C11)	2.037	1.935	0.203	3.170	64.0	1416	1611
Anode 2 (A02)	0.119	0.094	0.853	1.539	73.1	1100	1117
Anode 5 (A05)	0.272	0.246	1.006	1.692	61.3	1052	1092
Anode 8 (A08)	0.424	0.399	0.201	1.844	115.6	1523	1979
Anode 11 (A11)	0.577	0.551	0.277	1.996	109.7	1565	2162

*Analysis based on the time averaged thermocouple readings.

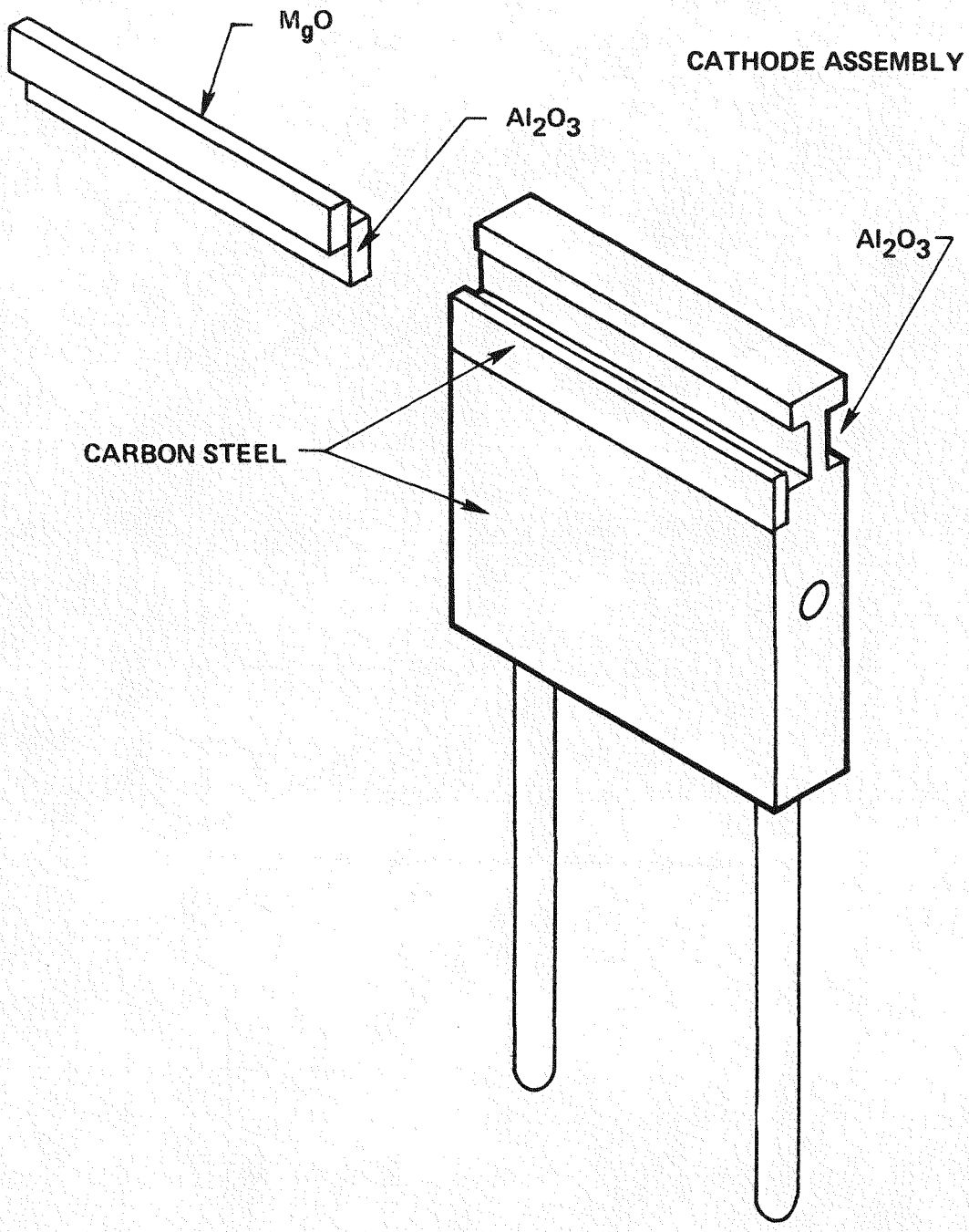

Figure 28. WESTF 43 Cathode

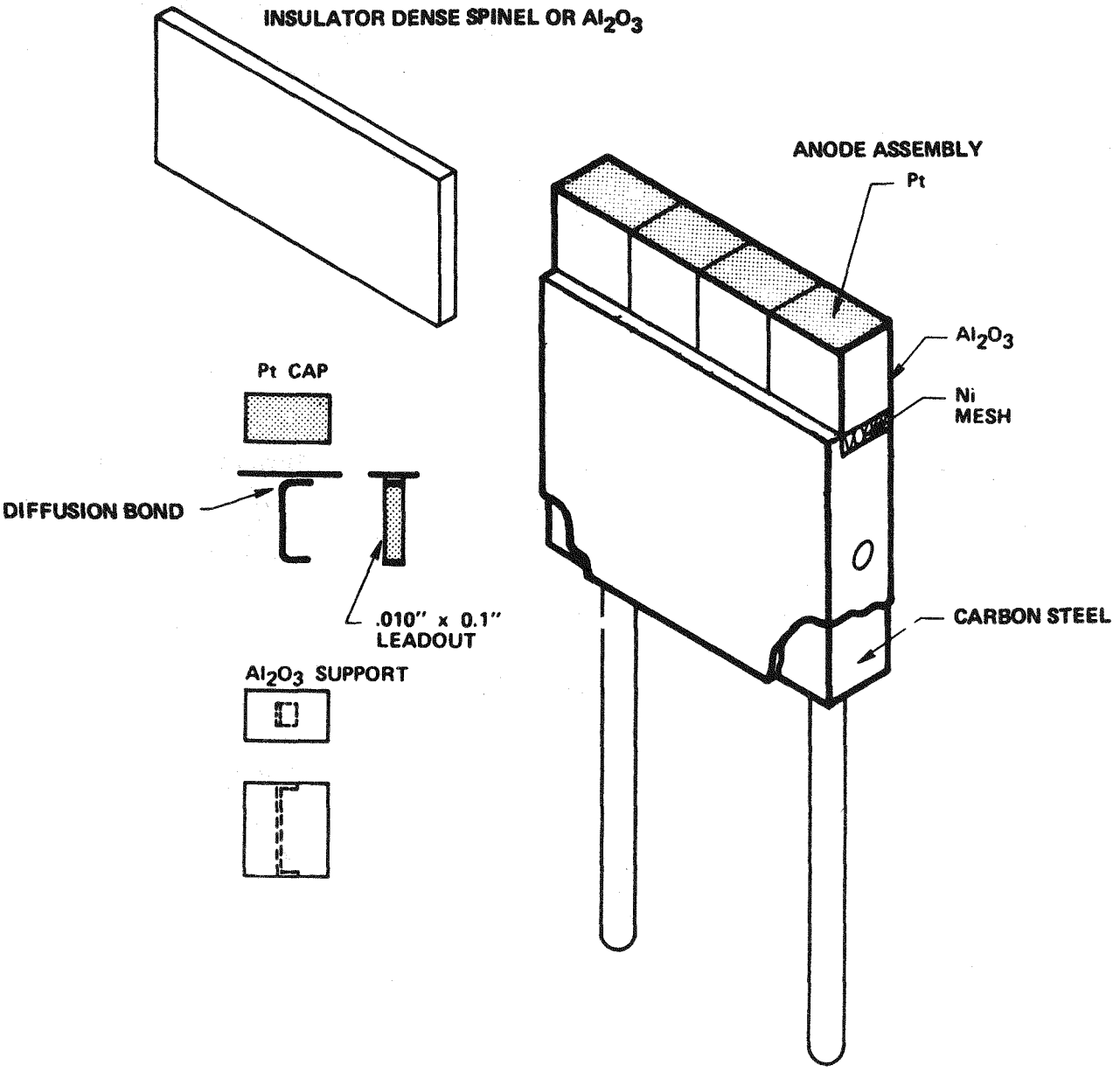

Figure 29. WESTF 43 Anode

differences betwen successive cathodes and anodes are the thicknesses of the insulator and the ceramic filler.

The heat fluxes and surface temperatures were computed from time averaged data from thermocouples in the electrodes. The heat flux, Q, was computed according to

$$Q = \frac{(T_1 - T_2)}{\sum_i R_i}$$

where T_1 is the temperature of the thermocouple near the electrode surface,

T_2 is the temperature of the thermocouple buried in the center of the electrode,

and $\sum_i R_i$ is the sum of the thermal resistances which are connected in series and parallel.

Each resistance, R_i, is defined by $\frac{L_i}{k_i f_i}$ where

L_i is the thickness of the electrode component (steel, Ni Mesh, spinel, Al_2O_3, etc.),

k_i is the temperature averaged thermal conductivity of the electrode component across distance L_i, and

f_i is the fraction of the total electrode cross-sectional area taken by each electrode component.

The surface temperature, T_s, was computed using

$$T_s = Q(R) + T_1$$

where Q is the calculated heat flux,

R is the thermal resistance of the electrode near the surface, given by $\frac{L}{K}$ of that electrode component,

and T_1 is the temperature of the thermocouple near the electrode surface.

Electrical

Light-off for WESTF Test 43 was at 1150 on 3/6/80. In order to minimize oxidation of the cathodes, the cathodes electrodes were kept at a negative potential of 10 volts relative to the anodes as the temperature of the system was increased. The anode-cathode resistances just prior to the introduction of seed at 1535 was generaally in excess of several hundred ohms.

The channel electrodes were connected in the CnAn+1 circuit discussed previously i.e., the first power supply was connected between electrodes C1 and A2 and the second power supply was connected between C2 and A3, etc. Electrodes C12 and A1, which were left "floating," were connected so that their potentials would be recorded during routine measurements.

About an hour after the introduction of seed it was possible to impress two amperes through the individual electrode-pairs of the channel with voltages varying between 50 to 70 volts.

Curves showing the distribution of voltages and currents as a function of electrode-pair position at different times during the run can be seen in the upper curves of Figures 30 to 39. The lower curves, which will be discussed later, give the potentials of selected water-cooled backing plates in the upper and lower insulating walls.

A very definite decrease in the voltage required to produce load currents of about 3.0 amperes in going from the upstream to the downstream section of the channel can be observed at times 1650 and 1700 in Figures 31 and 32. The failure of this effect to show up in Figure 30, which was taken 35 minutes after the introduction of seed was apparently due to an insufficiency of seed at 1610.

The currents through the channel were progressively increased to 7.0 amperes between 1700 and 1900. The changes in the electrical characteristics of the channel as the current density was increased can be observed by comparing Figure 37 with Figures 30 and 31.

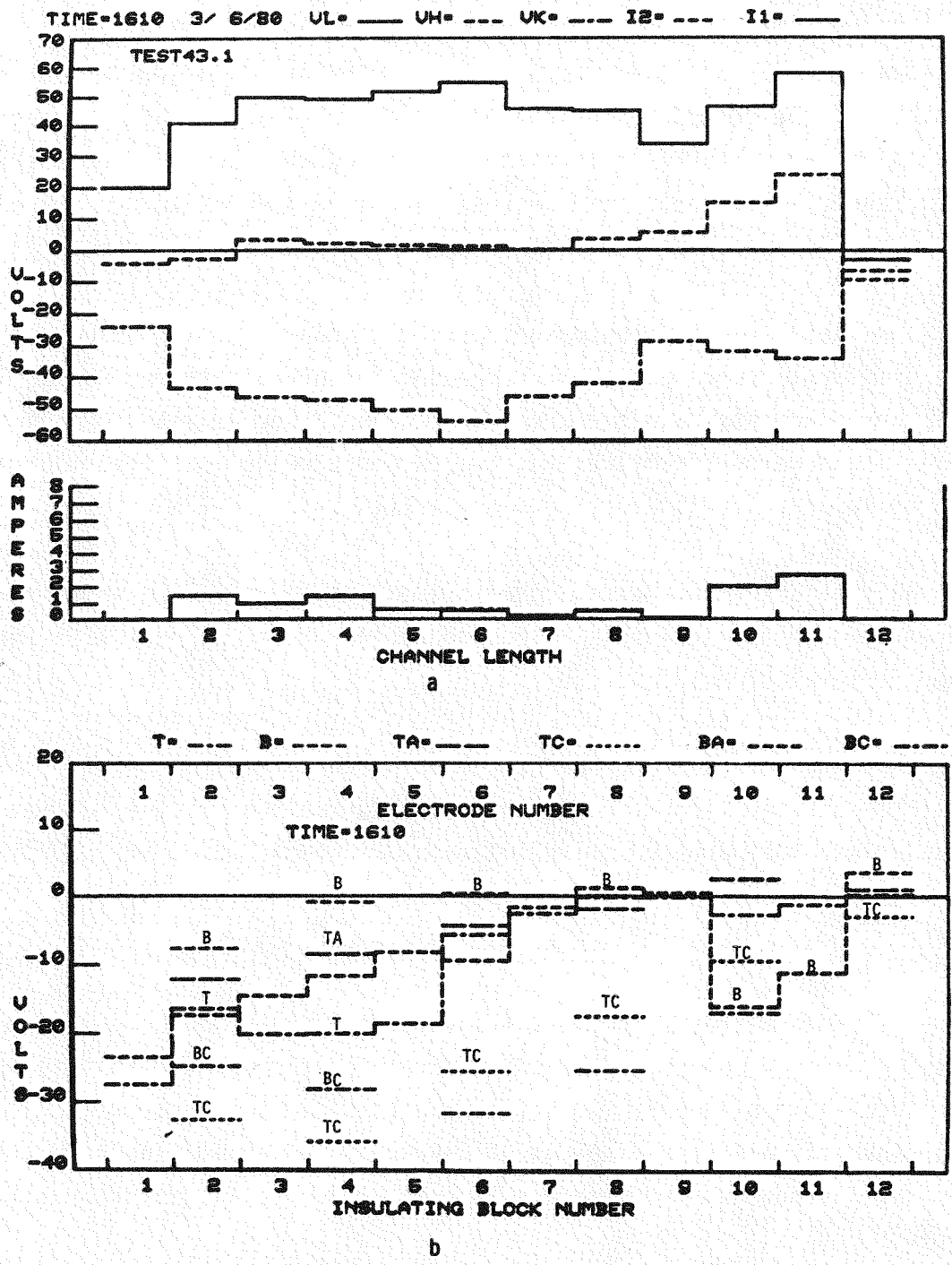

Figure 30. Voltage and Current Distribution, WESTF Test 43, 3/6/80

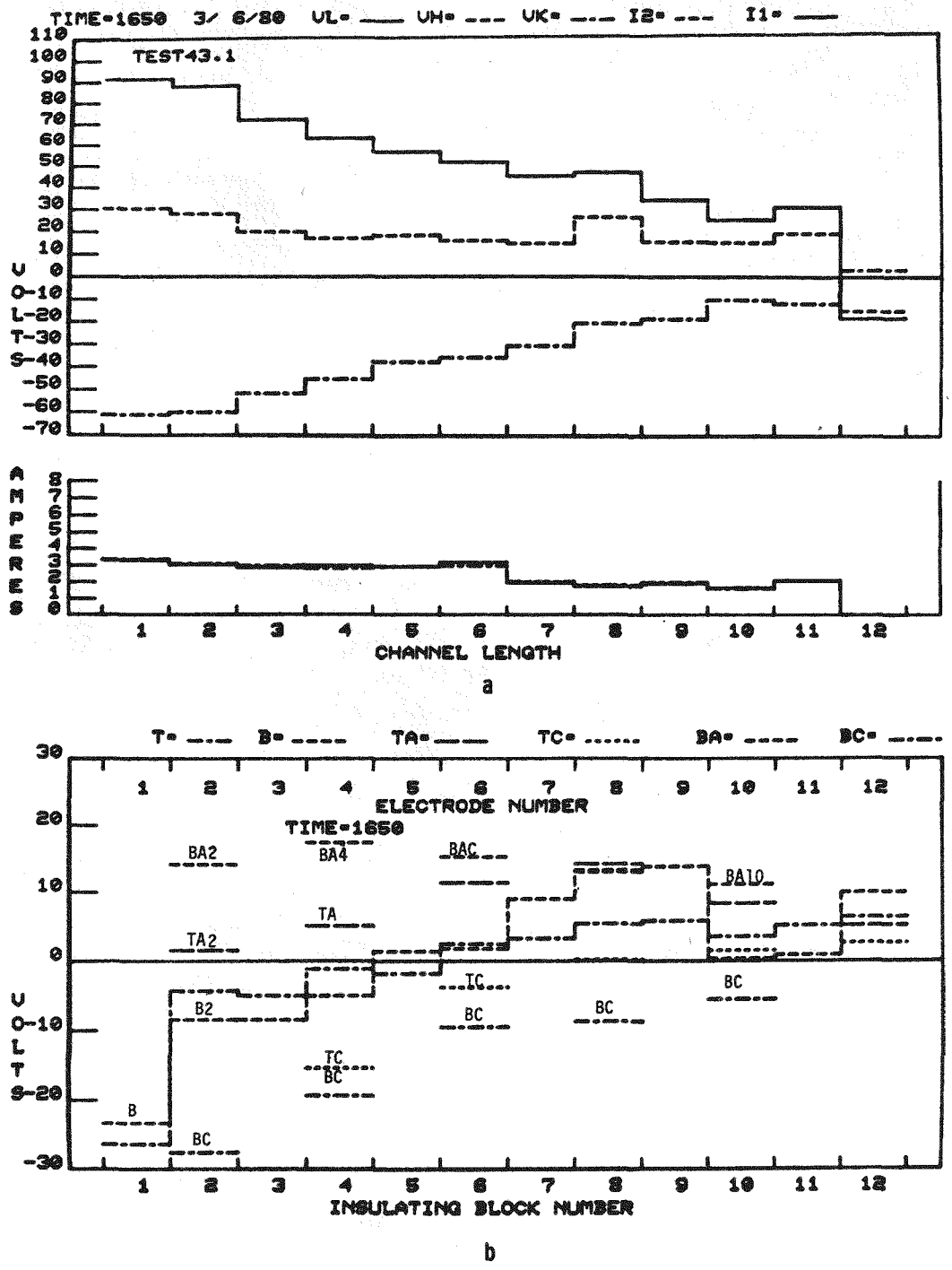

Figure 31. Voltage and Current Distribution, WESTF Test 43, 3/6/80

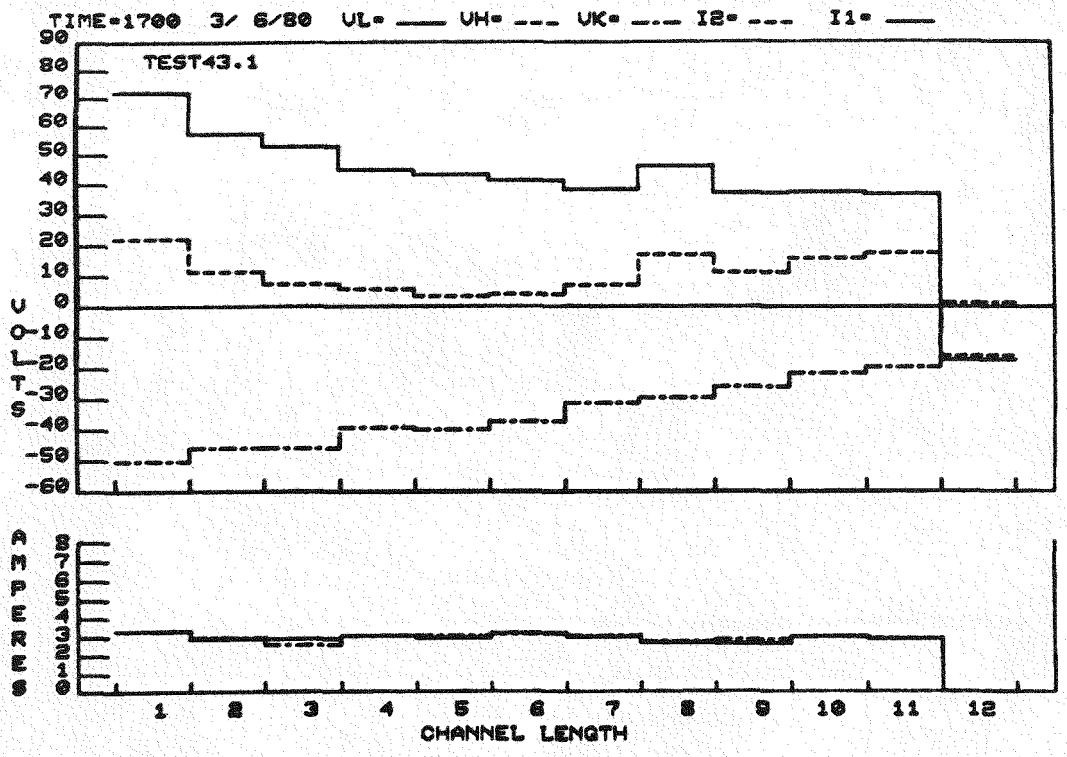

a

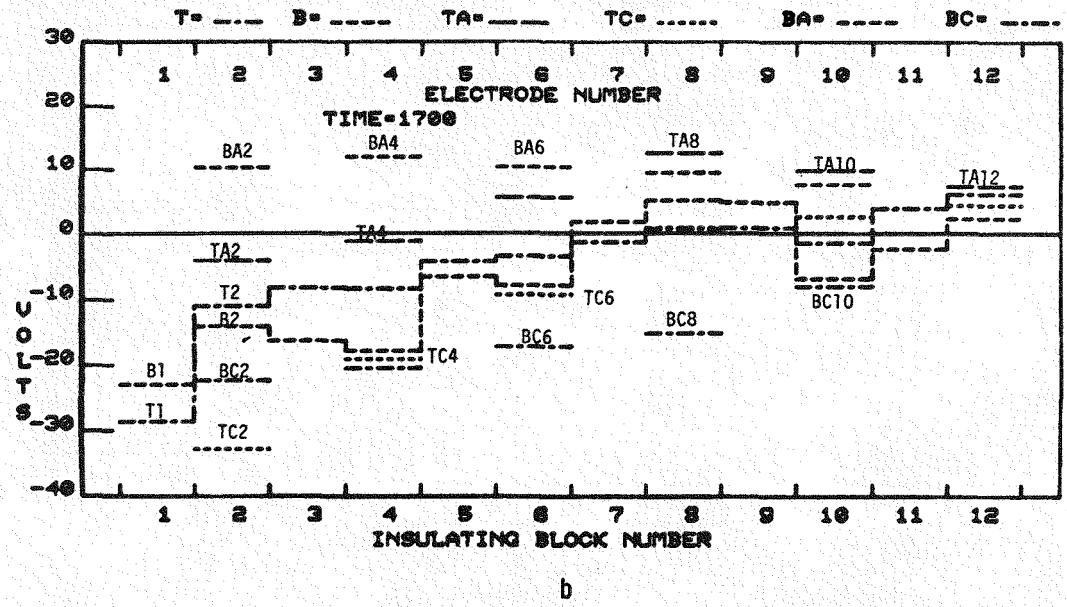

b

Figure 32. Voltage and Current Distribution, WESTF Test 43, 3/6/80

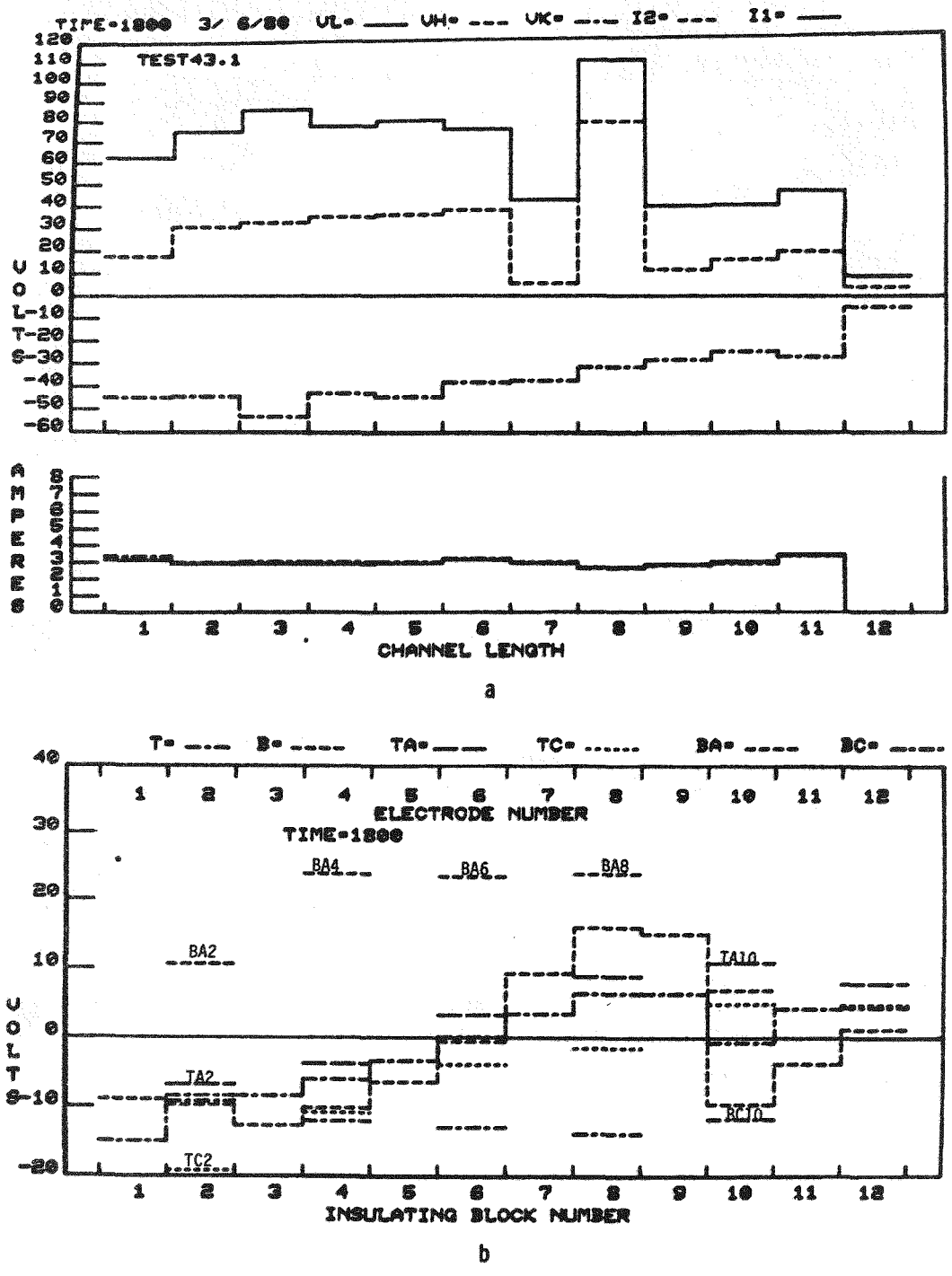

Figure 33. Voltage and Current Distribution, WESTF Test 43, 3/6/80

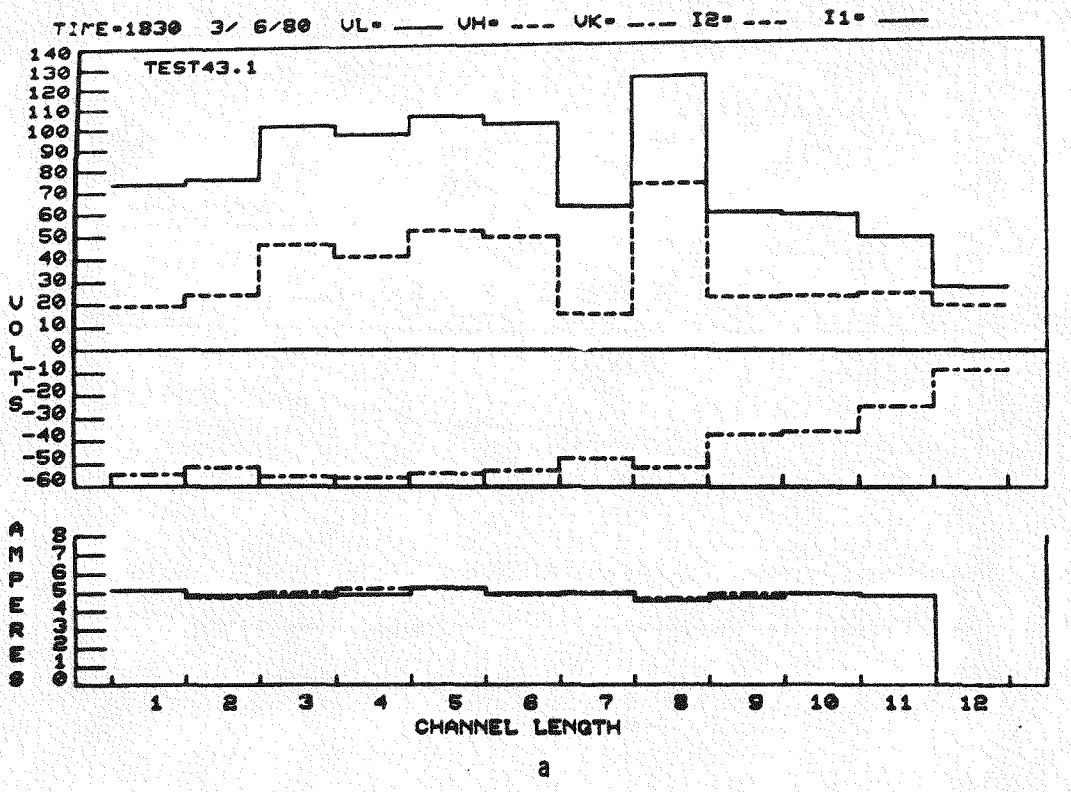

a

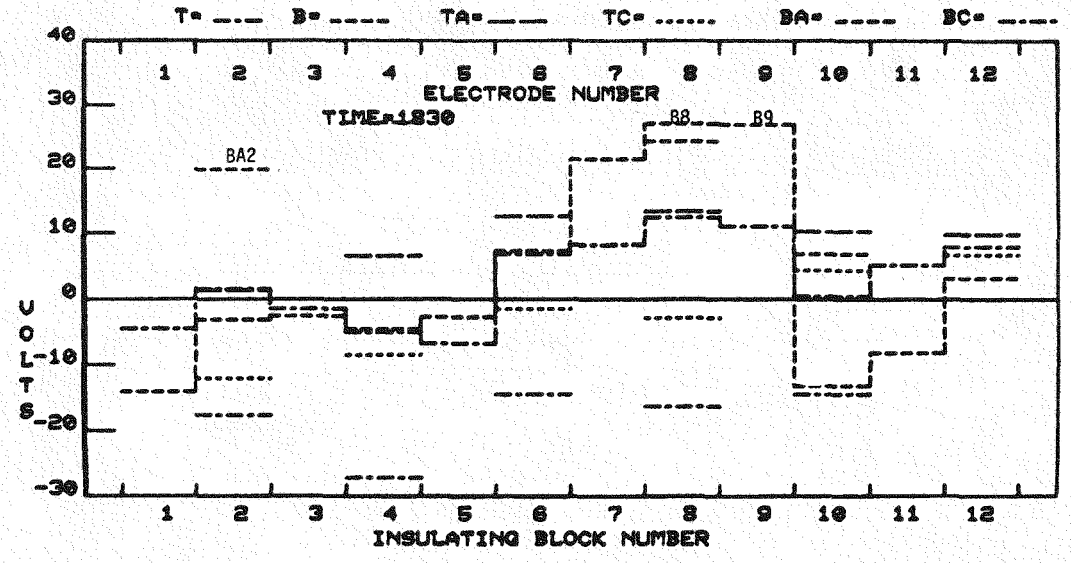

b

Figure 34. Voltage and Current Distribution, WESTF Test 43, 3/6/80

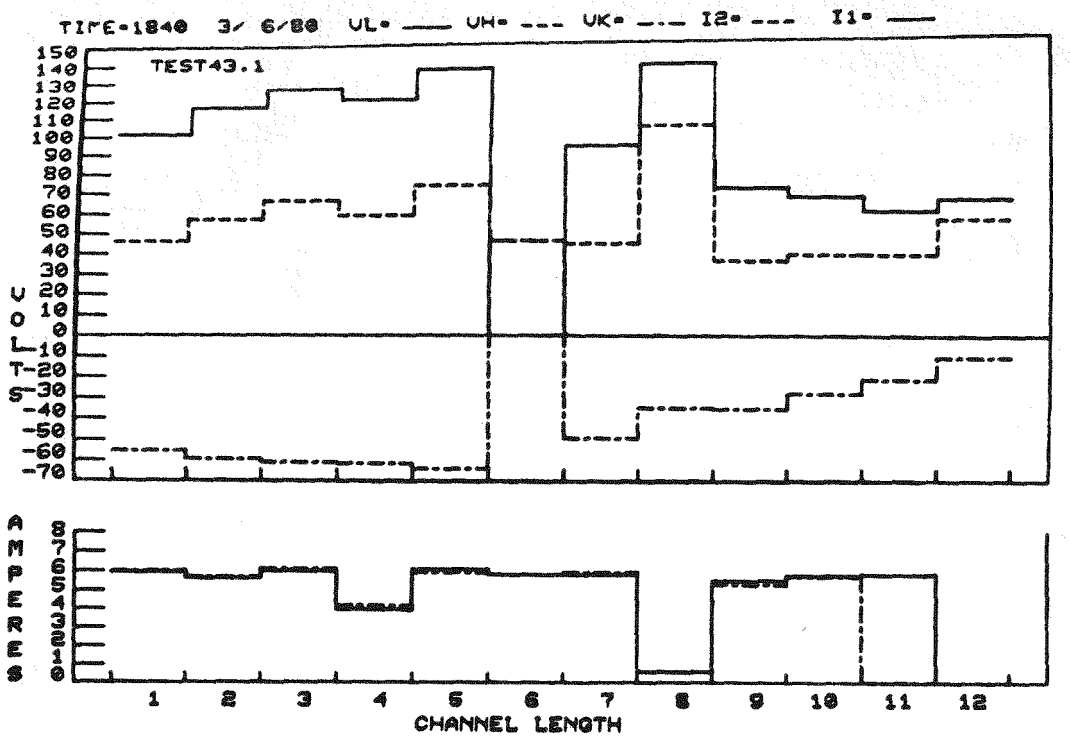

a

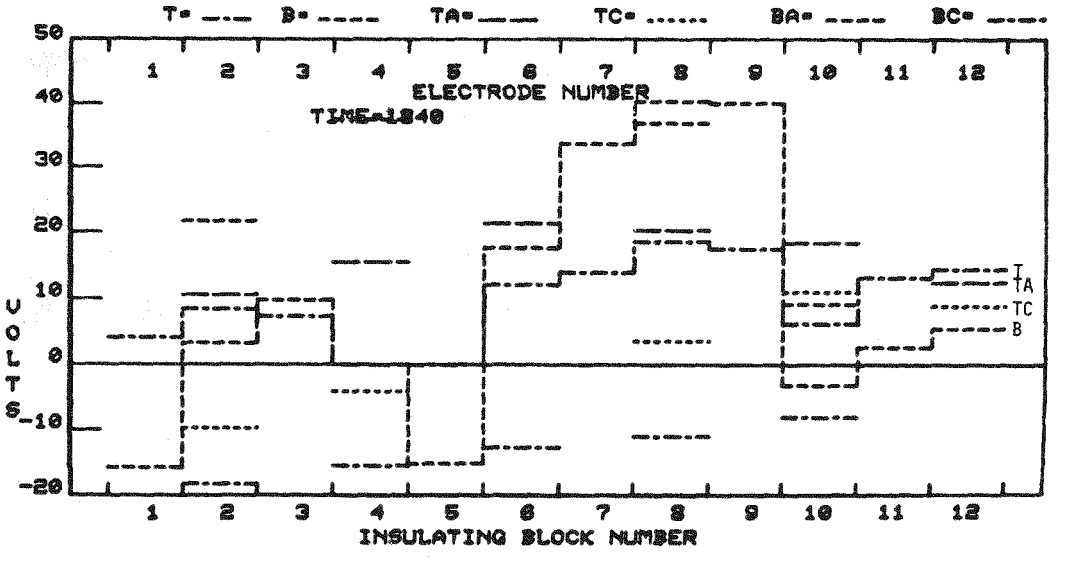

b

Figure 35. Voltage and Current Distribution, WESTF Test 43, 3/6/80

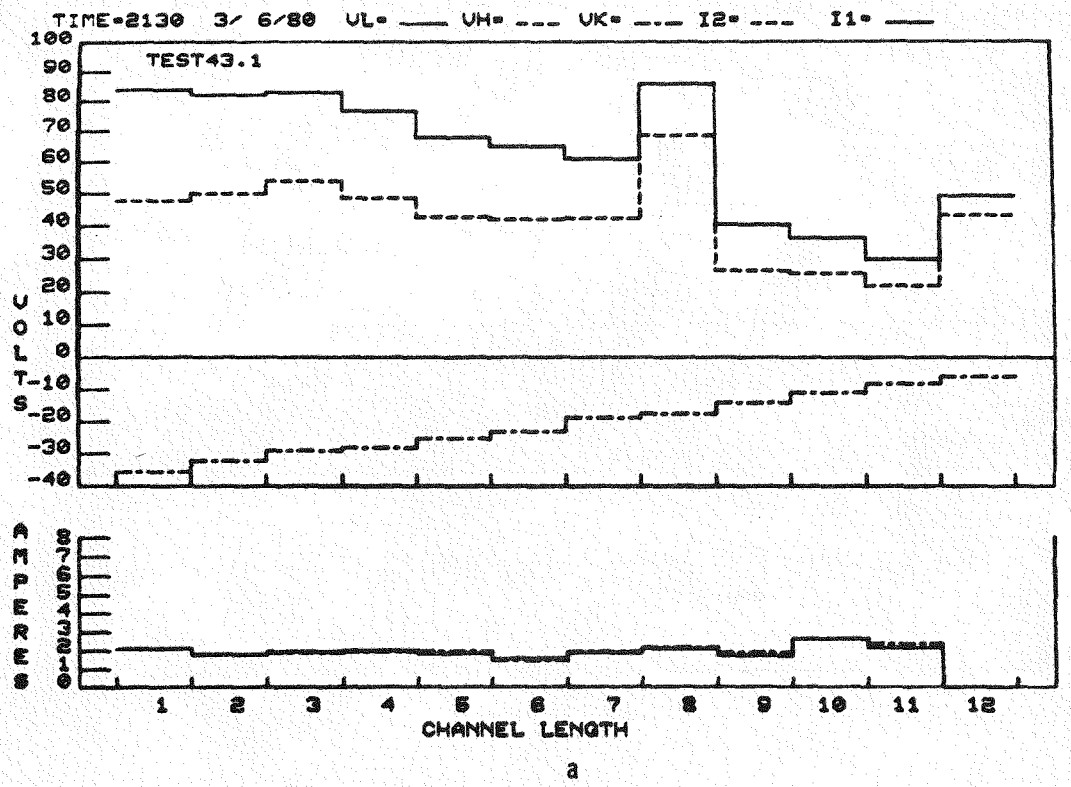

a

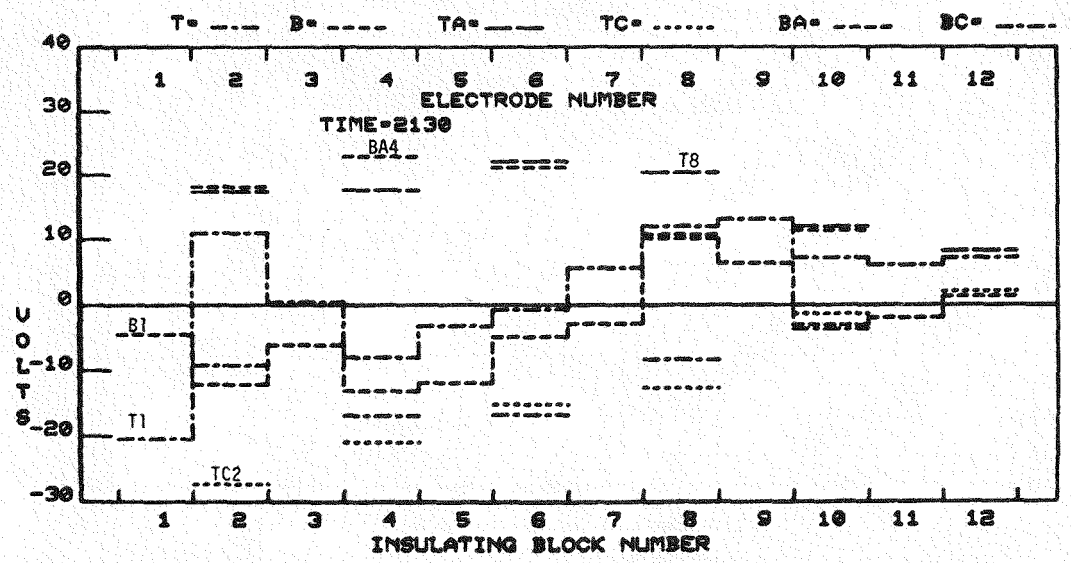

b

Figure 36. Voltage and Current Distribution, WESTF Test 43, 3/6/80

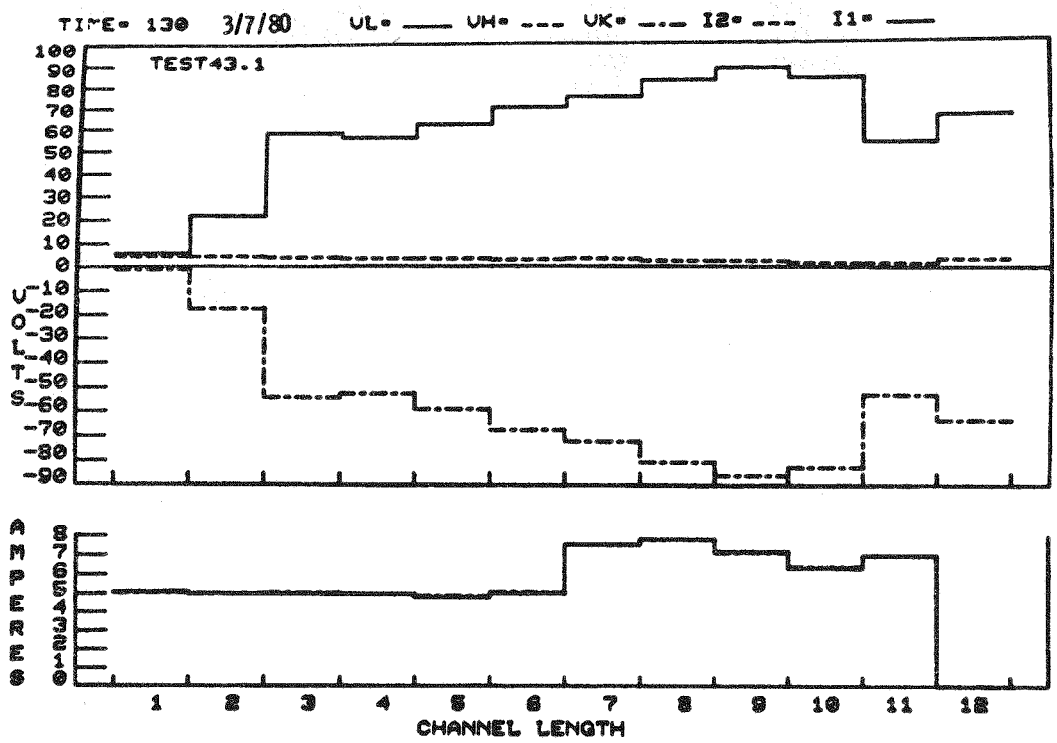

a

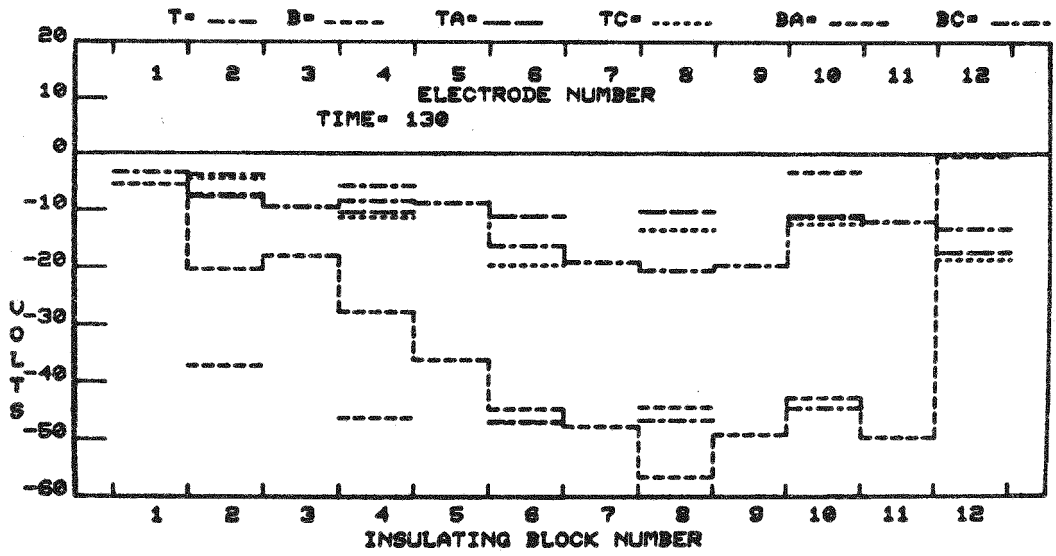

b

Figure 37. Voltage and Current Distribution, WESTF Test 43, 3/7/80

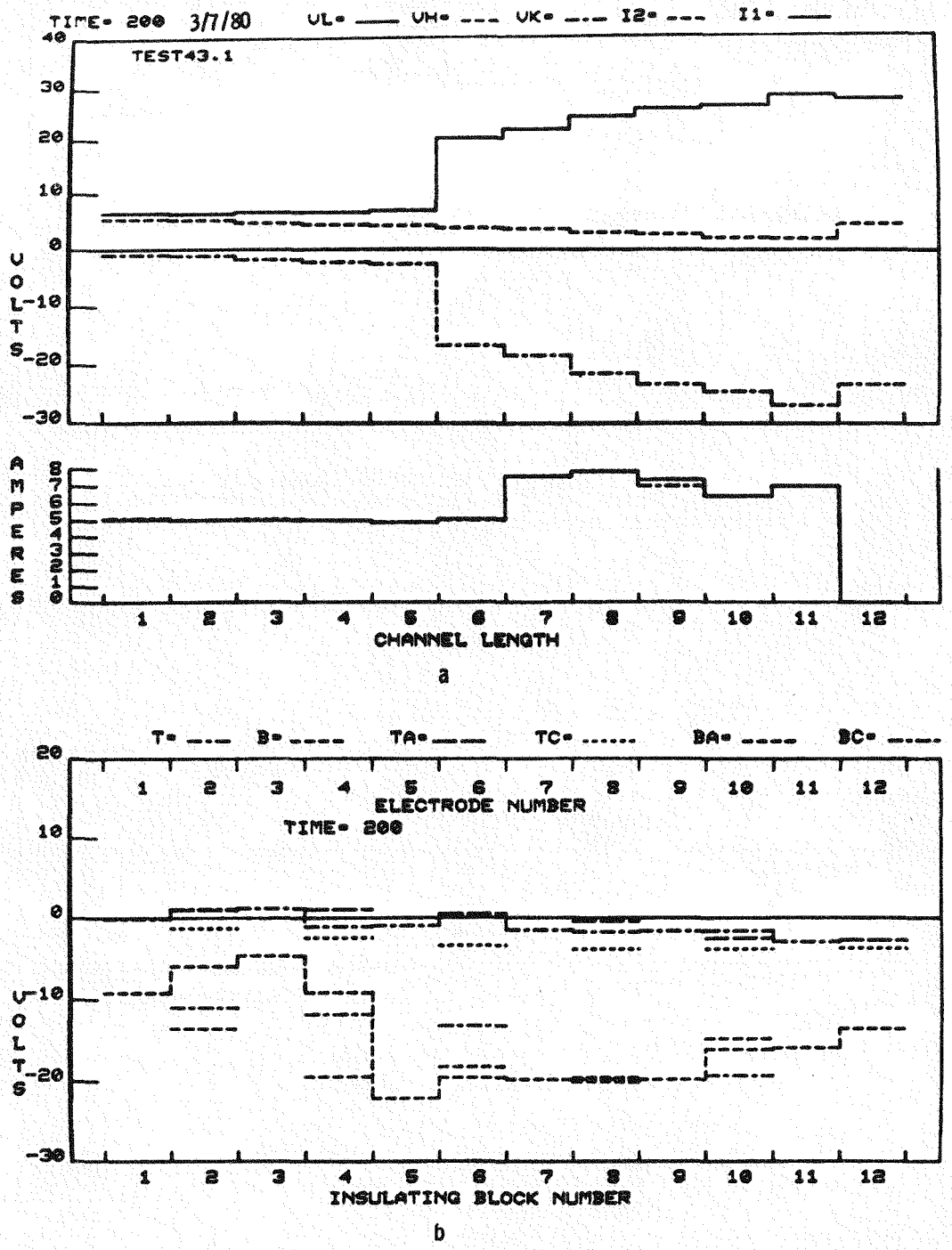

Figure 38. Voltage and Current Distribution, WESTF Test 43, 3/7/80

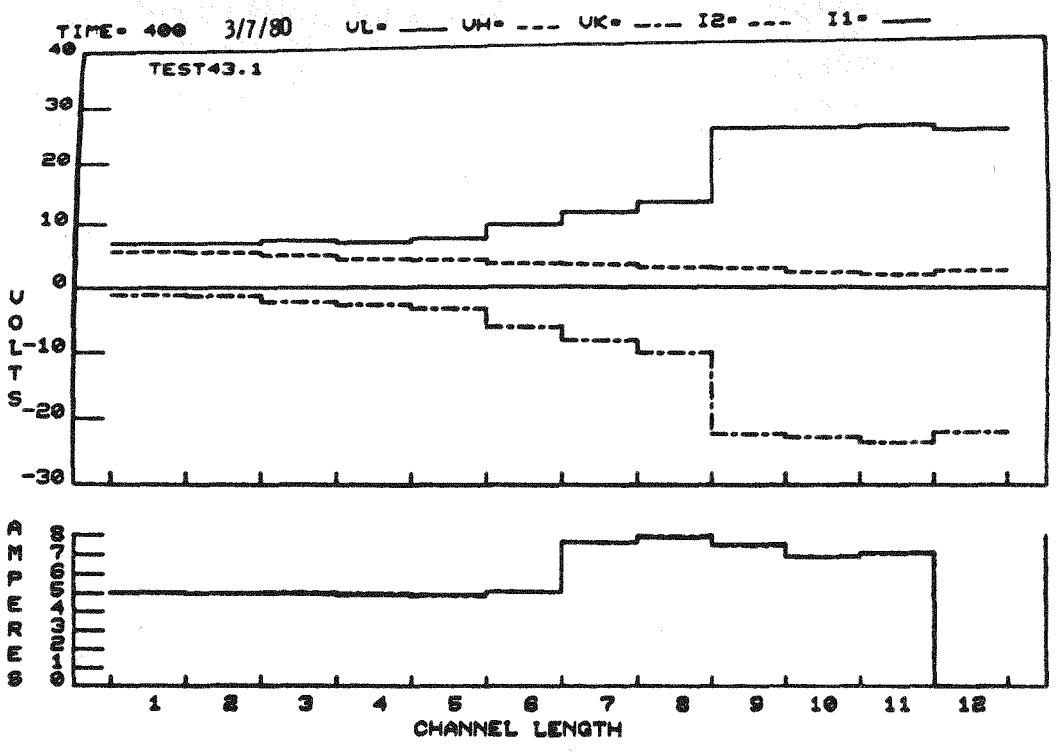

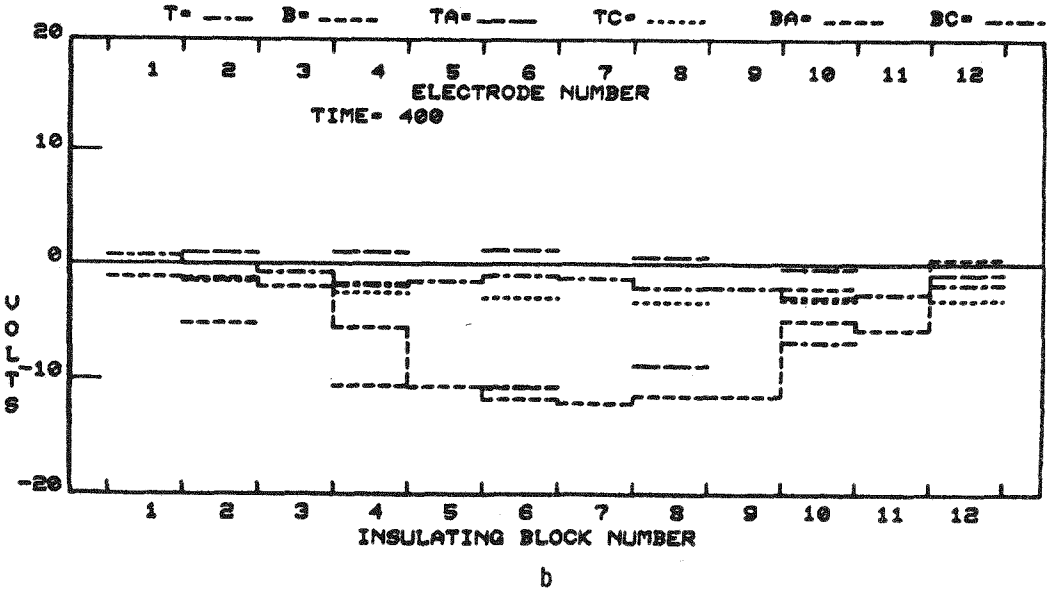

Figure 39. Voltage and Current Distribution, WESTF Test 43, 3/7/80

At 1900 when the currents in the channel were brought up to 7.0 amperes (corresponding to 1.2 A/cm^2), the electrical breaker controlling power to the combustor and to the first six power supplies opened up, interrupting fuel flow and shutting off the system.

The combustor was relit and brought up to temperature again. Seed was reintroduced at 2122; at 2130 the current in the channel was about 2.0 amperes (see Figure 36). The current level was gradually increased by time 2200 the current level was up to 5 amperes (.83 amps/cm^2). A voltage of about 120 volts was required to obtain this current level.

At 2300 the current levels in the last five electrode-pairs were brought to 7.5 amperes (1.25 A/cm^2). The currents in the first six power supplies were kept at 5 amperes for the remainder of the test to avoid retripping the system breaker.

It is evident from the curves taken at 2130 in Figure 36 that the reduction in voltage associated with the increase in electrode surface temperature still occurred after the power interruption. However, by 0130, 3/7/80, see Figure 37, it became clear that the decrease in voltage down the channel was no longer occurring. In fact the voltage distribution had reversed, and the voltage increased down the channel.

The change in the electrical characteristics took place gradually in the time period between 2130 and 2400. Figure 38, taken at 0200 and Figure 39, at 0400, shows radically altered voltage distributions in which the voltage required to transmit the required currents continues to increase with distance down the channel and was generally less than 30 volts.

It appears reasonable to conclude from the electrical data that the electrode system was reasonably intact until sometime between 2130 and 2400 on 3/6/80. It seems likely that the sudden change in temperature which occurred when system power was interrupted at 1900 damaged the Al_2O_3 substrate supporting the platinum sheet anodes. There were no obvious signs of damage to the Al_2O_3 anode substrates when the channel was dismantled after the test. From

the electrical data, however, it appears reasonable to conclude that the ceramic sections "popped off" as the channel was brought up to full loading after the power interruption.

As indicated previously the lower curves in Figures 30 to 39 give the potential distribution of selected backing plates in the insulating walls. The terminology used is defined in Figure 40. Because the number of circuits available for measuring the floating potentials of the backing plates were limited in number, it was not possible to read the potentials of all of the backing plates.

All of the central backing plates T1-T12, and B1-B12 were included in the measurements. However, only even number backing plates were used for the top and bottom of the channel. It was not possible however, to include BA12 and BC12 because of the lack of circuits.

At the beginning of the test the backing plates tended to assume negative potentials, see bottom of Figure 30. The negative potentials in Figure 30 indicate that leakage was more rapidly established to the negative electrodes. Within 10 minutes, leakage paths began to build up to the positive electrodes as well. The pattern of potentials which can be observed at the bottom of Figures 31 to 36 demonstrate that comparable substantial leakage paths had been established between the backing plates and the adjacent positive and negative electrodes. As can be seen in Figures 37 to 39, at the end of the test the leakage paths to the cathode electrodes predominated. This change in characteristic corresponds to the time period in which serious damage to the electrodes is surmised to have occurred.

WESTF Test 45

Visual inspection of the ZrO_2 - 20 m/o Y_2O_3 test electrodes (92% theoretically dense) indicated that the electrode surfaces had flowed under the shear forces of the plasma. Past experience suggested that this was due to the formation of a surface reaction layer with poor high-temperature creep resistance. Metallographic examination of sectioned electrodes showed a) blackening

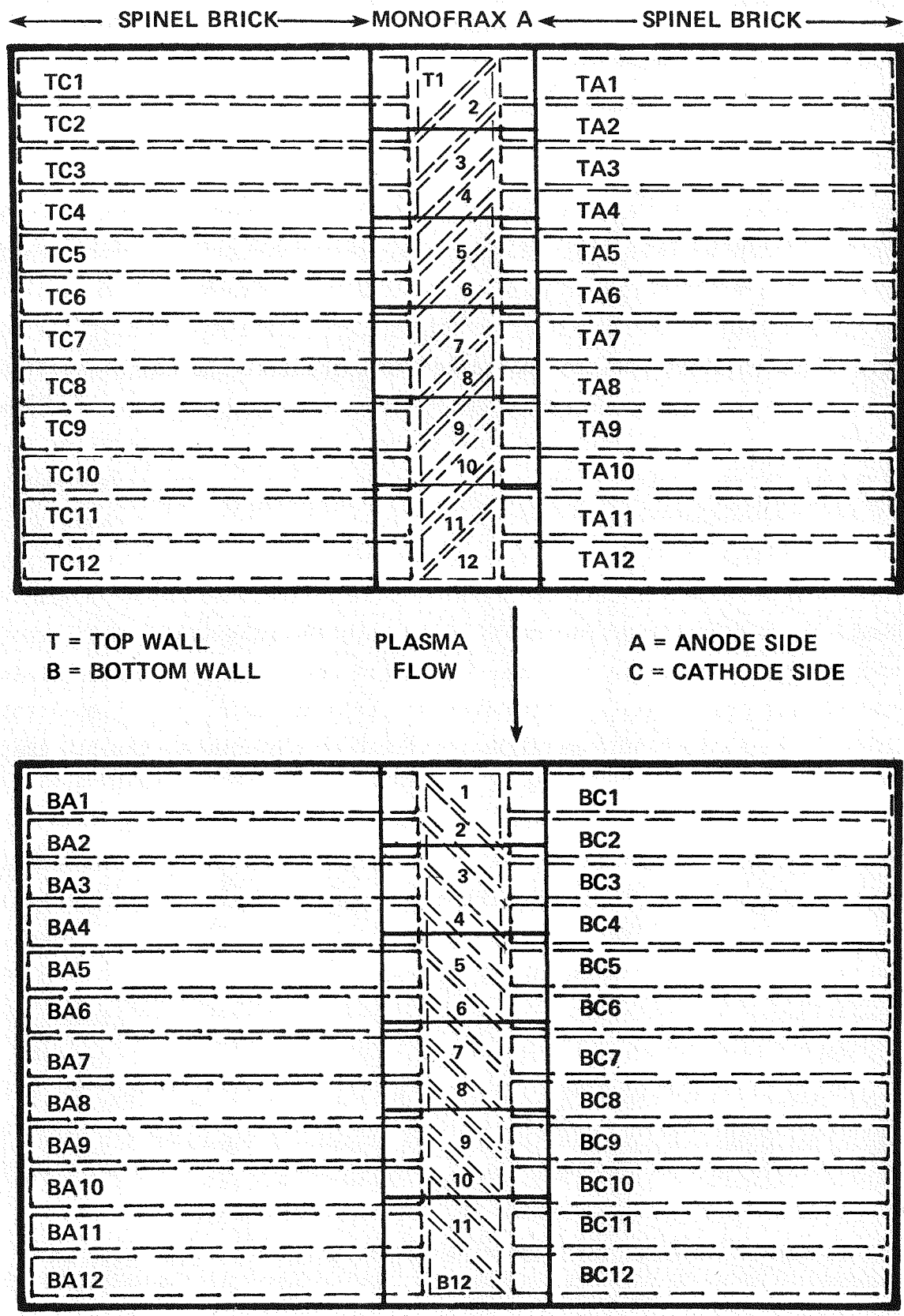

Figure 40. Schematic of Insulating Walls WESTF 41-Run 2 *615397-10A*

of the $ZrO_2(y)$ at the platinum/cathode interface and b) that the cathode was more severely cracked and bloated compared to the anode. To date SEM-EDAX analysis has been performed only on the anode. The following is a summary of these results.

Slag constituents have been deposited inside the anode to a depth of ~0.65 mm from the plasma/anode interface. Figure 40 shows part of this upper region of attack. The dark phase being slag rich while the light gray material is the ZrO_2 - 20 m/o Y_2O_3 phase. The fact that the ZrO_2 phase has recrystallized and spheroidized relative to the unattacked ZrO_2 phase at the colder section of the anode (see Figure 41) indicates that the slag constituents were liquid during the test. Clearly, the high volume fraction of liquid slag shown in Figure 40 explains why the surface of the electrodes sheared (flowed) in the test.

In all regions of the electrode where slag has condensed, it is very highly enriched in calcium compared to the original composition of the Rosebud flyash used in these experiments. The general trend in slag composition as one traverses from the electrode surface toward the interior is increasing Al, Si and K content but decreasing Ca content. However, even in the interior of the electrode, the calcium concentration is still greater than in the original flyash.

The surface regions of the ZrO_2 (Y) anode, in addition to having experienced grain growth and spheroidization, has undergone changes in chemical composition. At the hotter regions, the ZrO_2 has picked up calcium from the slag while yttrium and to a lesser extent the zirconium itslef has dissolved into the slag.

These data suggest that; a) calcia stabilized ZrO_2 would be a superior electrode material at superhot temperatures than yttria or other rare earth oxide stablized zirconia compositions, since the latter components tend to be quite soluble in molten coal slags; b) The fact that calcia rich slags deposit near the hot electrode surface and that more Al, Si and K rich slags (compositions that more closely approximate the initial flyash) deposit in the cooler interior of the electrodes suggest that thermal partitioning can be a very important factor determining the composition of the condensing slag, i.e.,

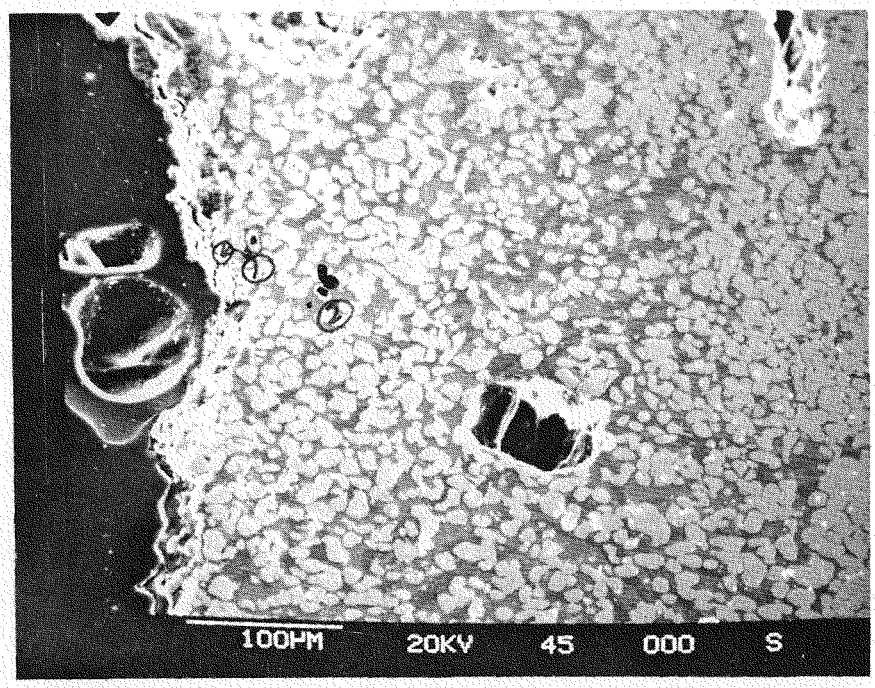

PLASMA ANODE

Figure 40. Top Region of ZrO_2-20 m/o Y_2O_3 - WESTF Test 45 (Dark Grey Regions are Slag)

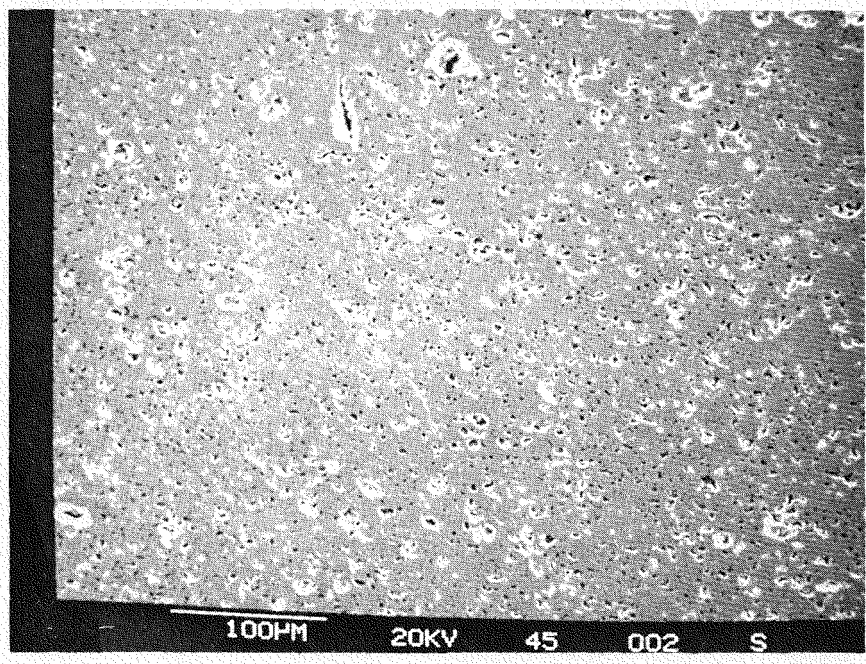

I. Interior Section of Unattached ZrO_2-20 m/o Y_2O_3 Anode after MTS Test 45

the more refractory slags condense out at the highest temperature regions of the electrode and visa versa. Since the chemical aggressiveness of slags are dependent on their composition, it is essential that future laboratory screening tests use slags whose compositions more closely reflects that which would condense from the plasma for the designed surface temperature of the electrodes.

WESTF Test 47

Post-test evaluation of WESTF Test 47 materials, platinum clad anodes and bare copper cathodes, operated under slagging cold conditions in the MTS II test section, have been performed using SEM-EDX analyses. In all cases there was no slag layer left adhering to the surfaces. The platinum anode surfaces exhibited localized melting due to arc impingement which was manifested as a "valley" and mountain pattern (see Figure 42). Arc damage was concentrated at the outer periphery of the anodes, a region of the 3/4 inch diameter samples which tended to run at the highest temperatures during the test. Some slag constituents were found to be physically incorporated into the once molten platinum globules or "mountains". The most dominant slag components were Ti, Ca, Si, K, S and Al. In some molten regions, there is evidence for the formation of intermetallic platinum compounds with titanium and silicon. EDAX indicates a persuasive presence of copper impurities, on the anode electrode surfaces, suggesting perhaps that it was transferred in the plasma phase from the cathode wall during the test.

As seen in Figure 43, there is evidence for chemical reaction and oxidation at the copper cathode surfaces but no direct signs of melting due to arc attack. Sulfur is the major impurity on the copper surface. Although, there is no slag layer remaining on the cathode to prove the following hypothesis, it is proposed that the principle mechanism of cathode loss during the test involved oxidation-sulfidation of the copper, followed by dissolution of the resulting copper compounds into the overlying slag layer.

Evaluation of Flame Pyrometer

The Flame Pyrometer is a relatively new instrument developed by IRCON, Inc. for measuring the temperatures of flames produced by burning fossil fuels.

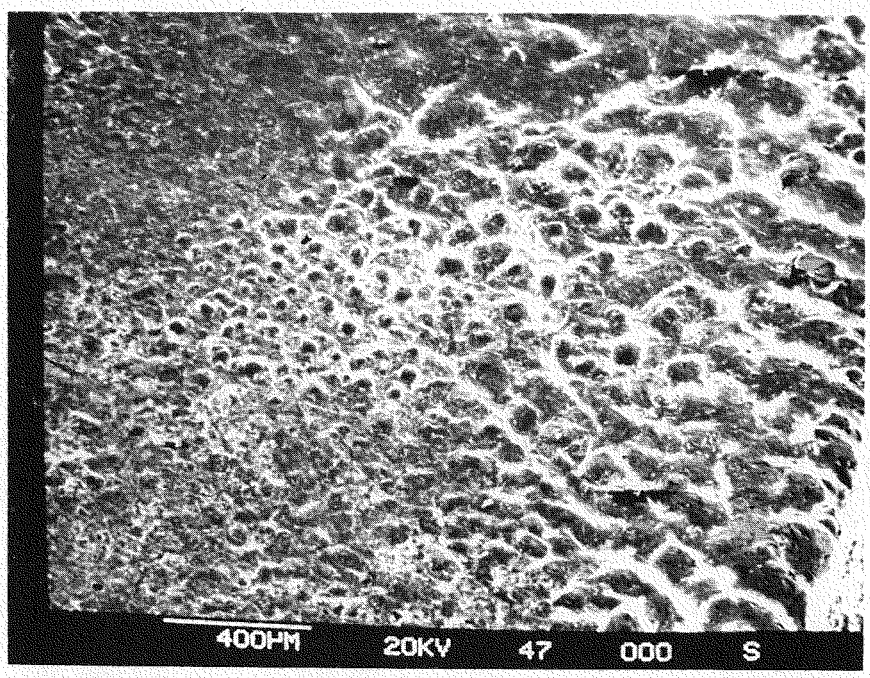

Figure 42. SEM Photograph of Surface of Platinum Coated Anode, WESTF Test 47 (Edge of Sample is at Right)

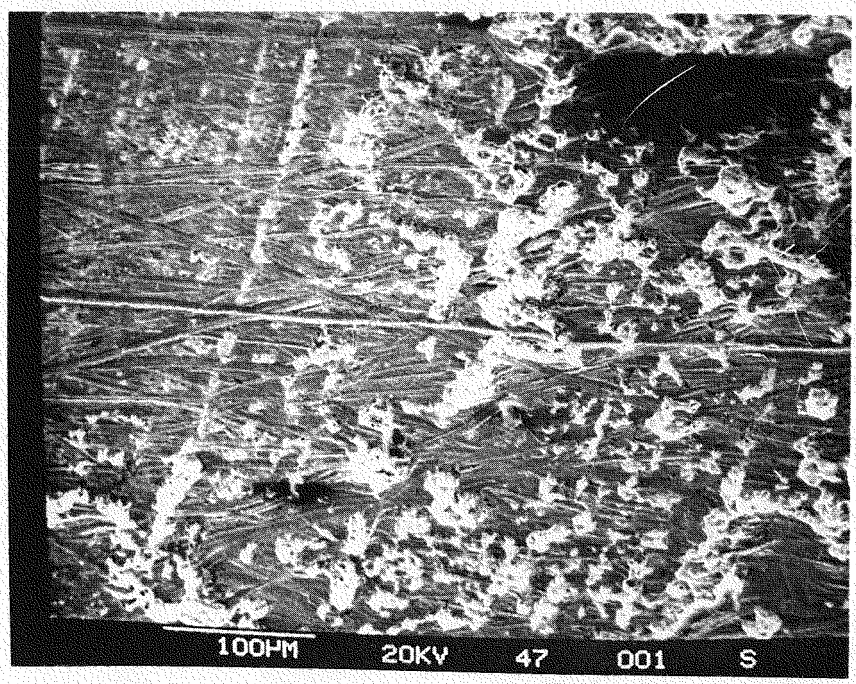

Figure 43. SEM Photograph of Surface of Copper Cathode, WESTF Test 47

The instrument works by sensing the emission radiated by CO_2 plasmas. Because it responds to radiation centered at 4.5 microns in a band 0.1 microns wide, the absorption of the cooler CO_2 layer situated at the boundaries of the system, which has an absorption maximum at 4.3 microns, is avoided.

The instrument has a dial control which permits correcting for the effective emissivity of the flame. Thus, correction can be made for absorption losses at windows, and for different flame thickness. Flames over 12 in. in diameter are treated as block bodies and require no emissivity correction. Emissivity corrections for flames between 3 in. and 12 in. are made according to a chart furnished by the manufacturer. According to the supplied curve a 6 in. diameter flame, which corresponds to the as-constructed diameter of the WESTF mixer, requires a flame emissivity correction of 0.83. The transmission correction for a 0.1 in. sapphire window is 0.88 according to IRCON data. The product of these two values, 0.73 was used in making the emissivity factor correction for WESTF Test 43.

The flame pyrometer used in the test was borrowed from IRCON in order to assess its potential usefulness for measuring MHD plasma temperatures. The construction used for mounting the instrument is shown in Figure 44. Because of the limited size of the penetration into the mixer, it was necessary to align the optical system of the instrument very accurately with the optical system of the window to avoid obstruction of signal. Any cut-off in the field of view would reduce signal output and result in excessively low temperature readings.

The 7/8" ball valve shown in Figure 44 was kept closed except when readings were being taken to minimize deposition of seed and ash on the window. By closing the valve it will be possible to remove the sapphire window for cleaning without shutting the system down. As shown in Figure 44 an air line was provided to permit bleeding air into the system to minimize deposition of seed and in the vicinity of the window.

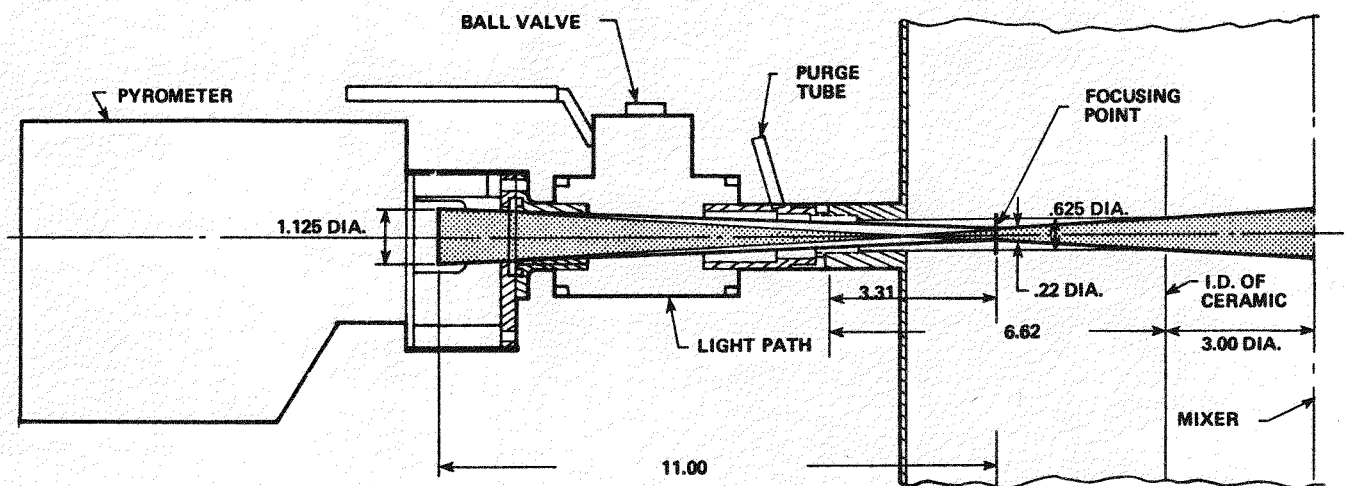

Figure 44. Installation of Flame Pyrometer on Mixer

WESTF Test 43

It became evident very early in WESTF Test 43, conducted on 3/6/80, that some of the signal to the sensor was being cut-off because of misalignment between the hole through the thick ceramic liner of the mixer and the metal flange supporting the sensor.

A summary of the flame pyrometer readings taken at different times during WESTF Test 43 is shown in Table 9. While the readings are low because of the misalignment referred to previously, the variation in temperatures appear to be reasonable. An initial substantial drop in temperature was observed both times, seed and ash were introduced, followed by a slow increase in temperature. The highest temperature observed during Test 43 was 2336 K which compares with anticipated theoretical temperatures between 2480K to 2670K for the combustion factors employed.

After the test the internal diameter of the mixer was measured and found to be 5.75 in., corresponding to a transmission factor of 0.82. The transmission of the 1.25 in. thick sapphire window at 4.5 microns was measured and found to be 0.805. The corrected value of emissivity as given by the product of these two revised factors is 0.66 instead of 0.73 used in the test.

The equation for correcting for a loss factor K at a wavelength of λ in cms is given by the following equation:

$$\ln K = \frac{C2}{\lambda} \left(\frac{1}{T} - \frac{1}{T_M}\right)$$

where T is the true temperature, T_M is the measured temperature, and the constant C_2 = 1.438.

Using this equation for the highest temperature shown in the Table 9, 2366K, the brightness or "measured" temperature at 4.5 microns for a "true temperature of 2366K, corresponds to 1919K. This is the temperature which would theoretically have been measured if the emissivity correction were set at unity.

TABLE 9

SUMMARY OF FLAME PYROMETER READINGS ON WESTF TEST 43, EMISSIVITY SET AT 0.73

TIME	TEMPERATURE K	REMARKS
1445	1911	System coming up in temperature
1452	2227	System coming up in temperature
1509	2227	System coming up in temperature
1533	2116	Seed on
1555	2033	Seed on
1600	----	Seed off
1620	----	Optical path blocked by ash
1900	----	Main circuit breaker opens
2029	----	Combustor relit
2055	1894	
2103	2666	
2108	2088	
2122	----	Seed on
2135	1894	
2207	2339	
2249	2366	
2300	2366	

Equation C1 can now be used to determine the "true" temperature for a brightness temperature of 1919K and an emissivity correction of 0.66. The corrected true temperature becomes 2557K instead of the 2366K temperature determined during the test with the emissivity set at 0.73. While the corrected temperature falls within the 2480K to 2670K theoretical range, it is clear that using an emissivity correction of 0.66 would be expected to give a still higher value of true temperature, since the field of view of the pyrometer was partially obstructed.

WESTF Test 49

The emissivity correction was set at 0.66 in. WESTF Test 49 based on the corrections discussed above. In addition the sensor was tilted to improve the optical alignment. The temperature readings observed were considerably higher than those obtained in WESTF Test 43. However, the passage way to the window was obstructed with deposits of seed and ash for a considerable part of the test. The following table summarizes some of the pertinent readings taken during the test.

SUMMARY OF FLAME PYROMETER READINGS, TEST 49,
EMISSIVITY SET AT 0.66

TIME	FLAME TEMP. K	REMARKS
1710	----	Seed on
1725	2689	Seed on
1804	2655	Seed on
1837	2727	Seed on

The expected theoretical plasma temperatures for the combustion factors employed was in the range between 2550 to 2650K.

It was hoped to compare plasma temperatures in combustor with plasma temperatures in the channel of Test 49, using the injection thermocouple/ technique described in last quarterly report. Unfortunately, mechanical misalignment prevented complete insertion of thermocouple.

From IRCON's calibration data a fossil fuel burning flame which is larger than 12 in. in diameter approximates a black body. With the configuration of combustor used in WESTF the ceramic liner once it comes up to temperature contributes radiation which increases the effective diameter of the flame, i.e., increases its effective emissivity. Radiation from any particles associated with the injection of seed and ash also increase the effective emissivity of the flame.

The observed drop in temperature when seed is introduced followed by a gradual later rise in temperature is not understood. The drop in temperature due to the injection of the water mixture of seed and ash would be anticipated. The later rise possibly is caused by a gradual increase in the temperature of the ceramic liner. Alternatively it could be due to more efficient vaporization of the seed and mixture with time or some preheat effect which occurs in the region where the seed volatilizes.

The flame pyrometer has the potentiality of being a very useful, possibly an indispensable tool per a large MHD installation in which the flame would have an emissivity of unity. It is a commercially available unit and simple to operate.

The instrument should also be very useful for WESTF, although further work is required to determine the appropriate emissivity values to use. Further effort is also required to provide a means of keeping the sight bore free of seed or ash. A mechanical system for periodically removing deposition products from the opening of the window would be very useful.

2.2 WBS 1.2.2 - Test Assembly Fabrication

During this quarter the following fabrication activities were completed or were in process.

- Completion of WESTF Test 43 Test Assembly
- Completion of WESTF Test 49 Test Assembly
- Completion of MTS II Viewport
- Fabrication of WESTF II Components

WESTF Test 43

The WESTF Test 43 section, designed for hot slagging operation, consists of an anode and cathode wall, each containing 12 electrodes, a top and bottom insulating wall, and an inlet and exit transition section. The anode is platinum, the cathode is iron (1018 carbon steel), and the lining for the insulating walls and transition sections is fused cast alumina. Interelectrode insulation is dense spinel on the anode wall and dense MgO on the cathode wall. Filler material is fused cast alumina and/or an alumina based adhesive.

The design and fabrication of the electrode sub-assemblies were discussed in Reference 3. Design details and dimensions are summarized in Table 10 for the anodes and in Table 11 for the cathodes. Photographs of the anode wall appear in Figure 45 and of the cathode wall in Figure 46. Electrode pitch on both walls is 1.36 cm. For each electrode, a surface area of 1 cm x 6 cm is exposed to the plasma.

The insulating walls consist of 36 cooling blocks on each wall, 12 long blocks on each side and 12 diagonal blocks within the center of the duct. A nominal 0.040 inch gap separates the blocks. The gap is filled with a low-viscosity heat curable silicone elastomer for electrical isolation. The cooling blocks on each insulating wall are covered with six interlocking fused cast alumina tiles, 0.600 cm (0.236 inch) thick in the duct (maximum design surface temperature = 900°C). A copper shim is used behind the tiles to adjust the height to 0.737 cm (0.290 inches) thick insulators used in WESTF 41. The side tiles are 82 percent dense spinel brick, 0.737 cm (0.290) inches thick. The ceramic insulators overlap the copper cooling blocks and are attached to them with RTV silicone adhesive. The center tiles extend beyond the electrodes so that they are locked in place and cannot move should the adhesive fail. A G-7 spacer backs up the cooling blocks and maintains them at a fixed distance from the G-10 outer wall.

Fused cast alumina, 600 cm (.236 inch) thick, is used to line the transition sections to give a maximum design surface temperature of 1650°C. The attachment is RTV silicone adhesive.

TABLE 10

NOMINAL DIMENSIONS AND TEMPERATURES - ANODE DESIGN - WESTF TEST NO. 43

Channel Position, Designation	1 201	2 202	3 203	4 204	5 205	6 206	7 207	8 208	9 209	10 210	11 211	12 212
Avg. Electrode Surface Temp(1) (K)	1400 ± 75			1475 ± 75			1550 ± 75			1625 ± 75		
Avg. Insulator Surface Temp (K)	1625 ± 50			1675 ± 50			1730 ± 50			1785 ± 50		
Avg. Insulator Back Face Temp (K)	835 ± 25			795 ± 25			767 ± 25			742 ± 25		
Avg. Electrode Ceramic Back Face Temp (K)	1050 ± 25			1035 ± 25			1025 ± 25			1012 ± 25		
Thickness of Insulator ($MgAl_2O_4$) (in.)	0.047 ± 0.002			0.107 ± 0.002			0.167 ± 0.002			0.227 ± 0.002		
Thickness of Platinum Surface (in.)(1)	0.01			0.01			0.01			0.01		
Thickness of Ceramic Substrate (Al_2O_3) (in.)	0.037 ± 0.002			0.097 ± 0.002			0.157 ± 0.002			0.217 ± 0.002		
Nominal Thickness of Nickel Mesh Compliant Layer (in.)(1)	0.200 ± 0.02			0.200 ± 0.02			0.200 ± 0.02			0.200 ± 0.02		
Nominal Distance of Electrode Surface to (OD) Outside of Heat Sink Cooling Passage (in.)	0.955			1.015			1.075			1.135		
Hydraulic Dia. of Cooling Passage (in.)	0.125			0.125			0.125			0.125		
Nominal Required Water Flow Rate for Cooling Passage (gph)	50 ± 5			50 ± 5			50 ± 5			50 ± 5		

TABLE 11

NOMINAL DIMENSIONS AND TEMPERATURES - CATHODE DESIGN - WESTF TEST NO. 43

Channel Position, Designation	1 101	2 102	3 103	4 104	5 105	6 106	7 107	8 108	9 109	10 110	11 111	12 112
Average Electrode Surface Temp[1] (K)	1300 ± 75			1375 ± 75			1450 ± 75			1525 ± 75		
Average Insulator Surface Temp (K)	1510 ± 50			1545 ± 50			1625 ± 50			1675 ± 50		
Average Insulator Back Face Temp (K)	730 ± 25			705 ± 25			658 ± 25			645 ± 25		
Thickness of Insulator (MgO)	0.440 ± 0.005			0.522 ± 0.005			0.752 ± 0.005			0.802 ± 0.005		
Thickness of Ceramic Filler (Al_2O_3) (in.)	0.400 ± 0.005			0.482 ± 0.005			0.712 ± 0.005			0.762 ± 0.005		
Nominal Width of Steel Rib (in.)	0.200 ± 0.005			0.200 ± 0.005			0.200 ± 0.005			0.200 ± 0.005		
Nominal Distance of Electrode Surface to (OD) Outside of Heat Sink Cooling Passage (in.)	1.340			1.422			1.652			1.702		
Hydraulic Diameter of Cooling Passage (in.)	0.125			0.125			0.125			0.125		
Nominal Required Water Flow Rate for Cooling Passage (gph)	50 ± 5			50 ± 5			50 ± 5			50 ± 5		

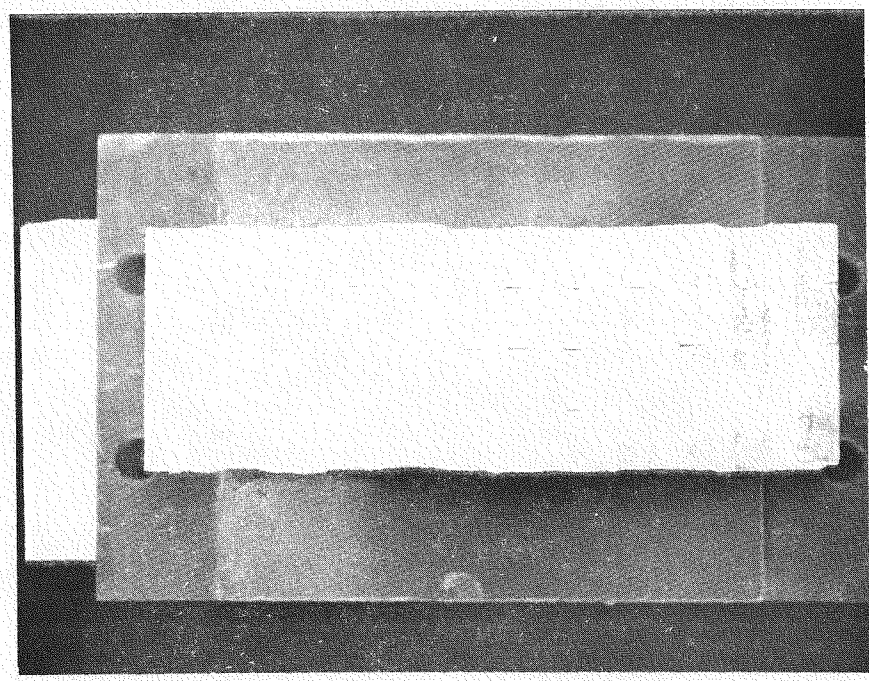

(A) Top View

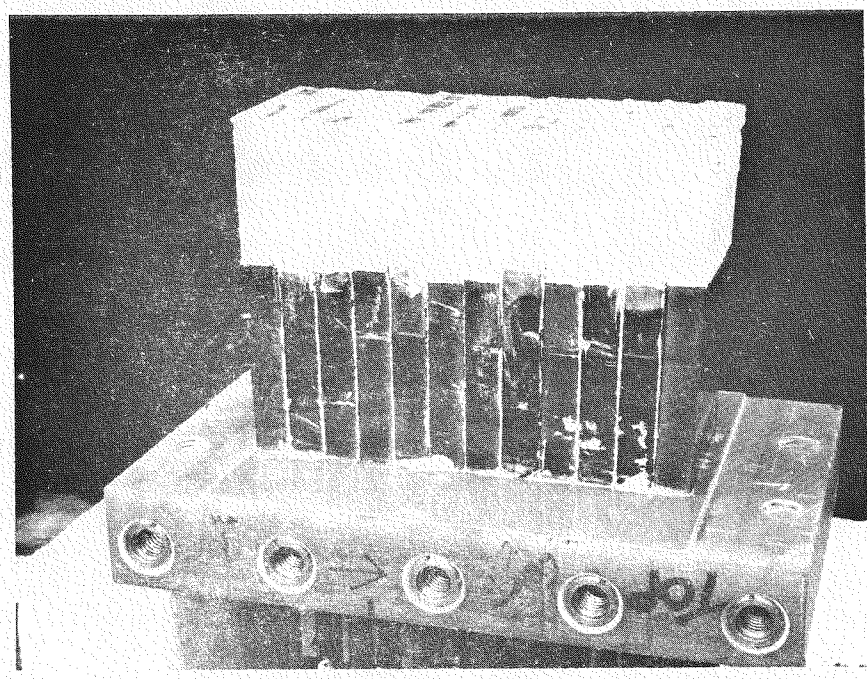

(B) Side View

Figure 45. WESTF Test 43 - Anode Wall

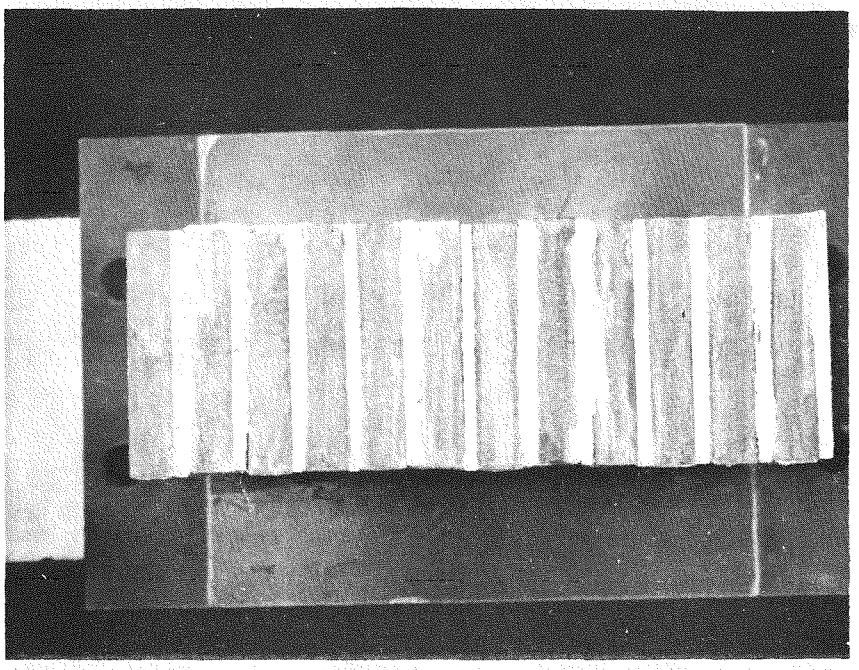

(A) Top View

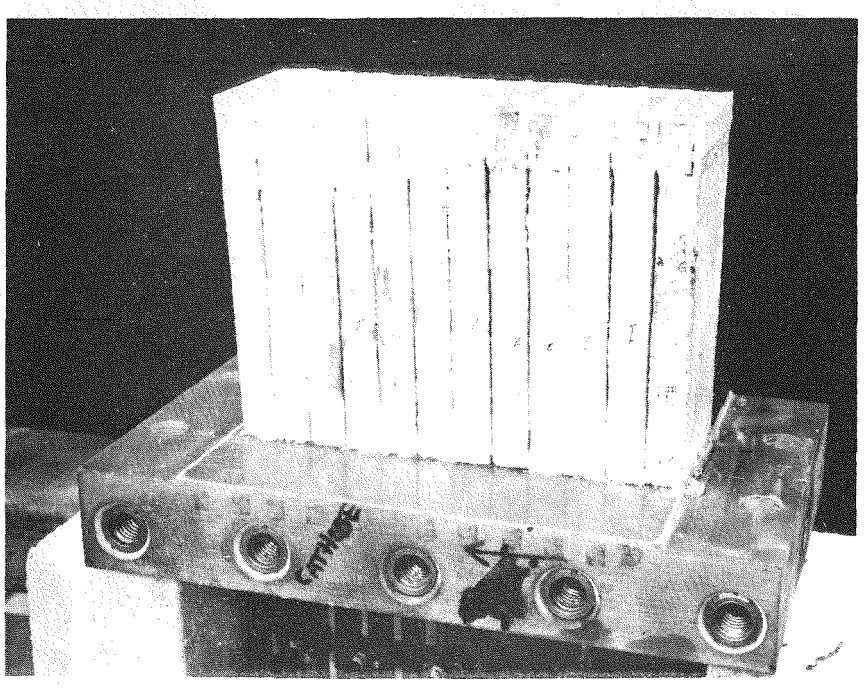

(B) Side View

Figure 46. WESTF Test 43 - Cathode Wall

Thermocouple types and locations for the electrode walls are given in Table 12. There are no thermocouples in the insulating walls. A type "R" thermocouple is located 0.35 cm below the surface of the alumina tiles in both the inlet and exit transition section. Also, an injectable Ir-Rh thermocouple will be used to measure plasma temperature in both the inlet and outlet transition sections.

A Type "E" thermocouple is located in the exit leg of each electrode to measure the temperature rise in each electrode water cooling passage. These are visible in a photograph of the assembled test section shown in Figure 47.

Resistance measurements were made on the assembled test section, and they showed that no conductive paths existed between components on each of the walls or between electrode walls, insulating walls and transition sections. Water flow measurements were also made through groups of three electrode in series on the electrode walls and on the top and bottom insulating walls as a function of supply pressure.

WESTF Test 49

WESTF Test 49 was fabricated to test three pair of 0.5 $SrZrO_3$ · 0.5 ($Sr_{.25}La_{.75}FeO_3$) electrodes supplied by MIT for testing in a non-slagging super-hot MHD environment. The electrodes were fitted in the MTS II test section, which consists of a water-cooled stainless steel casing lined with magnesia castable insulation. Each of the six electrodes was surrounded by a cylindrical MgO insulator 0.25 in. thick. The insulator extends 0.407 in. from the electrode surface and then is backed by boron nitride insulation. Both the anode and cathode walls contain 0.257 in. thick electrode discs brazed to copper mesh (0.062 inches thick) which, in turn, is brazed to water-cooled copper. The test section instrumentation included two Ir/Rh thermocouples, one positioned in the gas stream that can be retracted and one imbedded in the MgO insulation. These were both located in the top insulating wall. In addition, a Type S thermocouple sheathed with Inconel 600 was positioned in each ceramic electrode 0.157 in. from the plasma surface. Assembly was completed without incident.

TABLE 12

WESTF TEST 43 ELECTRODE THERMOCOUPLES

ELECTRODE	TYPE	NO.	THERMOCOUPLE DIMENSION FROM HOT SURFACE
Anodes			
A02	K	A-1	0.336"
A02	K	A-2	0.606"
A05	K	A-3	0.396"
A05	K	A-4	0.666"
A08	B	A-6	0.079"
A08	B	A-7	0.079"
A08	K	A-5	0.726"
A08	K	A-8	0.726"
A11	B	A-11	0.109"
A11	B	A-12	0.109"
A11	K	A-9	0.786"
A11	K	A-10	0.786"
Cathodes			
C02	B	C-1	0.080"
C02	B	C-2	0.080"
C02	K	C-3	0.892"
C05	B	C-4	0.080"
C05	B	C-5	0.080"
C05	K	C-6	0.974"
C08	B	C-7	0.080"
C08	B	C-8	0.080"
C08	B	C-9	0.080"
C08	K	C-10	1.204"
C11	B	C-11	0.080"
C11	B	C-12	0.080"
C11	K	C-13	1.248"

Totals = Anodes + Cathodes
(25) (12) (13)

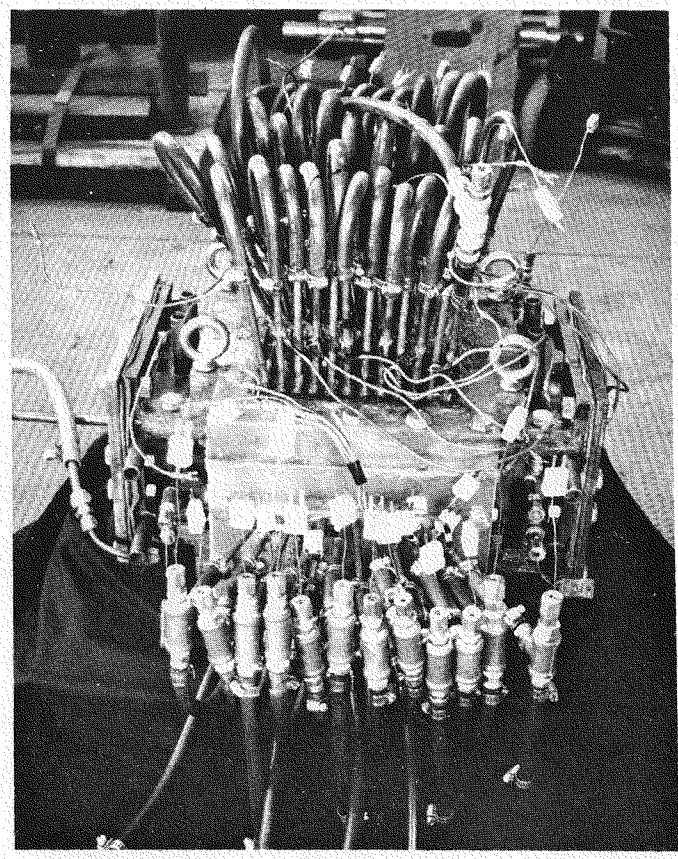

Figure 47. WESTF 43 Test Section

MTS II Viewport

The viewport which connects directly downstream of the Materials Test Section (MTS II) was fabricated. The vessel, shown previously in Figure 17, consists of two stainless steel tubes, the larger one used for the passage of the plasma and the smaller one for sighting on an upstream electrode. The viewing arm was welded to the main tube at a 20° angle for optimum observation of the electrode surface. Other weldments included a fitting for introducing an inert gas into the viewing chamber, a fitting and support hook for operating a manual metal shutter, and two 9 inch diameter stainless steel flanges slip fitted on the ends of the main tube. The end of the sight tube was threaded to receive a steel cap which contains the 0.375 inch thick quartz viewing window. An o-ring seats up against the metal and glass to seal the viewport. The whole vessel was stress relieved at 800°C prior to final machining. A hydrostatic pressure of 90 psi was to be met inside the chamber before its use in an actual test.

WESTF Component Fabrication

The installation of the 3 Tesla conventional magnet in WESTF makes it necessary to modify some parts and/or replace them with newly designed hardware. Relocation of the flow train gives rise to new dimensions for some parts. The test section designed for use with the magnet is constrained by the available space in the magnet bore and, consequently, the size of the duct in the test section has changed. Thus, changes in the nozzle and other components that contain hot plasma are required. The redesign and/or modification and the manufacture of these parts are underway.

Test Passage Hardware

The copper nozzle is being remade to have a 1.41 x 1.96 in. channel opening. Modifications that will only slightly impact the manufacturing schedule have been incorporated in the design of the new nozzle. These are an increase in the diameter of the water cooling passages near the square opening, an increase in the radius in the region of the transition from the round mixer

side of the nozzle to the square channel, and the addition of grooves in the square channel that, when filled with castable, will improve protective slag retention.

The interface between the nozzle and the flange is being adjusted to provide a better fit between the two. This is being accomplised by resurfacing the mixer flange in the area where it contacts the nozzle. As an adjustment to this, the nozzle will extend through the mixer flange and key to the adjacent downstream section for better alignment of the flow train components.

Dummy Test Section

"Dummy Test Section" is the term given to a refractory lined, water-cooled, flanged steel pipe section that is used for facility checkout runs in place of a more sophisticated test section. It is being remade to have a 1.96 in. x 1.41 in. flow area. It is also being mocked up to have the WESTF II envelope dimensions (9.88 in. x 5.25 in.) in the area where WESTF II would pass through the magnet. Thus, the dummy test section will be used to (1) ensure proper fitup of WESTF components up to, through, and beyond the magnet and (2) to be used for facility checkout runs without the magnet. The dummy test section will be bolted to a refractory lined, water-cooled spool section that in turn will be bolted to the mixer flange. Both of these parts are currently being fabricated.

WESTF-II Test Sections Components

Prototype WESTF II Test Sections are being fabricated and tested in support of the on-going design activity. Prototype G-11 window frame have been fabricated and tested to evaluate the leak tightness of the frame to frame joint. Using a formed in place silicon rubber gasket, these frames satisfactorily withstood an internal pressure of 150 psi with no leakage. A very strong bond formed between the frames that made them difficult to separate. When the frames were separated, the bond line was found to be nil. Specimens were prepared with a "zero" bond line and a 5 mil bond line and tested in tension and shear modes. The degree of separation made little difference in the test results. Values of the breaking load were 200 + 14 psi in tension

and 119 ± 16 psi in shear. In order to aid disassembly of the WESTF II Test Sections, the frames were modified to provide for the use of a wedge-shaped tool to separate the frames.

The thermal capabilities of the G-11 tube material was tested by placing a sample in an oven and increasing the temperature until an effect on the sample was noted. It wasn't until a temperature of over 200°C was reached that the originally light green sample began to char, turn tan in color, and delaminate. Also, creep tests were performed at 150°C in the three point mode at loads of 100 to 400 lbs, and times of up to 50 hours. At loads up to 300 lbs. the maximum deflection was 2.5 mils; at 400 lbs. the maximum deflection was 6 mils. At the end of these tests there was no permanent sample deformation. These data indicate that the G-11 tubular material is suitable for use as a structural member of the test section.

The capability for applying a nylon powder coating has been developed. It will be used initially to coat a part of one of the components of the water cooling assembly of the insulating peg wall design to provide electrical insulation between the inlet and outlet tubing. The nylon powder coating is adherent on the tube end and can be machined to the close tolerance required.

Parts are being machined to build and test one complete frame assembly containing two electrode pair with the new pitch of 0.7 cm. Based on the successful evaluation of that frame, a mini-WESTF test assembly will be fabricated.

2.3 WBS 1.2.3 - WESTF Operations

WESTF operations during this quarter included the completion of WESTF Tests 47, 42, 43 and 49 in that order. Following the completion of WESTF Test 49, the facility was shut down for scheduled facility modifications required in view of the addition of a 3 Tesla conventional magnet. This activity is discussed in Section IV-3.0.

2.3.1 Pre-Test Activities

There were no extraordinary pre-test activities completed during the reporting period. Those activities completed were those associated with

the post-test removal of the WESTF Test 45 test section and the subsequent installation, checkout and removal of test sections for the following WESTF tests:

- WESTF Test 47 (MTS II)
- WESTF Test 42 (WESTF)
- WESTF Test 43 (WESTF)
- WESTF Test 49 (MTS II)

2.3.2 Test Operations

WESTF Test 47

WESTF Test 47, MTS II test section, was completed on January 3, 1980 and provided performance and durability data to evaluate platinum clad copper electrode material in a slagging cold, western slag environment. Table 13 presents operating conditions and chronology. Seed flow time totaled 5.7 hours and exposure of electrodes at test conditions totaled 6.5 hours.

WESTF Test 42

WESTF Test 42 was a screening test of hafnia and zirconia electrode material coupons and insulating wall materials under non-slagging super-hot conditions. The primary objective of the test was to provide relative performance data for these materials over a range of temperatures and in the absence of electrical or magnetic fields.

The test was conducted on January 22-23, 1980 and the operating time, combustor on to combustor off, was 22.2 hours. A buildup of slag at the exit of the test channel was encountered which necessitated shutoff of the slag/seed injection system prior to completion of the test. As a result, only 8.7 hours of operation were with slag/seed flow. The hafnia materials were supplied by BPNL and BPNL participated in the conduct of the test.

The elapsed time from ignition to combustor shutoff was 22.2 hours. A summary chronology of the test and average values for the various parameters during the

TABLE 13

WESTF TEST 47 OPERATING CONDITIONS AND CHRONOLOGY

OPERATING CONDITIONS

Operating Mode	Slagging Cold
Gas Temperature, K	2650
Static Pressure, atm	1.1
Plasma Mass Flow, kg/s	0.067
K_2CO_3 Seed Concentration, w/o K	1.0
Flyash Concentration (Rosebud)	0.001
Heating Rate, °C/min.	20
Cooling Rate, °C/min.	Quick Ramp Down
Cooling Water Flow, gph	20
SO_2 in Plasma, m/o	0.3

CHRONOLOGY

Conditions	Date	Time	Elapsed Time, Hrs.
Start-up	1/3/80	0730	---
Air Preheat ON	1/3/80	0748	0.3
Combustor ON	1/3/80	0940	2.1
Test Condition Established	1/3/80	1020	2.8
Seed ON	1/3/80	1100	3.5
Seed OFF	1/3/80	1648	9.3
Cooldown Started	1/3/80	1648	9.3

test are shown in Table 14. Optical pyrometer readings taken during the test are shown in Table 15. Typical data are shown in Figures 48 through 50.

A buildup of slag/seed occurred at the exit of the channel which caused the static pressure within the channel to build-up excessively. When this occurred the seed/slag mixture was turned off and a low flow of water was injected through the seed/slag injection system until the problem cleared up. At 17.6 hours into the test a buildup occurred which could not be alleviated and caused a subsequent end to the test at 24.0 hours. A slow drift downward of the air preheat temperature may have aggravated the situation although the estimated plasma temperature and electrode thermocouple temperatures remained as required.

Large variations in the recorded city inlet water temperature for some unknown reason caused large perturbations in the calorimetric heat flux measurements The effect can be seen in the plots of heat flux.

WESTF Test 43

WESTF Test 43 was completed on March 7, 1980. The test conditions obtained subjected platinum anodes and iron cathodes to a slagging hot mode environment. The primary objective of this test was to assess the performance and durability of the electrode designs and of the interrelated performance of the associated electrical insulators. Table 16 presents the average conditions achieved during the test and the test chronology. An accumulation of 9.8 hours of seed flow time was acquired while temperature test conditions were maintained for 13 hours.

During this test, at 1850 on March 6, 1980, there was a temporary shutdown of the combustor due to a breaker trip. The combustor was restarted within 15 minutes. During the test there also was an intermittent build-up in internal pressure which necessitated shut-off of the seed supply.

WESTF Test 49

WESTF Test 49 was completed on March 14, 1980 and provided performance and durability data by which to evaluate the MIT electrode material $La_2FeO_3 \cdot SrZrO_3 \cdot SrFeO_3$. Test conditions simulated a non-slagging super-Hot operating mode in

TABLE 14

WESTF TEST 42 OPERATING CONDITIONS AND CHRONOLOGY

CHRONOLOGY	Time	Date	Lapse Time
Start-up	0830	1/22/80	0.0 Hours
Preheater Ignition	0850	1/22/80	0.3
Combustor Ignition	1058	1/22/80	2.4
Oxygen ON	1114	1/22/80	3.2
Calibration Hold at Conditions	1200	1/22/80	3.5
Seed/Slag ON	1500	1/22/80	6.5
Seed/Slag OFF Due to Pressure Buildup	2230	1/22/80	14.0
Seed/Slag ON	2300	1/22/80	14.5
Seed/Slag OFF Due to Pressure Buildup	0010	1/23/80	15.6
Seed/Slag ON Preheat Temperature Dropped	0300	1/23/80	17.5
Seed/Slag OFF Due to Pressure Buildup	0310	1/23/80	17.6
Cooldown Started	0830	1/23/80	24.0
Combustor OFF	0910	1/23/80	24.6
Preheat OFF	0915	1/23/80	24.65

AVERAGE TEST PARAMETERS

Mass Flow, kg/s	0.084 Kg/sec
Oxygen Flow, kg/s	0.018 Kg/sec
Air Flow, kg/s	0.055 Kg/sec
Fuel Flow, kg/s	0.006 Kg/sec
Air Preheat Temperature, °C	500°C
Slag Concentration, %	0.1
Potassium Concentration, w/o	1.0
Fuel	No. 2 Fuel Oil
Stoichiometry, Oxygen Equivalence Ratio	1.6
Plasma Temperature, Theoretical, K	2320
Plasma Velocity, m/s	400
SO_2 in Plasma, m/o	0.06

TABLE 15

WESTF TEST 42 OPTICAL PYROMETER READINGS

Time	Day	Reading
1505	1/22/80	1640°C
1530	1/22/80	1370
1600	1/22/80	1420
1630	1/22/80	1470
1700	1/22/80	1400
1730	1/22/80	1420
1800	1/22/80	1425
1900	1/22/80	1420
1930	1/22/80	1430
2000	1/22/80	1410
2030	1/22/80	1410
2100	1/22/80	1415
2130	1/22/80	1370
2200	1/22/80	1380
2230	1/22/80	1420
2300	1/22/80	1410
2330	1/22/80	1420
0	1/23/80	1410
0030	1/23/80	1420
0130	1/23/80	1420
0200	1/23/80	1420
0230	1/23/80	1410
0300	1/23/80	1410
0330	Sight Port blocked with seed/slag	

(1) Sighting on position 6 of anode wall.

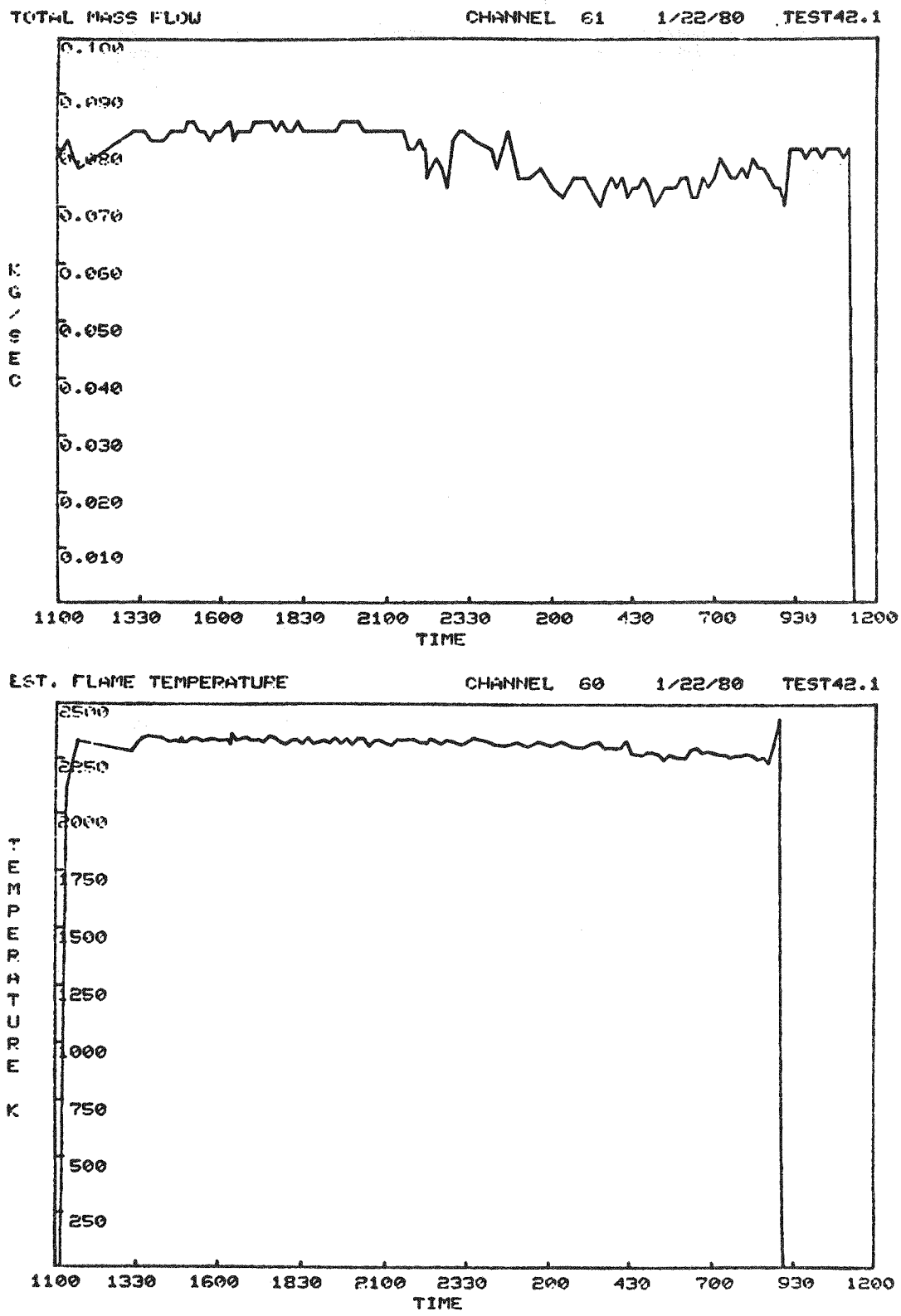

Figure 48. WESTF Test 42, Estimated Flame Temperature and Mass Flow

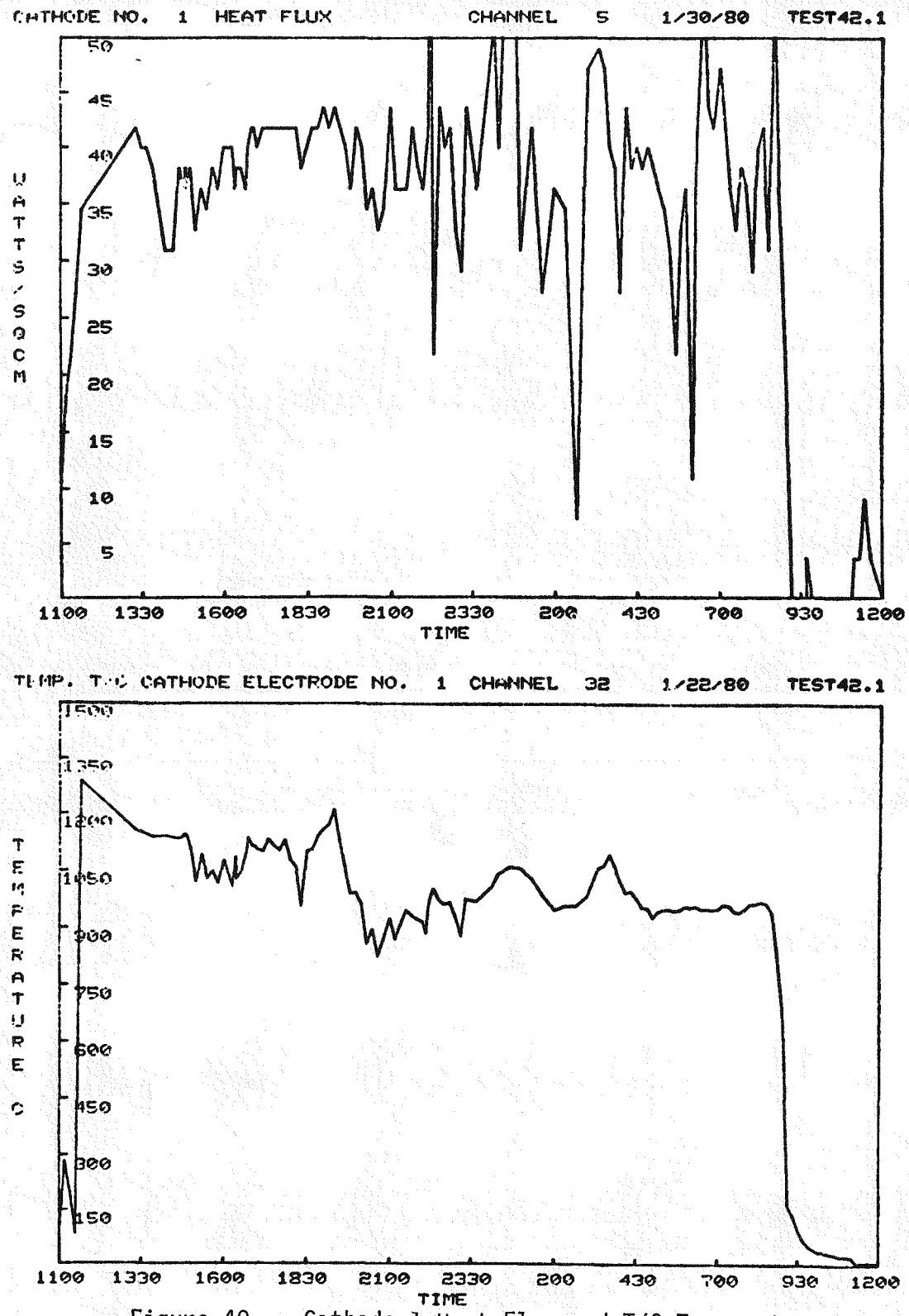

Figure 49. Cathode 1 Heat Flux and T/C Temperature

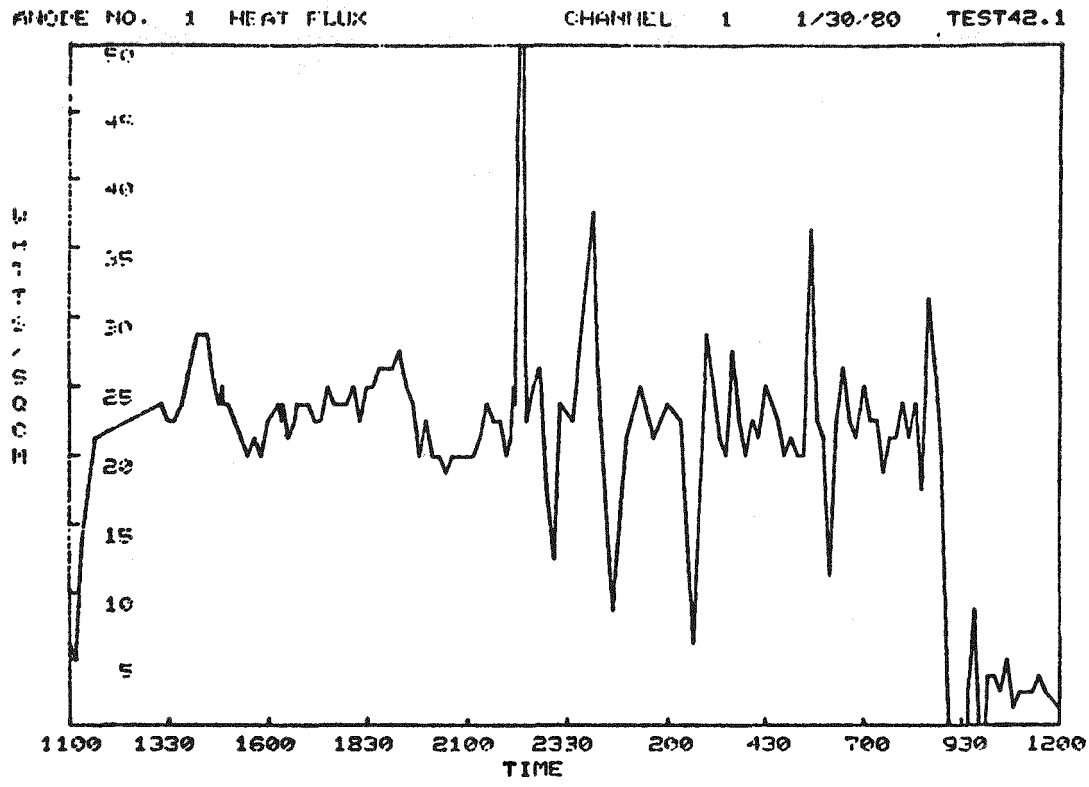

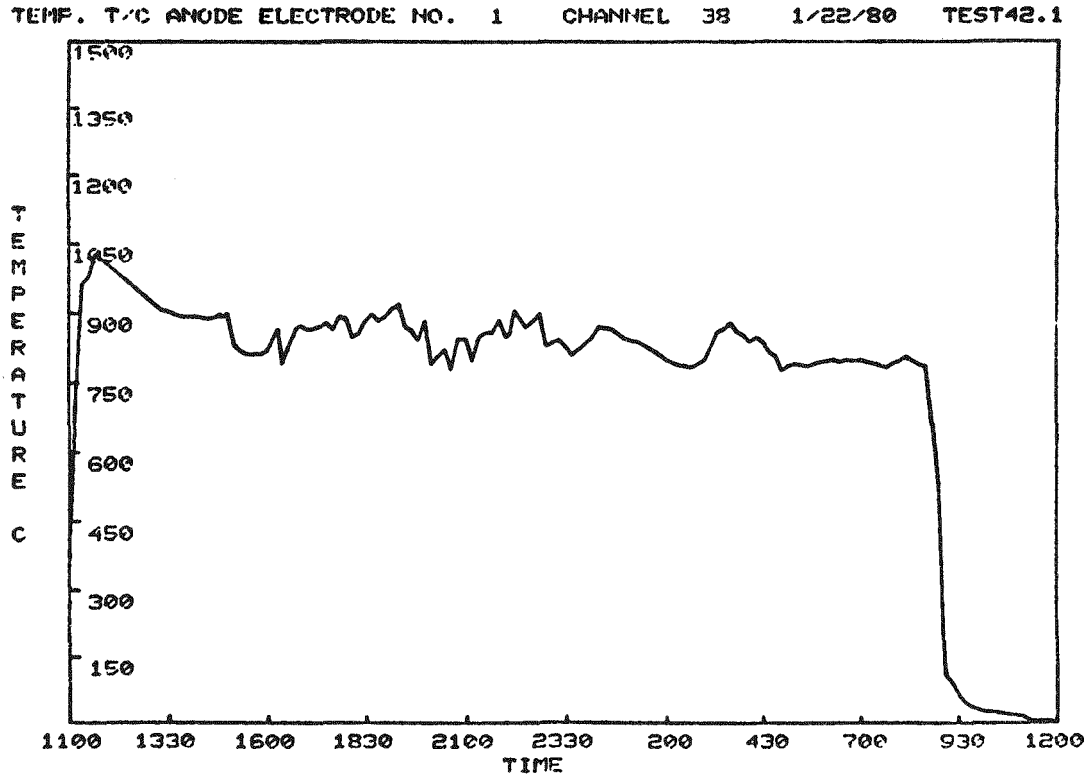

Figure 50. Anode 1 Heat Flux and T/C Temperature

TABLE 16

WESTF TEST 43 OPERATING CONDITIONS AND CHRONOLOGY

OPERATING CONDITIONS

Operating Mode	Slagging Hot
Gas Temperature, °K	2650
Static Pressure, atm	1.1
Plasma Mass Flow, kg/s	0.165
K_2CO_3 Seed Concentration, w/o K	1.0
Flyash Concentration (Rosebud)	0.001
Heating Rate, °C/min.	20
Cooling Rate, °C/min.	20
Cooling Water Flow, gph	55
SO_2 in Plasma, m/o	0.06

CHRONOLOGY

Conditions	Date	Time	Elapsed Time Hrs.
Start-up	3/6/80	0830	0
Air Preheat ON	3/6/80	0850	0.3
Combustor ON	3/6/80	1150	3.3
Test Condition Established	3/6/80	1310	5.7
Seed ON	3/6/80	1525	7.0
Seed OFF	3/6/80	1600	7.5
Seed ON	3/6/80	1605	7.5
Combustor OFF	3/6/80	1850	10.3
Combustor ON	3/6/80	1903	10.5
Seed ON	3/6/80	2025	12.0
Seed OFF	3/7/80	0404	20.0
Combustor OFF	3/7/80	0415	20.2
Preheat OFF	3/7/70	0435	20.5

the absence of electrical on magnetic fields. Table 17 presents the operating conditions and test chronology. Eight hours of seed time was accumulated at test conditions.

3.0 WBS 1.3 - WESTF MODIFICATIONS

3.1 MINI-COMPUTER/DAS

Upgrading of the mini-computer was completed this quarter with the installation and checkout of the additional core memory system.

3.2 MAGNET INSTALLATION

Satisfactory progress has been achieved in most areas associated with the magnet modification and supporting facility modification activities. Following the completion of WESTF Test 49, the facility was shut-down and major facility modifications initiated.

With the exception of the magnet power supply, all primary equipment items have been received. The power supply vendor identified a further slip in delivery to May 30, 1980, however, this schedule has been expedited. Milestones were established with the vendor in order to permit a tracking of progress. The current estimate is that the power supply will be delivered by the first week of May 1980.

Disassembly and removal of the flow passage has been completed to permit the major renovation of the WESTF test area. The 5KV feeder cables and load interrupter switches have been installed. Modifications to the water system, hook-up to the Recirculating Cooling Water System, are in process. Installation of the floor trench, for instrumentation wiring and cooling lines, is in process.

Design of the flow panel, load bank and isolation section for the air preheater line have been completed. Details are presented below for the load bank and isolation section.

TABLE 17

WESTF TEST 49 OPERATING CONDITIONS AND CHRONOLOGY

OPERATING CONDITIONS

Operating Mode	Non-Slagging Super-Hot
Gas Temperature, °K	2650
Static Pressure, atmp	1.1
Plasma Mass Flow, kg/sec	0.14
K_2CO_3 Seed Concentration, w/o K	1.0
Flyash Concentration (Rosebud)	0.001
Heating Rate, °C/min.	20
Cooling Rate, °C/min.	20
Cooling Water Flow, gph	55
SO_2 in Plasma, m/o	0.06

CHRONOLOGY

Conditions	Date	Time	Elapsed Time Hrs.
Start-up	3/13/80	0830	0
Air Preheat ON	3/13/80	0850	0.3
Combustor ON	3/13/80	1600	7.5
Test Conditions Established	3/13/80	1705	8.5
Seed ON	3/13/80	1710	8.7
Seed OFF	3/13/80	1750	9.3
Seed ON	3/13/80	1815	9.8
Seed OFF	3/13/80	0350	15.5
Cooldown STARTED	3/13/80	0355	15.5
Combustor OFF	3/13/80	0435	16.3
Preheat OFF	3/13/80	0440	16.3

The magnet coil final sizing fixture was received and subsequent magnet fabrication activities completed. These include:

- Final assembly and insulation of individual coils.
- Assembly and sizing of the magnet coil assemblies.
- Installation of the coils in the pole pieces.

Electrical and hydraulic testing of the modified magnet will be initiated and completed early in the following quarter.

Load Bank

Up to the present time the loading of the WESTF channel has been accomplished by impressing a series of DC voltages derived from a group of separate power supplies across each individual electrode-pair of the channel. The load current through each electrode-pair was brought to the desired level by adjusting its power supply to the appropriate voltage. All of the power produced by the supply, i.e., the product of the voltage across each electrode-pair and the current through it, was dissipated in the generator by means of I^2R losses within the plasma, as the result of potential falls at the electrode surfaces, and in the case of electrodes having significant resistivities, in ohmic losses within the electrodes.

When the WESTF channel is operated as an MHD generator using a magnet, the control of load current will be accomplished by means of a load bank, which is presently being constructed. The current in each electrode-pair in this load bank will be adjusted individually by its own rheostat as shown in Figure 51. Thus, the characteristic curve of each electrode-pair can be generated at will by using a switch to produce open circuit voltages and varying the rheostat to go from very low currents to short circuit conditions. With the rheostat at maximum resistance, the currents will be less than 0.25 amperes. Corresponding to current densities of less than $0.4 A/cm^2$, diffuse discharges would be expected at these densities.

The circuitry shown in Figure 51 can be used to operate the channel in the following modes:

1. as an MHD generator
2. as a simulated generator without a magnetic field using external supplies to simulate MHD loadings.
3. as an MHD generator using supplementary external power supplies to achieve current densities as high as 2 or 4 amperes/cm^2, and to increase Halls fields.

The revised electrical system will have the capability of energizing an MHD channel consisting of 16 electrode-pairs in either the MHD plus auxiliary power or the simulated MHD modes. In the case of operation exclusively as an MHD generator, the electrical system will have a 36 pair electrode-pair capacity, which could be used for tests on a multi-electrode Faraday connected channel having a very short pitch. Ordinarily the circuit will be used with less than 16 channels and the remaining circuits used to monitor floating potentials of selected water-cooled panels on the insulating walls. Eight of the external power supplies can be operated at loadings up to 18 amperes.

Voltage Isolation

The operation of WESTF as an MHD generator with a magnet requires that one end of the system be electrically isolated from ground to prevent shorting of the Hall field. A study of the relative difficulty of isolating the input versus the output end of the channel has led to the conclusion that the most reliable way of isolating one end of the generator would be to electrically isolate the mixer-combustor system.

In order to isolate the frame of the combustor and mixer the support frame will be mounted on insulating blocks fabricated from G-7 fiberglass. Insulating hoses will be used to isolate the water cooling. Voltage isolation of oxygen and air cooling lines will be accomplished by fabricating one foot insulating sections of pipe fabricated of a fire retardant fiberglass composition. These pipes will be threaded on both ends.

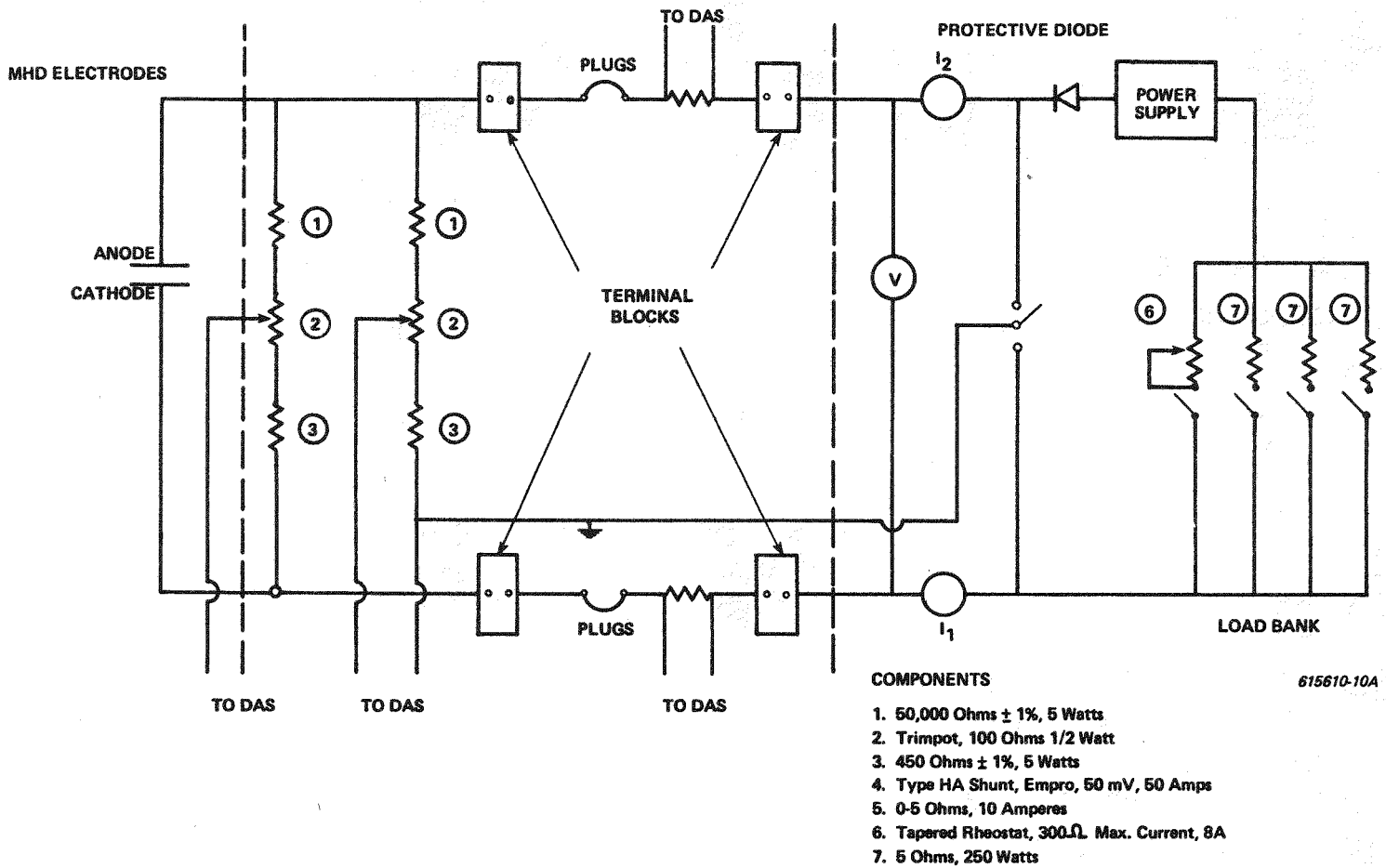

Figure 51. Individual Electrode Pair Circuit for Operation of WESTF with Magnet

The resistivity of the seed ash mixture employed in Test 43 was determined to be approximately 250 ohm-cm. A sufficient length of teflon tubing and some other insulating hose will be used to make the power loss in the seed line negligible during operation.

The design of an insulating length of piping for the preheater posed a more difficult problem since the preheated air can exceed 500°C in temperature. Figure 52, is an overall drawing of a water-cooled insulating section which will be constructed for this task. Insulation is accomplished by using a series of G-7 fiberglass cylinders, which are protected from the hot gas by an array of water-cooled stainless steel cylinders. Heat dissipation to the water cooled inner lining in this design is minimized by the use of a central mulllite cylinder which will be mounted over a 3/8" thickness of fiber-frax insulation.

It might be possible to isolate the downstream end of the channel using the general design features of Figure 52. However, the higher temperatures and the presence of seed, and ash would probably necessitate increasing the insulating paths.

Fabrication of the isolation section is in process.

4.0 WBS 1.4 - PROJECT MANAGEMENT AND DOCUMENTATION

The following required project documentation was issued during the reporting period:

- Monthly Report for December 1979
- Monthly Report for January 1980
- Monthly Report for February 1980
- Quarterly Report for the period October-December 1979

A technical review meeting was held with DOE personnel in January 1980 to review the direction of contract activities. As a result of this meeting and subsequent discussions the contract effort is being redirected to emphasize the engineering development and evaluation of slagging cold metallic electrodes. A work program

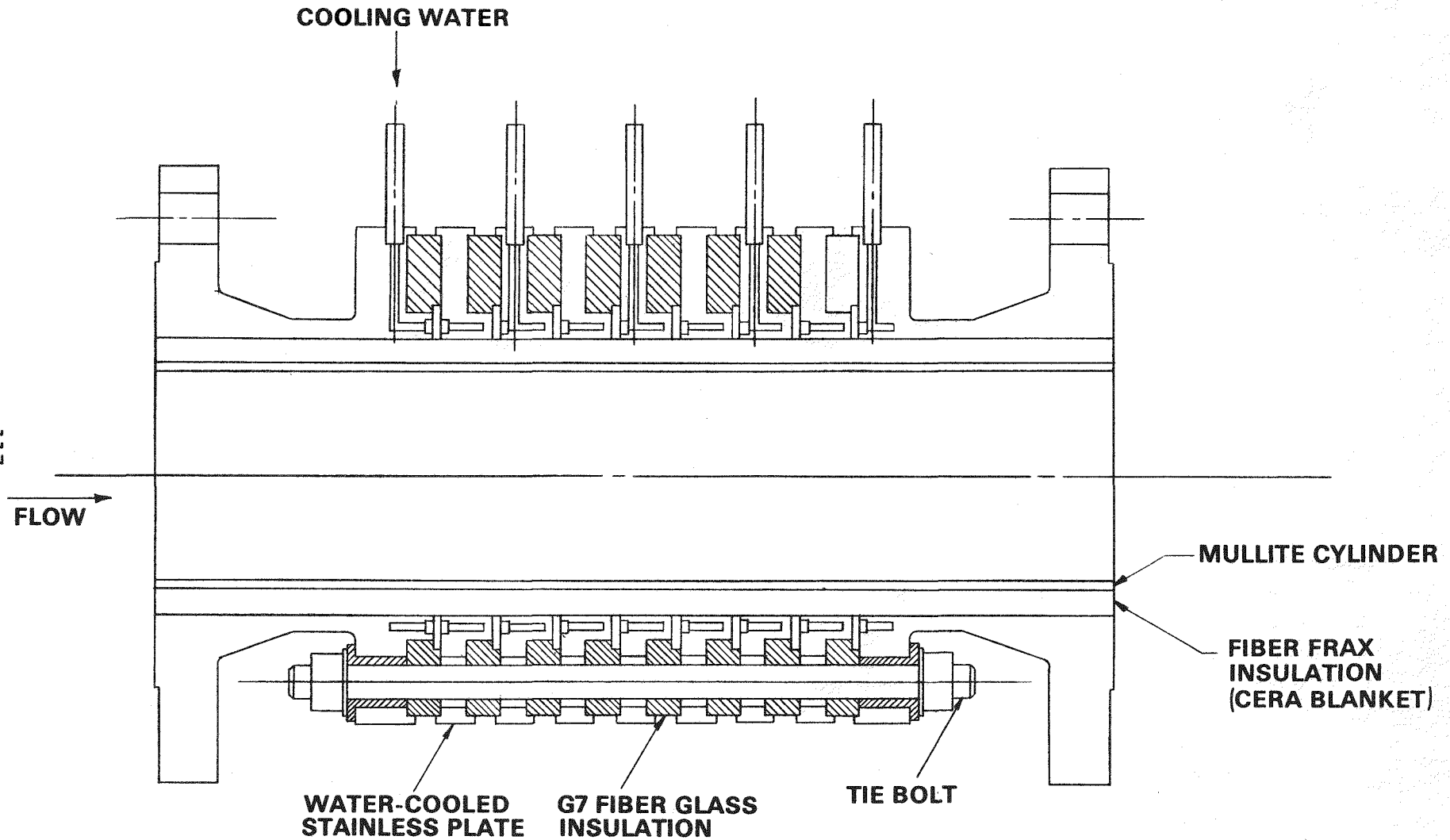

Figure 52. Insulating Section of Preheated Air Line in WESTF

is being formulated to outline this activity. Primary considerations are:

- To support near-term CDIF and ETF activities.
- To establish a WESTF - generator (and laboratory screening - WESTF) test correlation.
- To identify alternatives to the use of platinum as slagging cold electrodes.

In support of this effort, visits were made to the High Temperature Gasdynamics Laboratory at Stanford University, to the Sandia Laboratories and to the AVCO Everett Research Laboratory to review current activities.

V. SUMMARY PLANS NEXT REPORTING PERIOD

Summary plans covering significant activities during the next reporting period, April-June 1980, are presented below according to the Work Breakdown Structure primary tasks.

WBS 1.1 - ELECTRODE AND INSULATOR MATERIALS

- Initiate systematic study of attachment techniques for ceramic materials to be tested in the near future.
- Investigate the Pt/Cu system: assess copper diffusion, its effect on thermal and electrical properties, and examine possible solutions such as refractory metal barriers.
- Initiate and complete literature search of coal gasification and gas turbine corrosion resistant material alloys which offer potential for use as slagging cold metallic electrodes.
- Initiate the evaluation of electrochemical corrosion tests for screening metals, including use of aqueous K_2SO_4 and molten K_2SO_4 as electrolytes.
- Continue development and evaluation of anode arc erosion test.

WBS 1.2 - ENGINEERING TESTS

- Complete definition of work program which emphasizes the engineering development and evaluation of slagging cold metallic electrodes.
- Complete fabrication of the following test hardware:
  - Dummy Test Section (facility checkout)
  - WESTF II Test Section (facility checkout)
  - MTS II Test Section (non-slagging super-hot)
  - Viewport
  - WESTF II Test Section (slagging cold metallic electrodes)

- Complete post-test material evaluation of WESTF Test 43, slagging hot platinum and iron (Westinghouse) and WESTF Test 42, non-slagging super-hot hafnia and zirconia coupons (BPNL).

- Complete design of MTS II test of hafnia samples.

WBS 1.3 - WESTF MODIFICATION

- Complete magnet modification (electrical and hydraulic tests).

- Complete test passage reassembly, including installation of the magnet.

- Complete post-modification checkout of WESTF.

- Complete design of scrubber modification required to support WESTF operation at high sulfur levels.

WBS 1.4 - PROJECT MANAGEMENT AND DOCUMENTATION

- Issue January-March 1980 Quarterly Report.

- Issue monthly progress reports.

VI. CONCLUSIONS

Following the completion of four WESTF tests in this quarter, the facility was shut-down for major modifications. The primary element in the modification is the addition of a conventional 3 Tesla magnet. At the same time extensive rework of the test passage and test area are being implemented. Upon completion of this modification, WESTF will have the capability for simulating the realistic MHD environment which is necessary for the effective engineering development and evaluation of electrode materials and designs. Post-modification checkout of the facility is projected for the end of the next quarter.

Continuing laboratory electrochemical corrosion tests have shown that iron oxide additions to Rosebud slag are as effective as cobalt oxide additions in reducing electrochemical stress. The use of iron oxide additions offers significant economic advantages when compared with cobalt additions.

The current program activities are in a period of transition. Upon completion of the WESTF modification, primary emphasis will be given to establishing a correlation between WESTF and generator tests and the evaluation of slagging cold metallic electrodes. Laboratory investigations which are necessary to support this change in emphasis have been initiated. Testing of slagging hot and non-slagging super-hot electrodes will be continued at a reduced level.

VII. REFERENCES

1. FE-15529-2, "MHD Electrode Development, Quarterly Report, January - March 1979," DOE Contract DE-AC-01-79-ET-15529, Westinghouse Electric Corporation, May 1979.

2. FE-15529-3, "MHD Electrode Development, Quarterly Report, April-June 1979," DOE Contract DE-AC-01-79-ET-15529, Westinghouse Electric Corporation, August 1979.

3. FE-15529-5, "MHD Electrode Development, Quarterly Report, October-December 1979," DOE Contract DE-AC-01-79-ET-15529, Westinghouse Electric Corporation, February 1980.

4. FE-15529-1, "MHD Electrode Development, Quarterly Report, October-December 1978," DOE Contract DE-AC-01-79-ET-15529, Westinghouse Electric Corporation, January 1979.

5. FE-15529-4, "MHD Electrode Development, Quarterly Report, July-September 1979," DOE Contract DE-AC-01-79-ET-15529, Westinghouse Electric Corporation, October 1979.

6. Ronald R. Smyth, Fluidyne Engineering Corporation, private communication.

7. FE-2248-20, "Development, Testing and Evaluation of MHD Materials and Component Designs, Quarterly Report, April-June 1978," DOE Contract EX-76-C-01-2248, Westinghouse Electric Corporation, August 1978.

8. FE-2519-11, "MHD Generator Component Development, Quarterly Report, July-September 1979," DOE Contract FE-77-C-01-2519, AVCO Everett Research Laboratories, Ihc., January 1980.

9. Personal communication, M. R. Cannon, MIT, to B. R. Rossing, (W)R&D, January 1980.

☆U.S. GOVERNMENT PRINTING OFFICE: 1980-640-258/200